MULTI-OBJECTIVE OPTIMIZATION OF A GRID-CONNECTED PV-BATTERY-ELECTROLYZER FUEL CELL ENERGY SYSTEM

A CASE STUDY AT THE GREEN VILLAGE





Master Thesis

Submitted in partial fulfillment of the requirements for the degree of Master of Science in Sustainable Energy Technology (SET)

Riccardo MASELLI

Graduation Committee:

Dr. Hesan Ziar Dr. Özge Okur Dr. Na Li

Prof. Olindo Isabella

To be publicly defended in TU Delft on September 6th, 2023

Copyright © 2023 by R. Maselli

An electronic version of this Thesis is available at http://repository.tudelft.nl/.

CONTENTS

Li	st of	Figures	V
Li	st of	Tables	vii
Li	st of	Abbreviations	ix
Sı	ımma	ary	хi
A	knov	wledgments	xiii
1	Intr	oduction	1
	1.1	Background and Motivation	1
	1.2	Problem Statement	
	1.3	Case Study: The Green Village	6
	1.4	Outline	7
2	Lite	rature Review and Background Knowledge	9
	2.1	Energy Systems Sizing	9
		2.1.1 Optimization Techniques	12
		2.1.2 Multi-Objective Optimization	13
		2.1.3 Genetic Algorithm	14
	2.2	Pricing Mechanisms	17
		2.2.1 Electricity Retail Tariffs	
		2.2.2 Grid Connection Costs	18
	2.3	Knowledge Gap	19
3	Syst	em Simulation	21
	3.1	Components of the System	21
		3.1.1 PV Panels	22
		3.1.2 Batteries	24
		3.1.3 Electrolyzers	25
		3.1.4 Fuel Cells	
		3.1.5 Other Components	
	3.2	Energy Management	29
4	Inp	ut Data	35
	4.1	Solar Irradiance	
	4.2	Load Demand	36
	43	Electricity Prices	38

iv Contents

5	Opti	imization	41
	5.1	Optimization Parameters	41
		5.1.1 Objective Functions	41
		5.1.2 Variables and Constraints	44
	5.2	Implementation	46
	5.3	Optimal Solution Selection	48
		5.3.1 Weighting the Criteria	48
		5.3.2 Application of the TOPSIS Algorithm	50
6	Ana	lysis of the Results	53
	6.1	Base Case	53
		6.1.1 Pareto Set Analysis	53
		6.1.2 Use of Hydrogen Storage	54
		6.1.3 Economic Performances	56
		6.1.4 System's Behavior	57
	6.2	Infinite Grid	60
		6.2.1 Pareto Set Analysis	60
		6.2.2 Economic Performances	62
	6.3	Real Time Pricing	63
	6.4	Hydrogen Cost Decrease Scenario	65
		6.4.1 Pareto Set Analysis	66
	6.5	Unlimited PV Penetration	67
		6.5.1 Pareto Set Analysis	68
	6.6	Best Solutions Overview	70
7	Con	clusion	71
	7.1	Discussion	71
	7.2	Answering The Research Questions	73
	7.3	Limitations of the Work	74
	7.4	Recommendations for Future Research	75
A	App	endix - Literature Review Summary	77
В	App	endix B - Results of the Optimization	83

LIST OF FIGURES

1.1	Aerial View of The Green Village, retrieved from Google Earth	6
1.2	Graphic representation of the System Architecture	7
2.1	Example of a PV-wind-diesel-hydrogen-battery off-grid system, Dufo-López	
	and Bernal-Agustín, 2008	10
2.2	Examples of Three-Dimensional Pareto Sets from the Literature	14
2.3	Flowchart of the Optimization Algorithm employed	16
3.1	Graphic representation of the System Architecture	21
3.2	Beginning-of-life stack performance at reference conditions, ©Nedstack	
	Fuel Cell Technology	27
3.3	First Evaluation of the Energy Management Strategy function	30
3.4	Energy Management in Surplus Mode	32
3.5	Priority Choice in case of Deficit Energy	32
3.6	Energy Dispatch in the "Battery First" Mode	33
3.7	Energy Dispatch in the "Fuel Cells First" Mode	33
4.1	Annual irradiance on a 15° tilted plane in the different orientations	36
4.2	Total Electric Load	37
4.3	Day Ahead electricity prices in 2021 and 2022	38
5.1	Schematic of the Implementation Workflow	47
6.1	3-Dimensional representation of the Pareto Set, Base Case	54
6.2	2-Dimensional representation of the Pareto Set, Base Case	55
6.3	Base Case Best solution: Energy Flows during a Summer Week	58
6.4	Base Case best solution: energy flows during a winter week	59
6.5	Base Case most self-sufficient solution: energy flows during a summer week	59
6.6	Base Case most self-sufficient solution: energy flows during a winter week	60
6.7	Pareto Set, Infinite Grid Scenario	61
6.8	Cost increase of Infinite Grid Scenario Solutions with respect to the Base	
	Case	63
6.9	Imported power and electricity prices, Real Time Pricing Scenario top so-	C 4
C 10	lution	64
	Base Case and low Hydrogen Cost Scenario, Pareto Sets comparison	66
	Pareto Set, Unlimited PV Penetration Scenario	68
b.12	Distribution of the PV panels in the best solutions, Base Case vs Unlimited	00
	PV Penetration Scenario	69

LIST OF TABLES

3.1	Technical Characteristics of the Selected PV Panels	22
3.2	Selected Batteries Technical Characteristics	24
3.3	Techincal Specifications of the Electrolyzer	26
3.4	Fuel Cells Technical Specifications	27
3.5		29
4.1	Average Household Electricity Price Breakdown for the years 2012-2022. Prices in €/kWh, source Centraal Bureau voor de Statistiek, 2023	89
5.1	Constraints on the Maximum Number of Components	16
5.2	Options used for the <i>gamultiobj</i> function	18
6.1		55
6.2	8	55
6.3	0,7	6
6.4	0,	7
6.5	Infinite Grid Scenario, TOPSIS Best Solution: Sizing 6	61
6.6	Infinite Grid Scenario, TOPSIS Best Solution: Performances 6	61
6.7	Infinite Grid Scenario, solutions with increasing Grid Dependence : Perfor-	
		62
6.8	Infinite Grid Scenario, solutions with increasing Grid Dependence : Perfor-	
		62
6.9	1 7	63
	0 ,	64
	0 ,	64
	0	67
6.13	Low Hydrogen Equipment Cost Scenario, TOPSIS best solution: Performances	67
6.14		69
		69
		70
	· · · · · · · · · · · · · · · · · · ·	0
B.1	Base Case: Sizing Results	34
B.2		35
B.3		36
B.4		37
B.5		88

viii List of Tables

B.6	Real Time Pricing Scenario: Objective Functions Values Results	89
B.7	Hydrogen Cost Decrease Scenario: Sizing Results	90
B.8	Hydrogen Cost Decrease Scenario: Objective Functions Values Results	91
B.9	Unlimited PV Penetration Scenario: Sizing Results	92
B.10	Unlimited PV Penetration Potential Scenario: Objective Functions Values	
	Results	93

LIST OF ABBREVIATIONS

AC Alternating Current

AEM Anion Exchange Membrane
AHP Analytic Hierarchy Process
AI Artificial Intelligence
AOI Angle Of Incidence
ATC Annualized Total Costs

BAT Battery

CBS Centraal Bureau voor de Statistiek

CRF Capital Recovery Factor

CRITIC CRIteria Importance Through Intercriteria Correlation

CSA Crow Search Algorithm

DC Direct Current

DER Distributed Energy Resources
DHI Direct Horizontal Irradiance
DNI Direct Normal Irradiance
EC Energy Community
EES Electrical Energy Storage

EL Electrolyzer FC Fuel Cell

GA Genetic Algorithm
GD Grid Dependence

GHI Global Horizontal Irradiance
HRES Hybrid Renewable Energy System

HSS Hydrogen Storage System
IEA Ienternational Energy Agency
LCOE Levelized Cost Of Electricity

LOH Level Of Hydrogen

LPSP Loss of Power Supply Probability MOO Multi Objective Optimization

MOPSO Multi Objective Particle Swarm Optimization
NREL National Renewable Energy Laboratory
NSGA Non-dominated Sorting Genetic Algorithm

O&M Operation and Maintenance PEM Polymer Electrolyte Membrane

PROMETHEE Preference Ranking Organization METHhod for Enrichment Evaluation

PSO Particle Swarm Oprimization

PV Photo Voltaic

PVMD Photo Voltaic Materials and Devices

RTP Real Time Pricing
SC Specific Consumption
SoC State of Charge
TGV The Green Village

TOPSIS Technique for Order Preference by Similarity to Ideal Solution

TOU Time Of Use UL Unmet Load

WSM Weighted Sum Method

SUMMARY

The transition from a centralized to a decentralized energy infrastructure is one of the most discussed features of the future energy system. With the fast growth of renewable energy technologies, which can be integrated in the built environment and in contexts like small production centers, the development of distributed energy generation and storage systems closer to consumers is expected to play a significant role in driving the change. Within this context, the role of Energy Communities is emerging and is at the center of numerous studies. The Green Village in Delft is developing the 24/7 Energy Lab project, focusing on providing reliable, affordable and clean energy to a small-scale energy community by means of a system composed of solar panels for energy generation, batteries for electrical energy storage, and an hydrogen storage system consisting of electrolyzers, fuel cells and hydrogen tanks for seasonal energy storage.

Previous research has highlighted how an off-grid configuration would result in inconveniently high costs for the community's users, if compared to the average cost of energy in The Netherlands. The aim of this thesis is to study the system in a grid-connected configuration, and in particular to find the optimal sizes of the components in order to achieve the best trade off between three conflicting objectives: minimizing total costs, maximizing self- sufficiency and maximizing reliability. After modeling the system's components and their mutual interactions, the optimization was carried out on MATLAB using a variant of the NSGA-II algorithm, which provides a Pareto Set of equally optimal solutions for the problem. The solutions were then ranked with a Technique for Order Preference based on Similarity to the Ideal Solution (TOPSIS), to assist the decision-making process.

The simulations have determined that an installed capacity of 85.41 kWp (composed of 234 panels of 365 Wp each) results in the most effective choice for the solar energy generation, irrespective of the external conditions imposed. The optimal storage capacity, however, results significantly more influenced by factors such as grid imports limitations and price uncertainties. Under the conditions of limited imports from the grid, an optimal capacity of 75 kWh in the form of batteries was found. In general, the study confirms that the adoption of an hydrogen storage system is far from being convenient on a small scale residential level, regardless of the pricing conditions. The research has also posed an accent on the incremented costs incurred to reach full reliability of the system with low values of dependence from the grid, due to the high costs of the necessary storage equipment. Additionally, despite the best solutions found represent the optimal compromises balancing the conflicting objectives, reasonable solutions in terms of costs faced by the Community's users are usually not among the first choices of the ranking algorithm, mainly because they necessitate of at least 50% of the load to be supplied through grid imports.

ACKNOWLEDGMENTS

This work marks the conclusion of the most formative period of my life so far. I want to express all my gratitude to the people who made this achievement possible, all in different ways. First and foremost, I would like to thank my supervisors Hesan Ziar, Özge Okur and Na Li. Our frequent meetings were always a great occasion to exchange visions and ideas, and were of great help in guiding me towards to right direction while letting me in control of my work. Similarly, I thank Joep van der Weijden for his complete availability and for showing me the great environment of The Green Village. Additionally, a meaningful thanks goes to Prof. Olindo Isabella, who accepted to join my Thesis Committee.

The last two years have been an incredible emotional rollercoaster, and I was lucky enough to have fantastic people sharing the ride with me. First, my parents who never doubted me and whose unconditional support represent my safe port. A special mention goes to my friends in Delft, who simply made better every single one of my days here. I really can't express how much important they were to me. Of course, I want to thank my friends back home, for making it so hard to leave back to The Netherlands every time I had to. Last but not least I want to thank Chiara, because she often understands me more than I do. You were a wonderful gift too.

Riccardo Maselli Delft, August 2023

1

INTRODUCTION

1.1. BACKGROUND AND MOTIVATION

The necessity to tackle climate change and to decrease (and eventually terminate) carbon emissions is one of the most debated themes in today's society. It is also a crucial aspect of the 2030 Agenda for Sustainable Development adopted by all the United Nations members, and The Netherlands among these, in 2015. In particular, this is highlighted by two of the 17 Sustainable Development Goals, namely the necessities to "Ensure access to affordable, reliable, sustainable and modern energy for all" (Goal 7) and "Make cities and human settlements inclusive, safe, resilient and sustainable" (Goal 11). In order to pursue the said goals, disruptive changes of the current energy infrastructure will be likely to occur, not only in terms of organizational structure, but also for what concerns the technologies used and the policies applied.

One of the most discussed features of the future infrastructure is the transition from a centralized to a decentralized energy infrastructure. With the scaling up of renewable energy technologies like photovoltaic (PV) generation, which can be integrated in the built environment and in contexts like small production centers, the development of distributed energy generation (and storage) systems closer to consumers is expected to play a significant role in driving the change. Switching from a system mainly relying on traditional, fossil-based energy generators to one exploiting renewables based assets like PV and wind turbines also poses some significant challenges in the management of the power grid. The current energy infrastructure is designed in such a way that demand and supply are perfectly balanced in every instant, and the non-dispatchable nature of renewable energy technologies requires adequate solutions to deal with periods of high abundance of energy production (that can easily cause grid congestion) or scarcity of supply.

Different frameworks have been developed in the last decades for the integration of such distributed systems in the future power network. These have been often referred to with

2 1. Introduction

the term "microgrid". According to the definition given by the National Renewable Energy Laboratory (NREL) "A microgrid is a group of interconnected loads and distributed energy resources that acts as a single controllable entity with respect to the grid. It can connect and disconnect from the grid to operate in grid-connected or island mode". In the previously described context, microgrids can therefore act as a fundamental support to the main grid, by providing their excess power when necessary, and by decreasing their request from the main power grid when the latter faces congestion or scarcity of production. In addition to providing this kind of support, these systems also have the potential to benefit the loads to which they are directly connected, by supplying them with clean, affordable and reliable energy and preventing them from undesirable situations like faults from the main grid or price spikes resulting from energy crises.

More recently, the definition of microgrid has been replaced by the concept of integrated energy community, that comprises the previously mentioned microgrids' characteristics but also puts emphasis on the social and organizational aspects of the community involved in forming this system, for example by looking at the customer engagement. These communities are defined not only by their technical properties like the utilized technologies and the pursued goals of self-sufficiency and energy security, but also by the active involvement of the participants, who (especially in developed countries) "are being motivated by increased climate awareness and willingness to become autonomous among pro-active communities" (Koirala et al., 2016). Since the definition of Integrated Energy Community (IEC or just EC) is currently the most referred to in recent literature, this is the term the system will be referred to throughout this project.

The efficient design of an EC needs several aspects to be taken into account, not only under the technical but also under the economical and social point of view. First of all, the choice of the system's components shall be taken, and their sizing should be evaluated by taking into account the load requirements and additional boundary conditions. In particular, the conditions at which power flows are managed within the system, and the ways it interacts with the external main grid are of capital importance and can have a large influence on their optimal design.

The scope of this work is to study a real-life case of energy community, from the design to the analysis of its performances. By focusing on all the aspects (mainly the technical and economical analysis), this thesis project aims to represent a benchmark case study for the effective development of this and similar systems.

1.2. PROBLEM STATEMENT

The design of a semi-independent energy community is a complex task involving several different aspects to be taken into account. Apart from a technical overview of the project involving the components, its connections and management, factors like social acceptance, environmental and economical effects in the integration of energy communities should be covered to have an exhaustive overview of the project.

The Green Village is a dynamic center for experimentation, and previous studies on the

Energy Community on which this work is focusing have already being conducted. In particular, N. Li et al., 2023 have investigated the sizing of this system in an off-grid configuration, providing all the necessary electricity by means of self-produced power. Especially because of the high investment costs related to the hydrogen storage system (electrolyzers, tanks, fuel cells and surrounding equipment) the end-cost of the system resulted to be high if compared to the average electricity cost per kWh in The Netherlands.

Also Betere Marcos, 2022 approached the sizing of the system in an off-grid mode. The resulting costs were similarly high and not preferable for a local community that could have access to a grid connection, if necessary. However, the conclusion of such work also states that with a small reduction of the system's self sufficiency (and hence, with a grid connection) the system could enjoy significant economic benefit. This conclusion mainly comes from the fact that, considering the variability of energy generation from renewable sources, the system would end up being oversized if its scope is to provide 100 percent of the community's needs.

In this research, the system will be studied in a grid-connected configuration. This means that, in case of necessity, the Energy Community will be capable to both import energy in times of need and export its excess energy to sell it for profit. The introduction of the grid as an additional element of the system also poses questions on the interaction between the Energy Community and the external environment. If, on one hand, it is predictable that this would reduce the overall costs, importing energy from the grid represents a cost that its not completely straightforward to foresee.

In fact, the evolution of the energy system as a whole also entails a change with respect to the traditional ways of exchanging energy and electricity as a commodity. In order to deal with the previously mentioned congestion problems, and to accurately match the variable production from the renewables with the required loads, the future power network will need to consistently rely on demand side management techniques. Among these, Demand Response can be defined as the set of actions and incentives that influence the consumers' energy demand, both directly and indirectly.

An effective means by which the load can be indirectly influenced is by applying varying prices to the electricity purchased in different moments. By charging higher prices when the system is already stressed and lower ones when there is an excess of power produced, consumers which are aware of the instantaneous power price can choose to modify their consumption and be economically rewarded for this. This kind of policies, typically referred to as Dynamic Pricing, are one of the most relevant emerging areas in the future power industry (Sampson and Longe, 2021), and are likely to become widespread even in countries that are actually not employing it, as the energy infrastructure continuously evolves by incorporating a higher share of renewables and an increasing number of enabling technologies like smart electricity meters.

Differences in the adoption of distinct policies are expected to arise, with some that may

4 1. Introduction

prove to perform better under the economical point of view for energy communities (that is, by adopting different pricing mechanisms the overall cost of the electricity for the consumers is likely to vary). Because of this, an analysis is required to assess the response of different systems to their adoption. For example, in the case of the adoption of Dynamic Pricing schemes, as highlighted in Dutta and Mitra, 2017, "Market acceptance of dynamic pricing can only be achieved if its benefits to each stakeholder can be proved. This requires more and more well-planned pilot projects and a study of different aspects involved in this field". Since energy communities will play an important role in future energy systems, it would be necessary to evaluate the effects of these conditions on their design as well.

As earlier introduced, one of the most relevant aspects of distributed energy systems, is their capacity to operate independently from the main grid and when necessary even sell their surplus production to the retail market (through the mediation of the network operator). The regulations concerning the way these systems interact with each other, and in particular the ones determining under which conditions smaller systems like energy communities can inject their own produced power to the main grid, can also have a substantial impact on the systems' design.

In The Netherlands, the current policy for prosumers feeding power into the grid is the so called *Net-metering* (*salderingsregeling* in Dutch). According to this policy, power companies are required to reward the consumers for the energy they inject into the grid by deducting all said energy to the one they import. This means that prosumers receive a compensation that is exactly equivalent to the price they would have had to pay to buy that same energy they fed into the grid. The *Net-metering* policy has helped The Netherlands in boosting their domestic-scale share of installed PV, but it's now being under discussion by the Government itself. Several alternatives to this policy and their possible outcomes are being explored, as in Londo et al., 2020.

Policy intervention and regulations are very important aspects to be considered in the design of grid-connected energy communities, but surely not the only ones. While approaching these problems, decisive technical considerations shall be addressed. Firstly, a choice concerning the system's technical components shall be made. Energy communities are usually composed by loads, energy generators and (optionally) storage systems. Zero-emissions microgrids are characterized by the only presence of renewable energy sources as generators, like PV, wind turbines, hydrogen fuel cells, biomass generators or even small hydropower plants. As for the storage technology, several options can be taken into account, and usually the most considered alternatives include electrochemical storage in the form of batteries and chemical storage in the form of hydrogen molecules.

While the decision on the generation technology is usually location dependent (e.g. solar energy production through PV modules is usually the preferred choice when space limitation arise, due to their easily applicability in the built environment and low capital costs involved), the choice regarding the energy storage technology is less straightfor-

ward. Batteries are commonly the most common choice adopted in residential independent energy systems and microgrids, as their technology is well known and has reached levels of scale production. Their relatively low energy density, however, only makes them suitable for short term energy storage, while hydrogen storage systems (coupled with fuel cells acting as backup generators) can benefit a very high density and are therefore mostly used for long-term energy storage purposes. In this research, focusing on the case study of The Green Village in Delft and in particular on the 24/7 Energy Lab project, the considered system architecture is composed of PV generation, batteries, fuel cells and hydrogen storage system (HSS).

However, several factors might raise questions about the actual usefulness and effectiveness of hydrogen storage systems in grid-connected energy communities. The high capital costs of the hydrogen infrastructure can represent a detrimental aspect on its application, especially in systems that can benefit from power inputs from the grid in times when the prices are convenient. At the same time, the opportunity of exploiting medium and long-term storage to gain profits from exporting power at the right time could represent a significant added value. Moreover, the use of an HSS can surely provide better performances in terms of the system's self sufficiency, and safeguard its reliability in occurrence of grid faults.

The aim of this thesis is to cover these uncertainties and considerations, by analyzing a case study and transferring the most meaningful findings to a broader analysis. With regards to the selected case study, the first research question addressed will be:

What is the best sizing configuration for a grid-connected energy community in The Green Village under technical and economical aspects?

The mentioned price uncertainties also call for a second question, formulated as:

What is the influence of different electricity pricing conditions on the design and sizing of a grid-connected energy communities?

And lastly, concerns about the high costs for hydrogen equipment lead to a broader investigation of its usefulness:

To what extent the adoption of a hydrogen system can benefit a grid-connected energy community under different pricing conditions?

6 1. Introduction

1.3. CASE STUDY: THE GREEN VILLAGE

This project will partly act as a continuation of previous work conducted by Master students and researchers together with The Green Village. The 24/7 Energy Lab is an ongoing project that aims to provide reliable, affordable and clean Energy to the small-scale community of The Green Village, composed of 8 houses occupied by 12 households. To do so, the 24/7 Energy Lab involves the presence of solar panels for energy generation, batteries for electrical energy storage, electrolyzers, fuel cells and hydrogen tanks for seasonal energy storage in the form of hydrogen.



Figure 1.1: Aerial View of The Green Village, retrieved from Google Earth

Within the context of The Green Village, shown in 1.1, the system's microgrid can be seen as several individual components connected to a common AC bus. Components operating with direct current are coupled to the common grid through an inverter, while the regional grid provides a bi-directional energy flow to the Community. Figure 1.2 schematically represents the system's architecture.

The scope of this work will be to optimally design and size the system in a grid-connected configuration and to analyze both technical and economical performances of the Energy Community. The sizing will be based on real historical load data from the households provided by The Green Village, using those as an input for the optimization algorithm.

1.4. OUTLINE 7

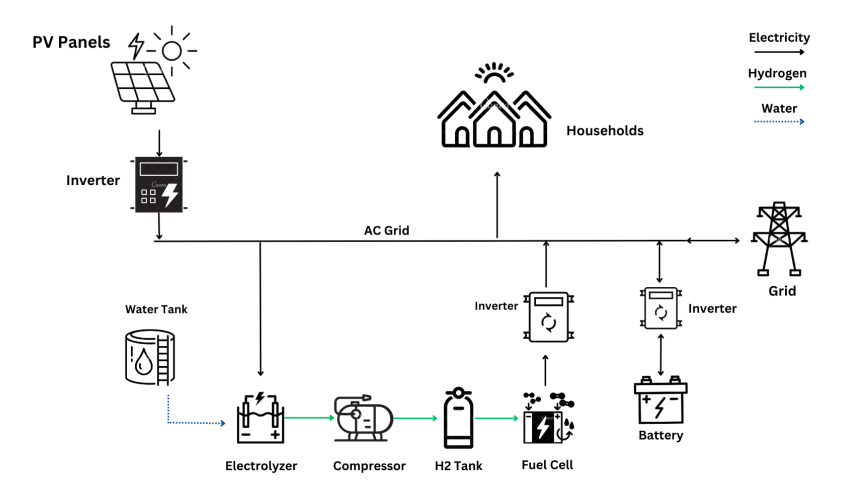


Figure 1.2: Graphic representation of the System Architecture

1.4. OUTLINE

The proposed approach to address the research questions is a scenario-based multi objective optimization, taking into account the different necessities of the Community, expressed as conflicting objectives. Before doing so, the available scientific literature on this topic was studied and discussed in Chapter 2. Trough the literature study, the most appropriate optimization method was selected, and a knowledge gap was identified so that this research can add a degree of novelty to the scientific community. The system needed then to be studied on a single component level. Therefore, modeling of all the elements forming the Energy Community was performed in Chapter 3. This includes the mathematical formulation of all the system's technical components, their behaviors and mutual interactions according to an energy management strategy. The processing of the necessary input data (about the load, the environmental conditions, and the prices) is addressed in chapter 4. Chapter 5 deals with the optimization itself, detailing variables, objectives, constraints and its practical implementation. The results of the optimization are shown and analyzed in Chapter 6, where several alternative scenarios are studied to address the sensitivity of the model. Lastly, Chapter 7 concludes the thesis, presenting final considerations, limitations of the project and reflections on future work.

LITERATURE REVIEW AND BACKGROUND KNOWLEDGE

The scope of this chapter is to analyze the reviewed literature served as a background for the research. This literature is comprised of journal papers, conference papers, articles, books and other publications mainly retrieved with the help of the databases Scopus and Google Scholar.

2.1. Energy Systems Sizing

Sizing is a critical aspect in the design of energy systems, influencing the final investment choices on the basis of the forecasted performances ad costs, and it is therefore a broadly discussed problem in scientific literature. Because of the vastness of the variables involved and the possible considerations to which these studies can lead, the research in this field is very heterogeneous. Generally, the use of optimization algorithms is a widespread approach to this kind of problem.

A considerable amount of earlier studies focus on the design of off-grid systems that can be more suitable in remote areas where a connection to the regional grid is too expensive or impossible for site-specific reasons. Narayan et al., 2019 employed Multi-Objective Genetic Algorithm to size off-grid solar home systems in a multi-tier framework. The authors highlight that "climbing the electrification ladder" in off-grid systems comes with large investment costs because of the over-sizing needed when no backup from the grid or other sources are available.

When systems are located in urban areas with easy access to a network connection, the interactions with the grid are also taken into account in the sizing process. Raja and Detroja, 2018 used single objective Linear Programming to optimize the sizes of a grid-connected PV-battery system that is also allowed to export power to the grid and financially benefit from this in conditions of dynamic prices for the electricity. To ex-

ploit this, the components result to be slightly oversized with respect to a base case with no possibility to export the self-produced power. Also the system sized in Gharibi and Askarzadeh, 2019 is able to export excess power to the main grid, but not capable of importing any. It is sized through a novel Crow Search Algorithm, and the operation is also taken into account in the multi-objective optimization with the introduction of a "grid-factor" variable, determining how much of the excess would be stored or sold.

The architecture of the systems considered in the reviewed literature is vary varied.PV panels are most of the times considered as the main power source in distributed energy systems, mainly because of the easy integration of this technology in small-scale systems and the low investment costs. Attia et al., 2021 designed a PV-only system in a grid-connected configuration with the use of the Augmented epsilon algorithm implemented in the CPLEX software in order to maximize the reliability and minimize cost and emissions (coming from the grid imports). However, several alternative or complementary generation options like wind turbines, biomass generators or diesel generators are investigated in other works

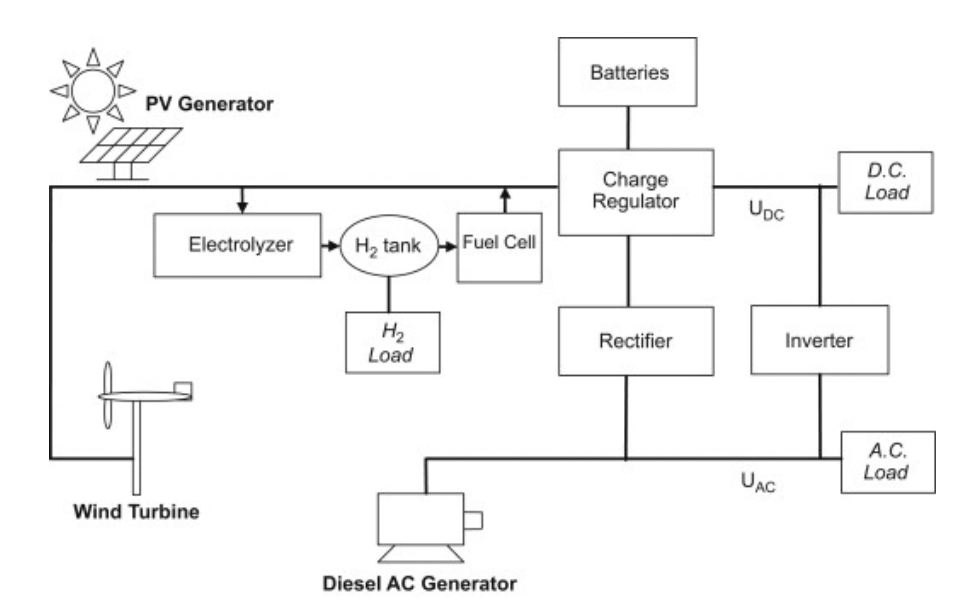


Figure 2.1: Example of a PV–wind–diesel–hydrogen–battery off-grid system, Dufo-López and Bernal-Agustín, 2008

The presence of some kind of energy storage is of particular relevance in the case of stand-alone systems, in order to avoid loss of load when the primary source of generation is not enough (e.g. at night, when the latter is only composed of PV). When grid-tied configurations are considered, energy storage is employed to guarantee to the system a certain degree of self sufficiency from the grid. Among all the possibilities for energy storage, electrical energy storage (EES) in the form of batteries is by far the most studied and firstly considered in the design of distributed energy systems, with an extensive

literature available in its support, especially when coupled with PV systems. A detailed review on this kind of systems is presented in Y. Zhang et al., 2022. Because of their relatively low energy density, however, batteries are more suitable for the so called short-term storage (e.g. the daily or weekly storage) rather than long-term, or seasonal, one. On the other hand, hydrogen has a very high energy density and the possibility to produce, store, and reuse it to generate electricity without pollutant emissions make it very often considered as a secondary energy storage system, usually employed together with batteries in the design of Microgrids.

Akhavan Shams and Ahmadi, 2021 employed the Genetic Algorithm to size a grid-connected PV-wind turbine system in two different configurations, using a battery energy storage system and hydrogen energy storage system (composed of electrolyzers, fuel cells and H_2 tanks) respectively. Even though the technical and economical performances of the two configurations are presented, the possibility of employing both system jointly is not taken into account. Paulitschke et al., 2015 in their study focused on the optimal sizing of a PV system equipped with both batteries and hydrogen storage, through the use of Multi Objective Particle Swarm Optimization (MOPSO). In this case, the fuel cells not only act as a backup when all the batteries are completely exhausted, but also charge the batteries when the state of charge reaches a predetermined low threshold level. hybrid batteries and hydrogen storage systems connected to renewable generation sources are optimized through the NSGA-II algorithm in B. Li and Roche, 2021. In this work, the sizing of a remote generating station and a local energy community connected to it was carried out together, with results showing the hydrogen system being of capital importance especially in ensuring continuous supply from the decentralized generating station.

The high cost of hydrogen systems components, however, represents a significant obstacle to their deployment, and often leads to sizing solutions in which they are very little or not employed at all, even at the expenses of reliability and self-sufficiency of the system. This is what happens in most of the optimal solutions evaluated in Dufo-López and Bernal-Agustín, 2008. In this study, the optimization is carried out on two levels in order to take into account the interdependence between the sizing and the operation strategy of the system, composed of PV, wind generation, diesel generators, batteries and hydrogen system. After a first algorithm randomly generates a set of possible configurations, a secondary runs to find the optimal dispatch strategy for each configuration. The solutions are then stored and the algorithm updates the found value until a predefined number of generations is reached. Among the optimal solutions found, most do not employ an hydrogen storage system, while the ones that do employ it prioritize the batteries in the dispatch operation. Similarly, also Human et al., 2014 performed a two-level optimization in order to optimize both the system's configuration and operation at the same time.

Generally speaking, the design of a hybrid renewable energy system (HRES) composed of generation and storage unit is not a trivial task. Choosing the optimal capacity of the system's components can benefit technical, economical, and social objectives. When single-optimization techniques are applied in the sizing, minimizing the system's cost is

usually the pursued goal by the optimizer. For example, Dash et al., 2018 sized a microgrid in a remote rural region of India under both grid-connected and off-grid configurations. To do so, they used the HOMER-Pro software to minimize the final energy cost. However, various other aspects can be considered when opting for a multi-objective optimization approach.

Shang et al., 2023 proposed a two stage optimization model to configure a grid-connected system comprised of PV, wind turbines, gas turbine, electrolyzer and fuel cells. The model considers electricity-price predictions and maximizes the net present benefit, while minimizing annual carbon emissions and loss of energy conversion. Yaghi et al., 2019 also consider emissions and cost as the optimization objectives for the sizing of a grid-connected system composed of PV, wind turbines, batteries and backup diesel generators. Together with cost, Baghaee et al., 2017 focus on the optimization of the reliability of the off-grid system under study. In particular, the loss of load is economically quantified and also the lost energy (extra production that does not serve the load) is minimized with the MOPSO algorithm. In their system sizing through NSGA-II, Wang et al., 2020 also considered social acceptance factors based on the land use and visual impact related to the installation of renewable power sources, in the context of a multiactor perspective to design energy communities.

2.1.1. OPTIMIZATION TECHNIQUES

As per the optimization techniques employed in the design and sizing of microgrids and distributed energy communities, the literature presents plenty of different alternatives. Single-objective optimizations are often dealt with Linear Programming algorithms, or specifically designed software such as NREL's HOMER PRO. As an example, Kusakana, 2019 only focus on the economic performances of a storage-only system under conditions of varying prices for electricity using Linear Programming. This method is also employed by Weckesser et al., 2021 to optimally size energy communities and analyze their impact on the distribution grid. In this case, a comparison is presented between multiple single objective optimizations and a multi-objective optimization considering all goals at the same time.

Optimizing multiple objectives simultaneously adds complexity to the problem. Recently, Artificial Intelligence (AI) based meta-heuristic algorithms have gained the interest of researchers because of their reliability, fast convergence towards towards optimal solutions and ease in their implementation. For these reasons, they have become the most common method to solve complex issues like the ones encountered in the design of energy systems.

A comprehensive review about the most relevant optimization approaches used to solve problems of placing and sizing distributed generation from renewable sources is presented in Abdmouleh et al., 2017. The authors conclude that "it has been noticed that GA and PSO are among the most promising optimization techniques to solve the DGs planning optimization problem". Ananth and Vineela, 2021 also have reviewed and com-

pared different optimization methods applicable to the energy sector, and in particular they indicate the Genetic Algorithm (GA) and Particle Swarm Optimization (PSO) as the most indicate to solve problems such as "Optimal Power Flow", "Multi-objective optimizations functions solving", "Large scale Unit commitment" and "Operational cost minimization with highly non-linear terms". New approaches have also been tested with very promising results, like the Crow Search Algorithm (CSA) presented by Askarzadeh, 2016, which is a fast-converging method inspired by the movements of flock of birds.

2.1.2. MULTI-OBJECTIVE OPTIMIZATION

A multi-objective optimization problem is defined by the presence of multiple objective functions to optimize. Most of the times these objectives are conflicting with each others, making the problem lacking of a unique optimal solution. Without losing generality, the optimization functions can all be considered to minimize (for objectives to be maximized, the same function with a negative sign can be minimized resulting in the same goal).

Following the description given by Konak et al., 2006, if J is the number of objectives and K is the number of variables, a minimization multi-objective problem can be defined as the problem of finding a vector $\mathbf{x}^* = \{x_1, x_2, ... x_K\}$ such that it minimizes the given set of objective functions $Z = \{z_1(x), z_2(x), ... z_J(x)\}$ inside a search space \mathbf{X} limited by some constraints and bounds on the K variables of the problem. Because of the conflicting nature of the objective functions, optimizing all functions at the same time is almost always not possible. This means that solutions resulting in optimal values for one objective may bring to unsatisfactory values for the others. Therefore, multi-objective optimization problems often result in a set of equally optimal solution, based on the concept of Pareto dominance.

Considering a minimization problem, a solution vector \mathbf{x} is said to dominate the solution vector \mathbf{x}' if $z_k(\mathbf{x}) \leq z_k(\mathbf{x}') \, \forall \, k = 1...K$ and if $z_k(\mathbf{x}) < z_k(\mathbf{x}')$ for at least one objective k. Similarly, the solution vector \mathbf{x} is said to be non-dominated if no other solution vector in the feasible search space \mathbf{X} dominates it. The set of all feasible and non-dominated solutions in the entire search space is referred to as Pareto Set, and their respective objective functions' values are called the Pareto Front. Figure 2.2 illustrates example Pareto Sets from the consulted literature, where the trade-off between three objective is visible.

Because of the absence of a unique solution for the problem, it is a task of the decision-maker to select the most appropriate from the Pareto Set. Alsayed et al., 2013 have compared the use of three different decision-making techniques and their performances when choosing between a three-objectives trade off: Weighted Sum Method (WSM), Technique for Order Preference by Similarity to Ideal Solution (TOPSIS) and preference ranking organization method for enrichment evaluation (PROMETHEE II). Both WSM and TOPSIS are based on the assignment of weights to the selected objectives and on ranking the solutions on the basis of their performances with respect to the weighted objectives. In addition to this, TOPSIS also compares the alternatives to two *ideal* solu-

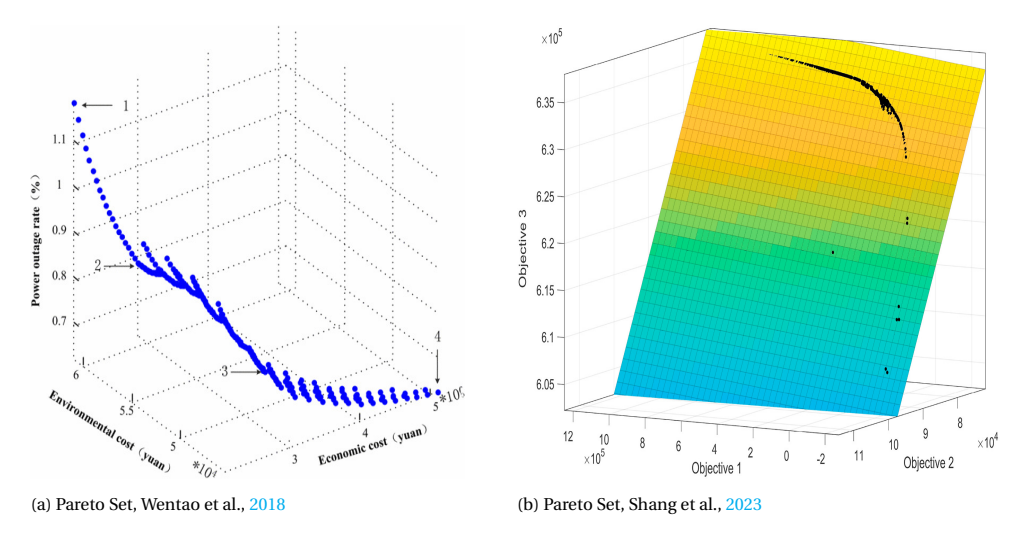


Figure 2.2: Examples of Three-Dimensional Pareto Sets from the Literature

tions and assigns the final score by looking at the relative distance of each solution from this ideal, as better detailed in 5.3.2. In a different way, PROMETHEE is based on comparing the solutions in couples, and sorting them according to a preference function.

Previous work have also opted for other selection methods, like Analytic Hierarchy Process (AHP), Criteria Importance Through Intercriteria Correlation (CRITIC) and Cumulative Prospect Theory. However, TOPSIS is by far the most applied in studies approaching similar problems to the one researched in this work and the most robust according to Alsayed et al., 2013. For this reason, it is implemented later in this work as well. This is detailed in 5.3.

2.1.3. GENETIC ALGORITHM

The Genetic Algorithm is inspired by Charles Darwin's evolutionary theory. Solution vectors in the feasible search space are called *chromosomes*, and their components (the optimization variables) are called *genes*. The algorithm performs its search for the optimal solution starting from an initial *population* of chromosomes, a set of randomly initialized vectors satisfying the bounds and constraints of the problem. According to the performances of a single chromosome with respect to the objective functions, a fitness value is assigned by the algorithm to every chromosome. The fittest elements are the ones with a lower score (in a minimization problem) and which have more probability to reproduce themselves. In fact, the GA is based on two main operators, called *mutation* and *crossover*, performed at every step (*generation*) of the algorithm.

Crossover consists in the generation of an *offspring* vector from two *parents* that are part of the initial population. By selecting the fittest chromosomes for the crossover operation, the algorithm makes sure that the best genes are passed to the offspring, so that

after a number of iterations the offsprings get fitter and fitter. On the other hand, the solution of the i_{th} generation should not be completely dependent on the initial population's vectors, otherwise the algorithm would incur in the risk of converging towards a local optimum of the problem without considering the whole search space. To avoid such problem, the mutation operation is applied to the offsprings, consisting in random variations applied at the gene level.

These two operations are determined by two parameters, called the Crossover Rate and Mutation Rate. The crossover rate determines the likelihood that any given pair of solutions will be selected for crossover, while the mutation rate determines the chance that any solution will be selected for random mutation. At each step of the algorithm, new feasible solution vectors are generated by means of the two operations, and a fitness value is assigned to them on the basis of their performances with respect to the objectives. Then, the initial population for the following step is updated with the fittest values of the offspring population, and the algorithm continues until a stopping criterion is met. The stopping criterion of the algorithm here employed is based on the *spread* of the objective functions' fitness, and explained below.

For the scope of this work, the MATLAB function *gamultiobj*, part of the Global Optimization Toolbox, is employed. This function is based on a variant of the well known Fast Non-dominated Sorting Genetic Algorithm (also called NSGA-II). An accurate description of its functioning is presented in the MathWorks documentation (The MathWorks Inc., 2023), but also described here for completeness. The algorithm is presented as a controlled elitist variant of the Genetic Algorithm. Elitist in the sense that it favours the fittest elements for reproduction in the next iterations, and controlled because it also favours solutions that help searching across the majority of the search space. In fact, after assigning a fitness value to the solutions of a certain population, these are ranked on the basis of dominance. Solutions with rank 1 are not dominated by other solutions, while solutions with rank 2 are dominated by rank 1 individuals, and so on.

To all the individuals in a certain population (remembering that each step of the algorithm is associated with its own population) *gamultiobj* also assigns a *Crowding distance* value, which is the sum of the distances in the objective functions space that a solution has with respect to all other solutions of its same rank. Solutions with the same rank and higher distance have more chances of being selected as parents for the following generation. In this way, the algorithm favours the search across the entire search space rather than only focusing on areas which are "densely populated" by solutions.

Each iteration concludes with the calculation of the *spread* in the population. With σ being the standard deviation of the crowding distance of all solutions, Q the number of solutions, d their average distance the factor μ is computed. This is defined as "the sum over the K objective function indices of the norm of the difference between the current minimum-value Pareto point for that index and the minimum point for that index in the previous iteration". Therefore, low values for μ correspond to small changes in the objective functions' values in the iterations, while low values for σ correspond to well

distanced solutions in the objective functions space. The spread is then obtained as:

$$spread = \frac{\mu + \sigma}{\mu + Qd} \tag{2.1}$$

And it is a measure of the relative change of the objective functions' values with respect to the previous iteration, and the variety of the solutions considered. The stopping criterion is met when the spread value is less than the average of recent iterations' spreads, and when the relative change in the value of the spread in the recent iterations is less then a certain tolerance value. The number of these recent iterations considered is set as 100 by default in MATLAB, while the default tolerance value is 10^{-4} . For the purpose of this application, these and other optimization parameters were modified, and their final values are later detailed in Table 5.2. A flowchart of the algorithm is visualized in Figure 2.3 for clarity purposes.

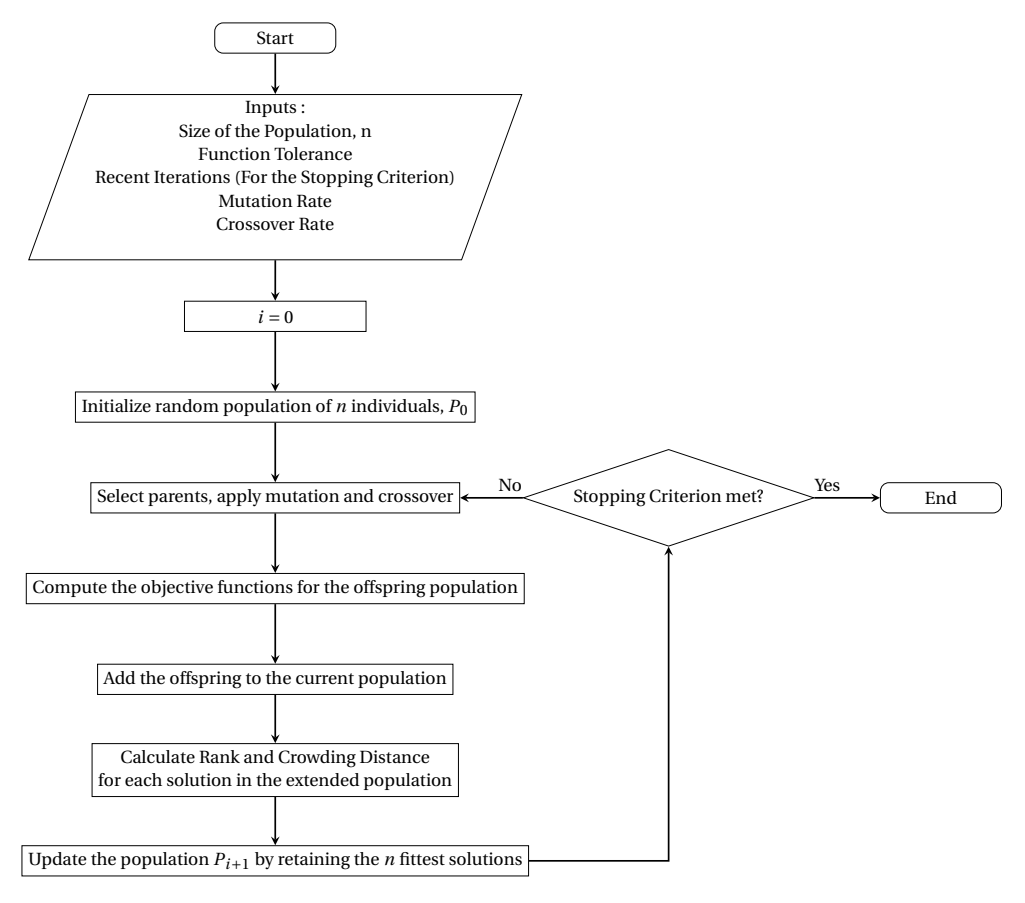


Figure 2.3: Flowchart of the Optimization Algorithm employed

2.2. PRICING MECHANISMS

2.2.1. ELECTRICITY RETAIL TARIFFS.

Extensive studies and reviews have recently focused on the evolution and analysis of electricity pricing mechanisms and their future directions, especially because of the fast development expected to happen in the energy infrastructure. Ryan et al., 2017 highlighted the necessity of adequate restructuring of electricity tariffs moving away from flat volumetric mechanisms, in favour of others that can promote energy efficiency and grid modifications. In their work, they analyze different retail tariffs and their effects on the aspects of renewable generation, demand response, energy efficiency and system cost recovery, also through the study of actual cases. According to the authors, most jurisdictions currently charge a fixed volumetric tariff (sometimes increased by a fixed amount) that does not take into account the amount of energy purchased and neither the time at which it is consumed. Therefore, energy efficiency is not incentivized if the price is low, because consumers could end up in purchasing more than it is socially acceptable. In their review of alternative pricing schemes, Time-of-Use (TOU) Pricing, which implies a distinction between peak and off-peak hours (or periods), is described as a blunter version of Real Time Pricing (RTP), in which prices will change on hourly or shorter timeframes according to the outcomes of electricity spot markets. This latter tariff's main drawback is that it may provide "too frequent and detailed price signals that consumers may not be equipped to engage", and is considered here to be suboptimal even though Nordic countries like Sweden have started implementing it.

Dutta and Mitra, 2017 focused on a review of different electricity pricing policies, with a particular focus on dynamic pricing tariffs. In addition to the mentioned Time-of-Use and Real-Time Pricing mechanisms, other tariffs are mentioned:

- Block Pricing, where consumers are charged at a flat rate per volume until a certain threshold, then switch to a higher price per volume until the next threshold and so on.
- Superpeak TOU and Critical Peak Pricing, variants of the Time-of-Use scheme with a shorter window for peak hours that guarantees a stronger price signal
- Seasonal Tariffs, according to which electricity is charged at higher rates in highdemand seasons and vice-versa

The paper also provides a comparison among the different policies introduced, and in particular on how the RTP scheme performs very good in terms of economic efficiency (because of the overall lowest bills payed by the consumers, and the ones that better reflect the actual value of the electricity purchased) and revenue stability for the utilities providing such power. Because of its fluctuating nature and dependence on spot market prices, however, this tariff is poorly performing with regards to bill stability, making it more risky for vulnerable customers which are exposed to frequent fluctuations that are difficult to predict. Besides stating that Real-Time-Pricing is the most complicated dynamic pricing scheme to implement, according to Shan et al., 2016 it is also the most direct and effective to stimulate mechanism to stimulate demand response. In particular, here the highlighted difficulty lies in the fast communication needed for the real-time

energy prices.

Aware of the main drawback regarding the application of Dynamic Pricing, especially if dictated by the spot market prices, Hammerstrom, 2022 proposes a method to harmonize such prizes, thus decreasing their tendency towards extreme variations while still preserving cost recovery for utilities and ensuring that clear price signals are launched to favour demand-responsive behaviors.

2.2.2. Grid Connection Costs

Apart from the costs related to purchasing electricity, grid-connected energy communities have (and will have to, with their expected future development) face costs related to their connection to the regional grid. For new projects, this is not an aspect of secondary importance: according to the Dutch Transmission System Operator Tennet, 2023, connection costs can range from 1.5 to 2.5 million $\[mathbb{E}$ for the most frequently occurring connections at low voltage levels. This aspect is of particular importance when the system not only wants to import, but also wishes to inject energy in the grid they are connected to.

In fact, in a recent report (ACER, 2023) the European Union Agency for the Cooperation of Energy Regulators recommended that, when consumers can both inject and withdraw energy from the grid, both uses should be considered when setting grid connection tariffs, which is not always the case as per today. As an example, in the Belgian region of Wallonia prosumers with a connected power up to 10 kVA are not charged injection fees among their connection tariffs. Similar regulations could represent a future incentive in investing in a smaller grid connection when planning distributed grid-connected energy systems.

In a future power infrastructure with a high penetration of Distributed Energy Resources (DER) and widespread bi-directional power flows with the grid network, it is more than likely that pricing schemes for distribution services will evolve as well. Among several options, Hledik and Lazar, 2016 have considered a demand charge based on the maximum instantaneous demand for electricity of the grid-connected users. In this way, according to the report's authors, fairness in cost recovery would be improved because this scheme would better reflect the peak-demand driven nature of distribution capacity investment. On the other hand, it is also mentioned that within the costs of distributed energy resources like energy communities: "to the extent that a customer participating in a demand response program can reduce its need for distribution capacity through a reduction in demand, the customer would simply avoid paying for a portion of the demand-related distribution capacity cost". Once again, the perspective of reducing the need for grid capacity could represent an economic benefit for consumers.

2.3. KNOWLEDGE GAP

Despite the extensive literature in support about the problem of energy systems and communities sizing, a knowledge gap was identified and it is within the scope of this thesis to provide insights about it. Over the studied references, the most relevant to the research questions approached in this work were sorted and analyzed, in particular the ones focusing on small and medium scale systems sizing by means of optimization algorithms. A table summarizing the highlights of these studies can be found in Appendix A.

This literature study has uncovered how the architecture of the systems (that is, the components of which they are composed) considered is extremely varied and location dependent. The 24/7 Energy Lab project under development in The Green Village is based on the usage of PV panels as a main source and the co-existence of batteries and an hydrogen system for short and long-term storage. The usage of different generation sources like wind turbines or diesel generators and other storage options obviously affects the studies' outcome. In particular, the mutual interactions of the two storage mediums here considered is often discarded in literature for residential systems applications, with most studies only considering one of the two options at the time.

An even more relevant influence on the process and the outcome of the sizing is given by the presence of a connection to the grid. As mentioned, a significant amount of studies focused on remote off-grid applications, thus not taking into account the possibility of interacting with the broader electricity network. This aspect has not only technical but also economical relevant consequences, which are not trivial to investigate because of the mentioned uncertainties about the future evolution of electricity and distribution network pricing schemes.

To the best of the knowledge acquired from existing literature, no system design have been carried out by combining these complexities, in particular taking into account at the same time:

- A system architecture composed of PV panels, batteries, and a hydrogen storagebackup system
- A Grid-connected system, interacting with the external network with bi-directional energy flows
- Varying conditions for the electricity prices, comparing a flat pricing with Real Time Pricing Tariffs (based on real spot market prices)

Lastly, it is worth to emphasize how this kind of work is extremely project-dependent, and thus relying on case studies referring to different geographical locations, consumption habits and needs in general can only be helpful to a certain extent. It is always necessary to tailor the study to one specific application in order to have reliable results. This work will specifically focus on the sizing of The Green Village Energy Community, without discarding more generical conclusions that may arise.

SYSTEM SIMULATION

The study carried out in this work started with a characterization of the system, in order to replicate its behavior and performances in a simulated environment. The scope of this chapter is to describe the modeling process of the system's components, and how these interact with each other to ensure coherent energy flows.

3.1. Components of the System

This section aims to describe the functioning of the system's different components. The system's architecture, already introduced in Figure 1.2, is reproposed below for clarity purposes. Technical characteristics like their input and output capacities and limitations will be presented together with operational and economic factors, providing a comprehensive overview of the elements of the system.

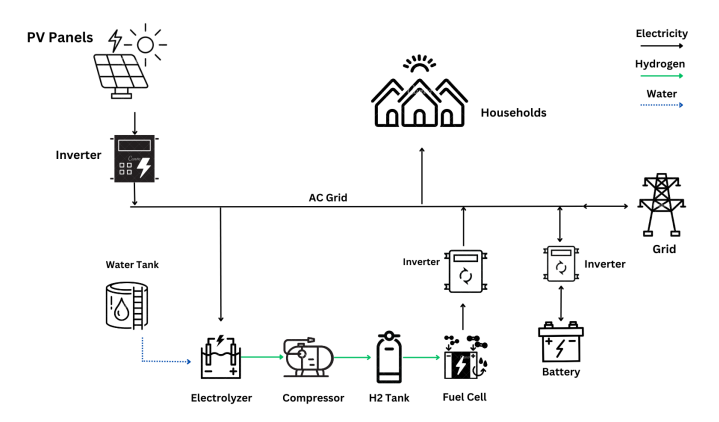


Figure 3.1: Graphic representation of the System Architecture

Parameter	Value	Unit
Rated Power	365	Wp
Open Circuit Voltage	49	V
Maximum Power Point Voltage	40	V
Short Circuit Current	9.6	A
Maximum Power Point Current	9.2	A

Table 3.1: Technical Characteristics of the Selected PV Panels

3.1.1. PV PANELS

The Photovoltaic panels represent the main source of electricity in the Energy Community under study. In this work, the panels selected are the Solo Lightweight 365 from the manufacturer ©Solarge, of which the major characteristics are reported in Table 3.1.

According to the technical data sheet provided by the manufacturer, these panels have a linear performance guarantee of 80 percent after 20 years of operation. In this work, 25 years of maximum operation have been considered, which was also selected as the total project lifetime. The cost for each of these panels is $260 \in$, and this cost is assumed to scale linearly with the total number of panels purchased.

The hourly electrical energy production from the PV panels was obtained with a model calculating the AC output based on meteorological data. In particular, the total irradiation on different tilted planes was calculated for the possible orientations in The Green Village, in order to find the optimal tilt for the modules, for each orientation.

The total irradiance on a tilted plane can be obtained with the sum of three different terms. More precisely, it can be expressed as the sum of the direct irradiance, the diffused irradiance and the albedo irradiance (Smets et al., 2016):

$$G = G_{dir} + G_{diff} + G_{alb} (3.1)$$

The direct irradiance is dependent on the Direct Normal Irradiance (DNI), which varies with the selected location and the position of the Sun. In fact, the Earth's movements throughout the year influence the component of the solar irradiance that directly hit the plane of the module. The Angle of Incidence, AOI, is defined as the angle between the normal surface to the tilted module and the incident direction of the sunlight, and it is calculated as:

$$AOI = \arccos(\cos a_M \cos a_S \cos(A_M - A_S) + \sin a_M \sin a_S)$$
 (3.2)

Where a_M and A_M are the altitude and the azimuth of the module, respectively indicating the module's tilt ($a_M = 90 - \theta_M$, with θ_M being the tilt of the module) and orientation. The factors a_S and A_S are the altitude and azimuth of the Sun at a given time. Because of the time-variance of these last two values, it was first necessary to calculate the position of the Sun at every hour of the day for the selected location through an external function. Thus, for every hour, the direct irradiance on the module was obtained as per 3.3.

$$G_{dir} = DNI \cdot \cos AOI \tag{3.3}$$

Secondly, the modules receive a diffuse component of irradiance, due to the scattering of solar light from the atmosphere. This component, G_{diff} , was computed with a function retrieved from the Sandia National Laboratories' PVLIB Matlab Toolbox (Stein et al., 2016), exploiting the model described by Reindl et al., 1990, and it's mainly dependent on the positions of the Sun and the modules, together with the DNI, DHI (Direct Horizontal Irradiance) and GHI (Global Horizontal Irradiance) components of the irradiance on the specific location.

The last term forming the incident irradiance is G_{alb} , indicating the light that is reflected from the ground. It is dependent from the reflectance of the terrain (the albedo, α) and the Sky View Factor, defined in 3.4:

$$SVF = \frac{1 + \cos\theta_M}{2} \tag{3.4}$$

$$G_{alb} = GHI \cdot \alpha \cdot (1 - SVF) \tag{3.5}$$

Once the general irradiance components (mainly DHI,DNI and GHI) were obtained through the ©Meteonorm software for the location of Delft, by knowing the hourly position of the Sun and the orientation of the panels it was possible to obtain the total irradiance on the tilted plane as per 3.1. In particular, the hourly irradiance was obtained with reference to data from the year 2020, for the three main orientations possible in The Green Village. These refer to the orientations of the buildings' flat roofs, the building's tilted roofs (2 different orientations) and the orientation of panels mounted on the ground, which are aligned with the flat roofs.

The panels are assumed to be installed with a tilt of 15°, and with a row-to-row spacing of 0.7 meters. Such configuration is not the optimal in terms of energy gain, for which a higher tilt, e.g. 30° for the flat roofs mounted in a southerly direction, would have been more effective. However, the choice of the configuration lies on considerations about typical installation tilts in The Netherlands (de Vries et al., 2020), where the strong winds in winter make low tilts more effective for the stability of the modules. Moreover, this configuration is the same used in a report by Zhou et al., 2022, where the maximum potential PV panels penetration in The Green Village was assessed. Such study was also used in this work to set the maximum number of panels in every area as an upper bound for the optimization.

The irradiance incident on the plane of the module is finally used to obtain the DC output of the modules. Taking into account their rated power under Standard Test Conditions irradiance ($1000 \ W/m^2$), this can be estimated with :

$$P_{PV,DC} = P_{STC} \cdot \frac{G}{G_{STC}} \tag{3.6}$$

Parameter	Value	Unit
Usable Energy	15.36	kWh
Max. Cont. Output Current	250	A
Peak Output Current	375	A
Nominal Voltage	51.2	V
Operating Voltage	40-57.6	V
Round Trip Efficiency	95	%
SoC Limits	15-90	%
Depth of Discharge	75	%
Cost	6000	€

Table 3.2: Selected Batteries Technical Characteristics

Which is valid for one single module placed in that particular configuration. For each orientation, such output is then multiplied by the number of modules to be placed with a certain orientation as per the optimization's results.

3.1.2. BATTERIES

The batteries selected for this work are the ones currently in use, on a smaller scale, at The Green Village. These are the ©BYD Battery Box Premium, based on Lithium Iron Phosphate (LFP) technology and coupled with external ©Victron Multiplus II Inverters. As per the manufacturer's technical Data sheet, these batteries have a 10 year warranty. Again, for conservative reasons a life span of 8 years was considered for this application.

The maximum depth of discharge is not indicated, but some limitations on the maximum and minimum SoC still apply. In fact, in accordance to the state-of-the-art for similar applications, the maximum Soc was selected to be 90 percent, while the minimum was set to be 15 percent, achieving a maximum depth of discharge of 75 percent. While the minimum SoC is fixed, the cycling of the battery depends on the threshold State of Charge selected as an optimization variable, determining the switching from the discharge of the batteries and the activation of the fuel cells in case of deficit.

The input and output power capacity of the battery is also dependent on the rate, hence the velocity, at which these are charged or discharged. According to the manufacturer's indications, the total usable energy of 15.36 kWh was exploitable with a depth of discharge of 100 percent, at a temperature of 25° and at a C-rate of 0.2C (with this C-rate, the battery would be completely discharged in in a time frame of $0.2^{-1} = 5$ hours). By assuming that charging and discharging of the batteries would occur at the same rate and that the batteries would operate at a fixed voltage of 48V, the input and output limit power is imposed as 3.7:

$$Power = Voltage \cdot Current \tag{3.7}$$

With a maximum energy of 11.25 kWh (75 percent depth of discharge), the battery completes a full discharge cycle in 5 hours with a current of 46.875 A. With this current, the

charge/discharge power of a battery is taken as 2.25 kW, then multiplied by the total number of batteries to obtain the total limit power.

The batteries are the first component activated in case of surplus production from the PV panels, exceeding the load demand. In these cases, the batteries are charged. The rate at which this occurs depends on both the state of the battery and the amount of surplus produced. If the batteries can accommodate all the surplus, these will be charged with the corresponding power, provided this is lower than the limit power. The energy stored in the batteries is then updated:

$$E_{bat}(t) = E_{bat}(t-1) + min(P_{PV,DC} \cdot \eta_{inv} - L(t); P_{bat,max}) \cdot \eta_{bat} \cdot dt$$
 (3.8)

If the surplus is so big that it would exceed the batteries' charging limits, then the maximum possible energy will be used for the charge :

$$E_{bat}(t) = E_{bat}(t-1) + min\left(E_{bat,max} - E_{bat}(t-1); P_{bat,max} \cdot dt\right) \cdot \eta_{bat}$$
(3.9)

In the discharge mode, the behavior of the batteries is opposite to the one just described. When they are prioritized over the fuel cells, they are the first component providing the missing power from the PV. If the energy stored is enough to provide all the required load, they are discharged at the necessary rate:

$$E_{hat}(t) = E_{hat}(t-1) - min(L(t) - P_{PV,DC} \cdot \eta_{inv}; P_{hat,max}) \cdot 1/\eta_{hat} \cdot dt$$
 (3.10)

Otherwise, they are discharged until their lowest limit, exploiting all the energy available at the moment:

$$E_{bat}(t) = E_{bat}(t-1) - min\left(E_{bat}(t-1) - E_{bat,min}; P_{bat,max} \cdot dt\right) \cdot 1/\eta_{bat} \tag{3.11}$$

The same holds for the cases in which discharging the batteries is evaluated as secondary to the activation of the fuel cells to supply additional energy. The only difference, in this case, is that the second term of equation 3.10 would take into account the energy already provided by the hydrogen backup system.

Whatever the input or output in the batteries, the State of Charge is always updated as per 3.12

$$SoC(t) = \frac{E_{bat}(t)}{E_{hat.max}}$$
(3.12)

3.1.3. ELECTROLYZERS

The electrolyzer selected for this application is from ©Enapter, model EL 4.0, based on an Anion Exchange Membrane technology and working with AC current. The electrolyzer is activated in cases of overproduction from the PV panels, either when the batteries are fully charged, or when their charging limit power has been reached. Its technical features are summarized in Table 3.3.

Parameter	Value	Unit
Hydrogen Production Rate	Up to 1.0785	kg/ 24h
Output Pressure	Up to 35	bar
Hydrogen Output Purity	99.9 at 35 bar	%
Operative power consumption	2.4	kW
Peak power consumption	3	kW
Heat Dissipation	0.6	kW
Water Consumption	420	mL/h
Cost	9000	€

Table 3.3: Techincal Specifications of the Electrolyzer

According to the manufacturer, the expected lifetime of this electrolyzer is more than 35000 hours of operation, corresponding to around 4 years of continuous operation. In this work, the lifetime for this component was considered to be an indicative 8 years, with this choice being probably conservative as the electrolyzers will almost surely be operative for less than half of the time during a whole year. Moreover, in order to ensure a prolonged life, in the user manual it is indicated to limit the intermittent operation of the electrolyzer, and operate it in a steady way as much as possible. In particular, no more than 5 on/off cycles per day and 1 on/off cycle per hour shall be performed, and these conditions are taken into account in the model.

Furthermore, the electrolyzer is subject to ramping limitations. The ramp-up time depends on the electrolyte temperature, and it is lower with low temperatures. Enapter indicates that " starting the device with an electrolyte temperature of e.g. 25 °C it will take about 30 min to be fully operational and perform at its maximum efficiency at 55 °C". Because the time-resolution of the model in this work is hourly, it was considered that in the first hour of operation of the electrolyzer would produce hydrogen at a maximum reduced rate of 80 percent of the nominal capacity. The electrolyzer also has a defined operating range, and its minimum input power is equal to 60 percent the rated power.

If the excess power at timestep t is higher than the minimum power inlet in the electrolyzer, this is started according to 3.13

$$E_{EL}(t) = min(P_{PV,DC}(t) \cdot \eta_{inv} \cdot dt - L(t) - E_{char}(t); P_{elec\ max} \cdot dt)$$
(3.13)

Where $E_{char}(t)$ is the energy employed to charge the batteries at time t, as described in the previous section.

3.1.4. FUEL CELLS

Fuel cells are employed as a backup generator when the power provided by the PV panels is not sufficient, and the batteries have low energy at their disposal or have already reached their discharging limits. The Green Village is employing Polymer Electrolyte Membrane (PEM) fuel cells from ©Nedstack, model FCS 7-XXL, which were also selected

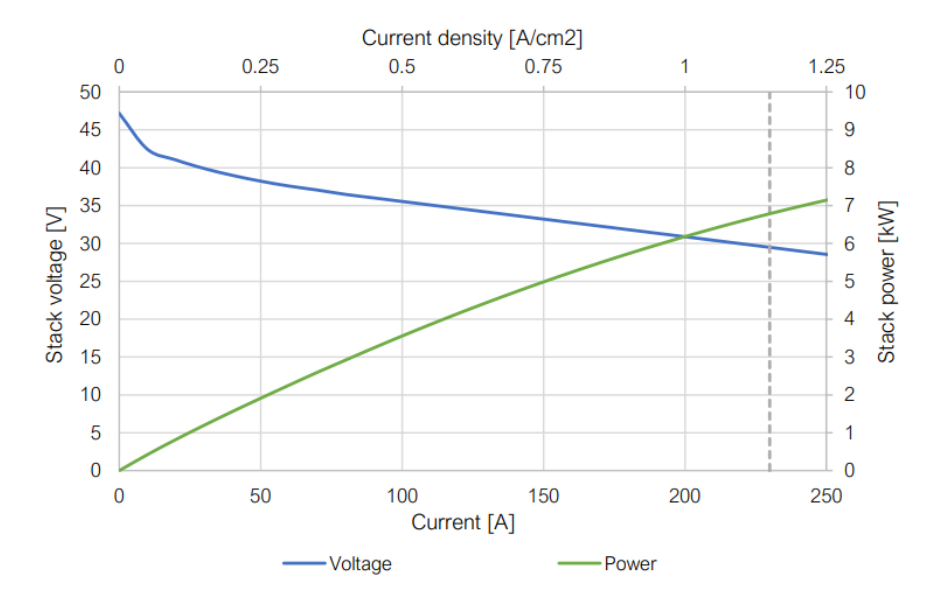


Figure 3.2: Beginning-of-life stack performance at reference conditions, @Nedstack Fuel Cell Technology

in this research.

Through the Technical specifications provided by the manufacturer, it was not possible to retrieve info about the ramping constraints of the fuel cells. It was therefore assumed that within the first hour of operation, the fuel cells would only be able to provide half of their nominal output. After the start up phase, PEM fuel cells can provide a flexible power output (Nikiforow et al., 2018 have achieved a ramp-up from 2 to 3.7 kW in less than 1 second), therefore no additional ramping constraints were considered in this work. Since they generate electricity in direct current, the fuel cells are coupled with a @Victron Multiplus II inverter.

Like the electrolyzer, the lifetime of the fuel cells is assumed to be 8 years. The operating conditions of the stacks can vary, following the Voltage-Current curve in Figure 3.2. Other technical specifics are shown in Table 3.4.

Parameter	Value	Unit
Rated Power	6.8	kW
Voltage Range	29-47	V
Current Range	0-230	A
Number of Cells	48	-
Maximum Hydrogen Consumption	77	Nl/min

These components are activated to supply additional energy to the load in case of deficit. Their output is not only limited by the fuel cells' own characteristics, but also by the availability of the hydrogen used as a fuel. Assuming that the fuel cells always operate at the maximum hydrogen consumption rate indicated by the manufacturer, the fuel cell would consume approximately 0.05 kg of hydrogen per kWh of electricity produced. This value has been introduced in the model as the fuel cell specific consumption.

When the fuel cells are used as the last backup source, after depleting the batteries, they provide as much energy as possible to fulfill the load requirements:

$$E_{FC}(t) = min\left(L(t) - P_{PV,DC}(t) \cdot \eta_{inv} \cdot dt - E_{disch}(t); P_{FC,max} \cdot dt\right) \cdot 1/\eta_{inv}$$
(3.14)

Where, in 3.14, E_{disch} is the amount of energy provided by the discharge of the batteries. The operation of the fuel cells, as mentioned, may be limited by the availability of the fuel. In these cases, the fuel cells exploit all the available hydrogen, even if this cannot provide for all the remaining load:

$$E_{FC}(t) = min\left((LOH(t-1) - LOH_{min}) \cdot 1/SC_{FC}; P_{FC,max} \cdot dt\right) \cdot 1/\eta_{inv}$$
(3.15)

Where LOH is the level of hydrogen present in the tanks, expressed in kg, and SC_{FC} is the hydrogen specific consumption of the fuel cells expressed in kg/kWh.

3.1.5. OTHER COMPONENTS

Apart from the main components just described, several additional pieces of equipment are necessary for the system to be fully operational.

The PV panels produce electrical energy in the form of direct current, which has to be switched to alternating lurrent through the use of an Inverter. The modeling of the inverter's characteristics and working mechanism is out of the scope of this work, but for the scope of this application it was selected to employ the ©Solaredge SE5K Inverter, already available at The Green Village. According to the manufacturer's indication, the maximum power in Standard Test Conditions that this Inverter can support is 6.75 kW. Therefore, by coupling it with the selected panels, it was assumed that a maximum of 18 panels can be coupled to each inverter. In order to have a precise estimate of the costs of the inverter (considering the scale of the system) a study from TU Delft's PVMD Group for the INNOZOWA floating solar park was considered. The cost for the inverters can be estimated with a polynomial fit of the kind:

$$f(x) = p_1 \cdot x + p_2 \tag{3.16}$$

Where x is the target kWp installation, and f(x) represents the inverse cost in W/ ϵ . For the ©Solaredge inverters coupled with a power optimizer, $p_1 = 0.0753$ and $p_2 = 1.939$.

The hydrogen storage also requires ancillary equipment. Upon the hydrogen is produced with the electrolyzer, it needs to pass through a compression step to be stored

in the tanks at a pressure of around 400 bars. The compressor selected for this application is the Skid model from ©HyEt Hydrogen, a Dutch company that is partner of The Green Village. Some technical features about the compressor are summarized in Table 3.5.

Table 3.5: Selected Compressor Technical Characteristics

Parameter	Value	Unit
Throughput	2	kg/day
Input pressure	3-200	barg
Output pressure	0-410	barg
Power consumption	0.7	kW
Price	300	€

Compressed hydrogen is then stored in appropriate tanks. The total capacity for the hydrogen storage, expressed in kg, is also one important factor influencing the behavior of the whole system, and its maximum degree of self-sufficiency from the grid. For this reason, the total storage capacity is one of the optimization variables of the problem. The estimated cost for the hydrogen storage tanks is $200 \, \text{€/kg}$ (N. Li et al., 2023).

Also the fuel cells and the batteries need an inverter to be fully operational within the system. The ©Victron Multiplus II was selected to be coupled with such components.

3.2. ENERGY MANAGEMENT

After detailing the behavior of each component of the system, it is necessary to integrate them together in order to distribute the energy flows at every moment. The system detailed in this work is governed by an energy management strategy, mainly dependent on the instantaneous mismatch between load requirements and energy production from the PV panels. The energy management strategy is integrated in the Optimization formulation as described in 5.2.

The function describing the energy management is based on a hourly timesteps resolution. For every timestep t, it calculates the hourly difference between the PV production and the load, Based on the Irradiance data and the number of PV panels. If the production from the PV panels exceeds the load, the system is in Surplus status. Else, the status is a Deficit, as shown in Figure 3.3.

In case of surplus from the PV, the battery is charged first. Then, the electrolyzer is activated if some spare energy is still available, and finally energy is exported to the grid in case of excessive overproduction. Throughout the surplus mode, the capacity limits of the energy storage must be always respected. For example, if one of the storage systems cannot host all the energy left (i.e. the batteries or the tanks are already almost full), they get first completely filled and then the excess energy is utilized for the following operation in the line. Figure 3.4 schematically shows the functioning of the Surplus mode.

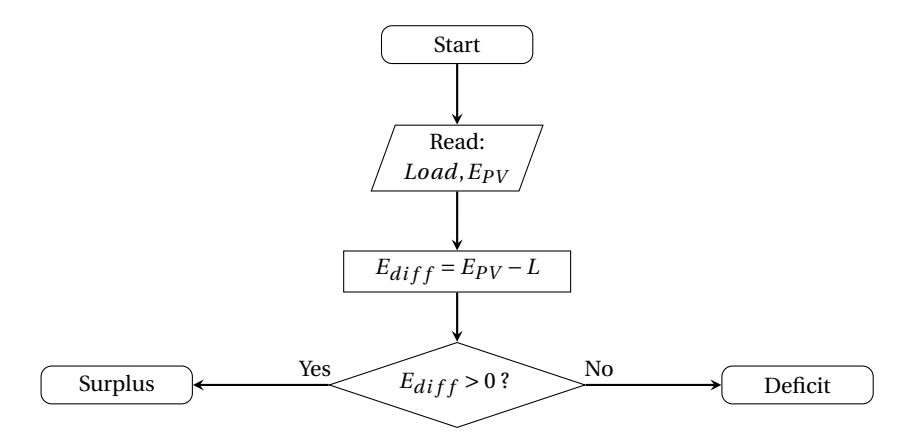


Figure 3.3: First Evaluation of the Energy Management Strategy function

Before charging the batteries, the overall SoC is checked, as it is similarly done with the level of hydrogen before powering the electrolyzers. It is also worth to notice that the energy dispatch (both in Surplus and in Deficit mode) is always subject to the components' input and output power limitations. As it can be seen from the flowchart in Figure 3.4, the batteries are either charged to store the whole surplus (if the remaining capacity allows to do so) or at maximum charging power. The same holds for the electrolyzers, which are either activated at a power level capable of converting the whole remaining surplus to hydrogen or at their nominal power rate. Power limitations also hold for the energy that is exchanged with the grid. In Surplus mode, when the excess energy overtakes the maximum exportable to the outer grid, part of the produced energy is dumped.

In case of deficit production form the PV, the system has two alternative behaviors. In fact, the missing power can be either provided by the fuel cells or by the batteries. This choice is determined by the instantaneous level of the batteries' state of charge and by the threshold level of the selected solution. The battery is prioritized when its SoC is high enough (that is, when it is above the threshold): in these cases, the batteries are used as the first backup source, and discharged to supply to load. When the remaining capacity in the battery is not sufficient, or when the discharge power limit is reached without fully providing the load, the fuel cells are switched on and employed to supply the remaining energy. Should the combined inputs of all these sources be insufficient, the remaining energy would be withdrawn from the grid.

Conversely, if the SoC of the batteries is below the threshold level during a Deficit situation, the "Fuel Cells First" strategy is adopted (Figure 3.5). The primary source of backup for these cases would be the fuel cells, exploiting the hydrogen produced for long-term storage purposes and to prevent the batteries to be completely depleted. In fact, the batteries would only be employed if the fuel Cells are not able to fulfill the remaining demand, because of either power or capacity limitations. Also in this case, the system makes use of the grid as the last option to supply the load.

When the deficit is so large that the selected equipment is not able to fulfill it entirely, the other is activated. Power will be imported from the grid if the storage systems are depleted. Also in the deficit cases, the operation is subject to limitations from the components that make the priorities and switching among the components more complex. For example, the fuel cells can be activated even if the SoC of the batteries has not reached its lower limit, but they cannot provide enough energy because of output power limitations.

Like in the previous case, also in Deficit mode the connection to the grid presents some capacity constraints. The loss of Power Supply is in fact a direct consequence of this limitation, because after deploying the system's storage the load cannot be met when the energy imported from the grid reaches the maximum imposed value and not all the demand is satisfied. In these cases, the difference between load and the energy inputs in the system is accounted for as Unmet Load (UL), as can be seen also in the schematic of Figure 3.6.

The behavior of the system in Deficit mode is influenced by the results of the optimization itself. The higher the threshold SoC selected by the algorithm for a certain solution, the more frequently the "Fuel Cells First" strategy will be employed, resulting in the need for a larger number of fuel cells and electrolyzers in that particular solution.

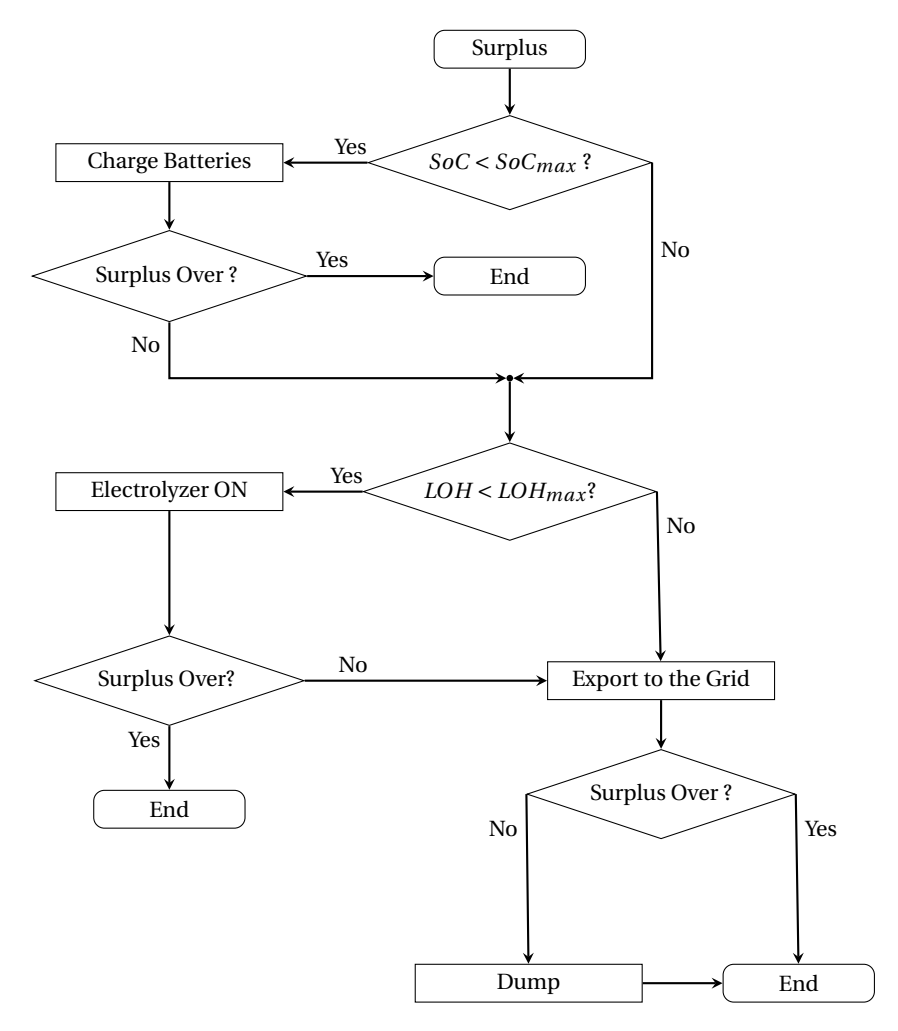


Figure 3.4: Energy Management in Surplus Mode

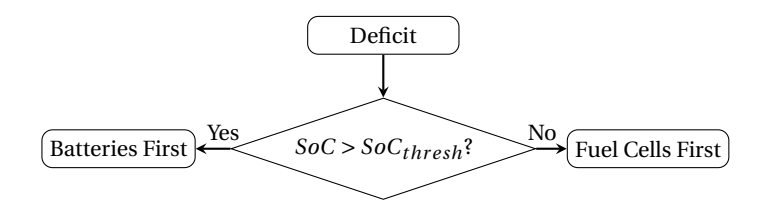


Figure 3.5: Priority Choice in case of Deficit Energy

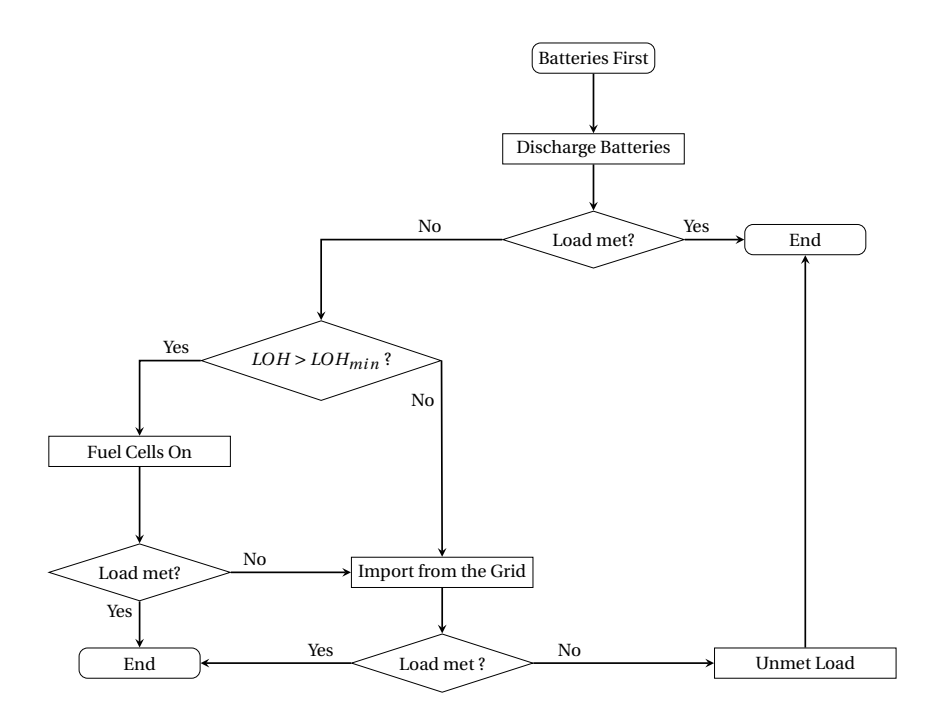


Figure 3.6: Energy Dispatch in the "Battery First" Mode

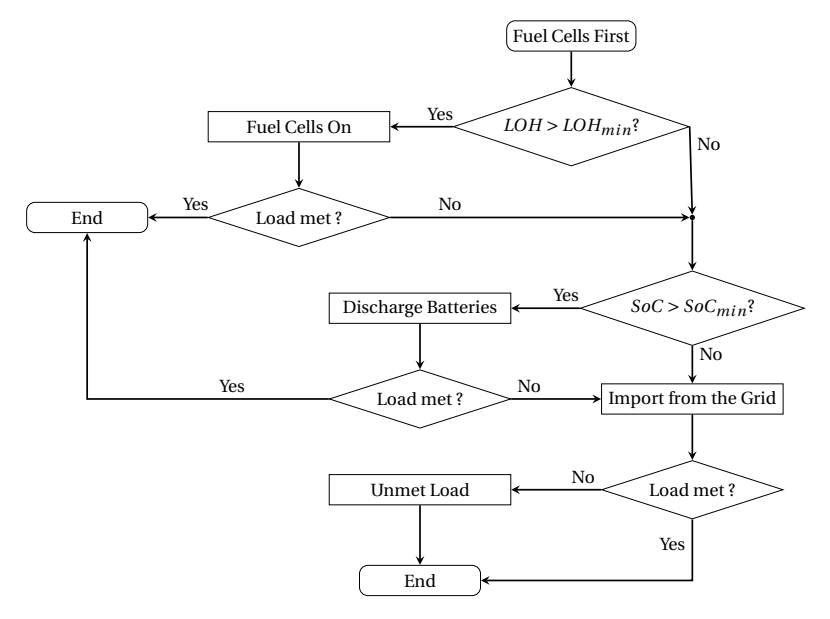


Figure 3.7: Energy Dispatch in the "Fuel Cells First" Mode

4

INPUT DATA

The scope of this chapter is to describe the input parameters of the model describing the Community's behavior and its optimization. The system's simulations are based on fixed input data, serving as a basis to obtain the results which are dependent on the final values of the optimization variables. Such input data are the irradiance data, thanks to which the energy produced from the PV panels is calculated, the load data representing the Community's electricity demand to be satisfied by the optimized system, and the Price data for the electricity exchanges with the outer grid, impacting on the economics of the community.

4.1. SOLAR IRRADIANCE

In section 3 the modeling of the PV energy production was described, and the irradiance calculation on a tilted plane was shown. The final irradiance per square meter on the tilted plane considered was obtained for a time period of one year as per equation 3.1. Thanks to the ©Meteonorm software, the data for the DHI,DNI and GHI were retrieved for the full year of 2019, and used to obtain total irradiance.

As previously mentioned, more than one orientation was taken into account. In a clockwise reference systems where North is at 0°, the flat roofs in The Green Village have an orientation of approximately 153°(southerly-oriented), while the tilted roofs have orientation of 75° (easterly-oriented) and 255°(westerly-oriented). Furthermore, the possibility to place some panels on the ground in some so-called 'free-spaces' was considered, and such panels are considered to have an orientation of 180°, exactly towards South.

Since no preference has been assigned for the placement of PV panels in an area over another, the algorithm will most likely select the orientation with the highest potential first, and fill them to their limit, before selecting to place in other areas. Figure ?? shows the annual irradiance for reference year 2019 on a 15° tilted plane in the four investigated orientations. Despite the similar peak values, it can be noted how the two orientations of

36 4. INPUT DATA

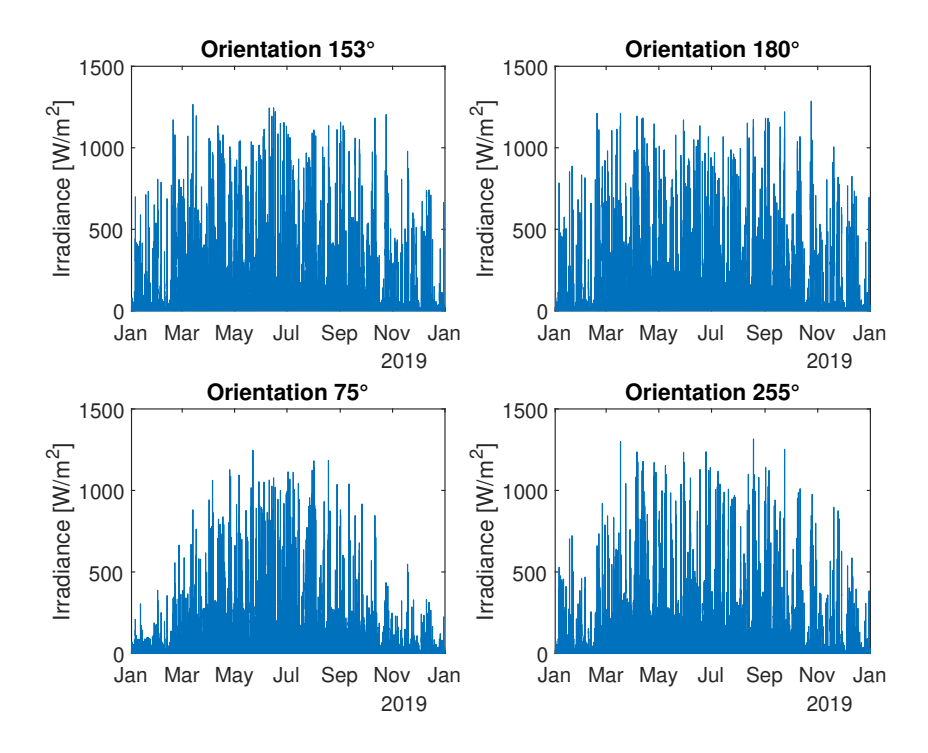


Figure 4.1: Annual irradiance on a 15° tilted plane in the different orientations

the flat roofs (153°) and the ground-mounted panels (180°) have a higher performance, particularly in the winter months. It is therefore no surprise that some solutions will only employ panels with such orientation, discarding the last two.

4.2. LOAD DEMAND

Together with the irradiance data used to obtain the solar production, the very first input to the model is the electrical energy demand of TGV's Energy Community. In total, the load from 8 houses was considered, each occupied by a maximum of 2 households. Such data needed some pre-processing, mostly to uniform their resolution and fill some minor gaps (up to 15 days).

In order to fill the gaps, a method intended to preserve both daily and seasonal variability was employed. Whenever a certain amount of data was missing, two or more reference sets from the available data were selected, from the same seasonal period of the missing ones (e.g. if a week in February was missing, the reference periods would be a week in January and another week in February). From the reference sets, the average consumption at each hour was extracted, and a normalized daily profile was obtained. The normalized profile was then multiplied by a vector of random factors, so that the scale of these consumption would be similar to that of the available data around those,

4.2. LOAD DEMAND 37

but different each day.

Out of the 8 houses, 3 of them resulted in having non-consistent data because of large gaps and faults in measurements. Since all the houses have similar characteristics (in particular for what concerns the number of people occupying them) it was decided to rely on the 5 houses for which the data was consistent, and add the missing parts of the load by scaling up the 5-houses aggregate load by a factor 8/5.

Another issue to be solved consisted in the unification of such data, with respect to their resolution and the total period considered. The single houses' consumption were collected in different periods over time, and with different metering appliances. While some data was available with a per-minute resolution, other houses only had a 15-minutes or hourly resolution. The final choice was to unify the demand dataset with a 1-hour resolution, also used for the simulations nested in the optimization algorithm. Of course, a shorter timestep would have allowed for higher precision, but on the other hand it would have brought to inevitable uncertainties and inaccuracies for the fitting of longer resolution data. Lastly, the most consistent period in terms of data availability was identified in 1 year, from February 19, 2021 until February 19, 2022.

The reference houses are completely electrified, and therefore the heat demand was not taken into account in this study. For privacy reasons the profile demands of the single houses cannot be shown separately. However, the cumulative load is depicted in Figure ??. Seasonal patterns can be easily identified, by focusing on the differences of both the peaks and medium consumption in the cold and warmer months. In particular, the start of the month of March presents the very high peaks, with the consumption starting to decrease in spring and reaching its lowest levels during the summer. Towards the end of the month of October, consumption levels start to rise again (due to the usage of electric heating) and later stabilize until the end of February, with the only exception of the holiday period straddling the beginning of January.

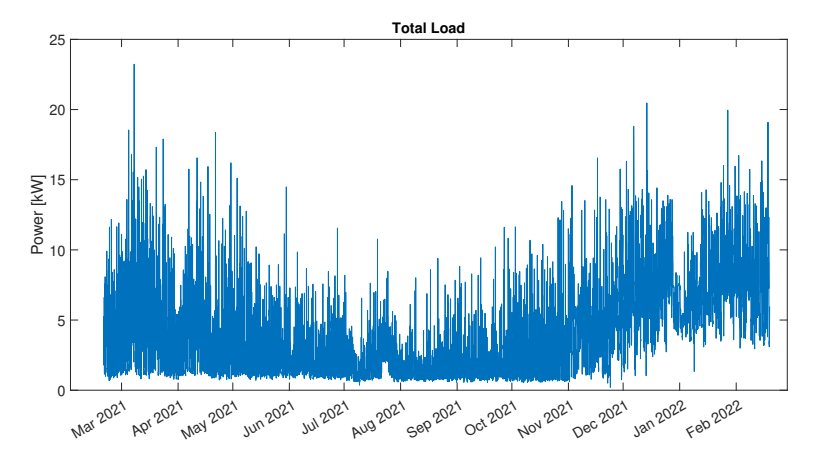


Figure 4.2: Total Electric Load

38 4. INPUT DATA

4.3. ELECTRICITY PRICES

For the calculation of the cost minimization objective, the model makes use of an input vector of hourly electricity prices, which changes throughout the scenarios analyzed. The first reference analyzed for such prices is the ENTSO-E Transparency Platform, 2023, from where it was possible to access The Netherlands' spot market's day-ahead prices for the years 2021 and 2022, shown in Figure 4.3. Here, negative prices were neglected and set to zero, since this occurrence is unlikely when the electricity is actually sold to end-consumers.

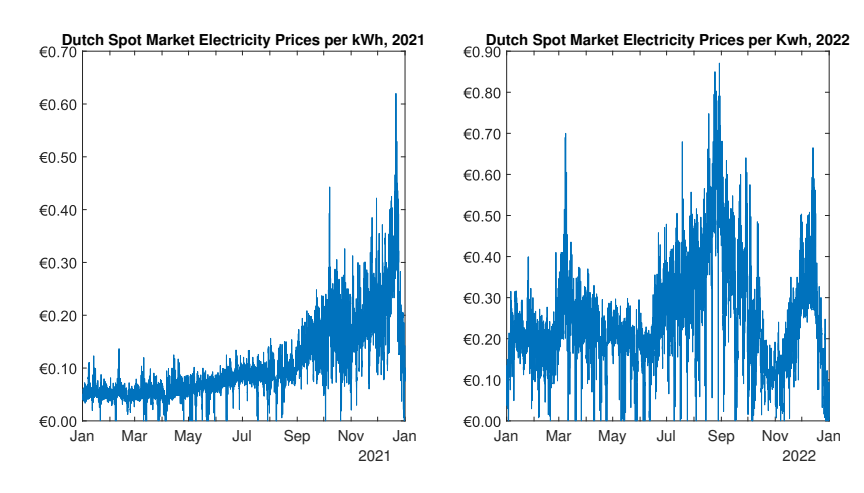


Figure 4.3: Day Ahead electricity prices in 2021 and 2022

Such data has the advantage of having a high resolution of 1 hour for every year, reflecting the evolution of transaction in the spot market. The behavior of the spot market prices is significant in showing the gradual increase in the mean price in 2021, followed by the extreme oscillations occurred in 2022 due to the energy crisis after Russia's invasion of Ukraine. These prices, however, are not entirely representative of the prices payed by the end consumers. In fact, taxes and levies are not considered and neither are additional factors, like distribution and network costs.

To take into account these factors, another reference was considered. The CBS database (Centraal Bureau voor de Statistiek, 2023) provides, among the other data, a breakdown of quarterly an annually average electricity prices from the year 2007, divided into transaction, delivery and network prices and including taxes. Unlike the generic spot market data, the prices retrieved from CBS are specific for the households class consuming less than 5 MWh per year. Table 4.1 provides an overview of the average electricity price breakdown over the last 10 years:

For the Base Case simulations, in which the tariffs are considered to be flat, the price considered was the average household electricity price over the last 10 years, equating to 0.33 €/kWh. The variable pricing case considered hourly-varying prices. For this case,

Table 4.1: Average Household Electricity Price Breakdown for the years 2012-2022. Prices in €/kWh, source Centraal Bureau voor de Statistiek, 2023

Year	Transaction	Delivery	Network	Total Price
2012	0.186	0.118	0.068	0.372
2013	0.19	0.118	0.072	0.38
2014	0.182	0.112	0.07	0.364
2015	0.192	0.126	0.066	0.384
2016	0.161	0.094	0.066	0.321
2017	0.156	0.091	0.065	0.312
2018	0.171	0.104	0.067	0.342
2019	0.205	0.136	0.069	0.41
2020	0.139	0.068	0.072	0.279
2021	0.134	0.057	0.076	0.267
2022	0.105	0.029	0.076	0.21

the input prices used refers to spot market prices in the year 2022. Despite not completely reflecting the price payed by the end consumers, this represents the best reference for a Real Time Pricing Scenario, the purpose of which is precisely to provide price signals on the basis of the spot market behavior.

5

OPTIMIZATION

To solve a complicated problem like the one under study in this project, the use of computational tools like Artificial Intelligence-based algorithm appears of particular relevance and usefulness. The literature review has highlighted how meta-heuristic evolutionary algorithms have been widely used to solve sizing and planning problems related to the energy sector, and for this reason one of those was used in this project as well. In particular, in this study a variant of the Multi-Objective Genetic Algorithm was implemented through a MATLAB code. This section aims to provide a description of the optimization process, from the formulation of objectives, variables and constraints to the actual implementation and the choice of the optimal solutions within the final Pareto Set.

5.1. OPTIMIZATION PARAMETERS

5.1.1. OBJECTIVE FUNCTIONS

The scope of this section is to describe the formulation of the three objective functions of the optimization problem. Because of their conflicting nature, optimal performances with respect to one of the three comes at the expenses of at least one of the remaining. The selection of these three objectives is based both on studies on similar systems through the literature review, and on the specific needs of the Energy Community under study for this project. After a consultation with the advisor from The Green Village, the following objectives were selected:

1. Annualized Total Cost Minimization:

Economic benefit is one of the most important drivers for the development of energy communities. Ideally, the whole cost sustained by the participants should be lower than the one they would incur in if they were to satisfy all the demand from the main grid. Because of other advantages related to the Energy Community, slightly higher costs might be acceptable, within certain limits. The Annual-

42 5. Optimization

ized Total Cost to minimized is thus defined, of which the single components will be analyzed:

$$minATC = C_{cap} + C_{rep} + C_{O\&M} + C_{grid_{IMP}} - C_{grid_{EXP}}$$

The capital cost is the investment cost payed to purchase the necessary system's components and make the system operational. It is given by the sum of the cost for a single component, C_k , times the number of components needed, N_k . Since the initial investment is made to ensure a project over a certain lifetime, it is necessary to take into account the time-value of money in this analysis and calculate the annualized investment cost, i.e. the annual cost that, for the duration of the project's lifetime, has to be payed in order to recover the initial investment. Hence, the Annualized Capital Cost also depend on the Capital Recovery Factor, CRF.

$$C_{cap} = \sum_{k=1}^{K} C_k \cdot N_k \cdot CRF \tag{5.1}$$

The replacement costs take into account the lifetime of the single components with respect to the total project's lifetime. Since the PV panels are the components with the longer lifetime (25 years), the total lifetime of the project is considered to be equal as the one of the panels, and hence they do not need any replacement during the project's lifespan. Equation 5.2 takes into account the necessity to substitute the batteries, electrolyzers and fuel cells at the end of their lifetime, which is 12,12 and 8 years respectively. In the equation, r, k indicates the number of replacements of component k during the project's lifetime, and l_k is the lifetime of component k (Baghaee et al., 2017).

$$C_{rep} = \left(\sum_{k=1}^{4} C_k \cdot \sum_{r,k}^{R} \frac{1}{(1+i)^{r,k} \cdot l_k}\right) CRF$$
 (5.2)

As mentioned, both previous equations are used to obtain annualized costs taking into account the total project's lifetime and the time-influence on money. To do so, they both contain the Capital Recovery Factor:

$$CRF = \frac{i \cdot (1+i)^{l}}{(i+1)^{l} - 1}$$
 (5.3)

Where I is the total project lifetime and I is the annual real interest rate, depending on the inflation rate and the nominal interest rate. In this project, the real interest rate is 5 percent, which is an indicative value on the basis of the reviewed literature on similar projects.

Under the assumption that Operation & Maintenance costs and the prices for electricity increase over time with the same rate as the general prices, there is no need

to take into account the time-value of such costs, and therefore no need to consider the CRF for these costs components. The annual O&M costs are assumed to be equal to 20 percent of the investment costs, regardless the component. Therefore, they can be formulated as follows:

$$C_{O\&M} = \sum_{k=1}^{K} 0.2 \cdot C_k \cdot N_k \tag{5.4}$$

Lastly, the total cost of importing power from the grid and the total profit gained by selling power to the main grid are considered in the last two terms of equation 1:

$$C_{grid_{imp}} = \sum_{t=1}^{T} P_{imp,t} \cdot E_{imp,t}$$
 (5.5)

$$C_{grid_{exp}} = \sum_{t=1}^{T} P_{exp,t} \cdot E_{exp,t}$$
 (5.6)

Where $P_{imp,t}$ and $P_{exp,t}$ are the prices for importing and exporting power during the timestep t, expressed in \in /kWh and $E_{imp,t}$, $E_{exp,t}$ are the amounts of energy imported and exported during the timestep t, in kWh.

2. Grid Dependence Minimization

The Energy Community is equipped with its own power production and storage sources, and one of its major goals is to be as much independent as possible from the main grid. By aiming at maximum self-sufficiency, the system would not only make the most out of its self-produced energy, but can also relieve the grid under stressful conditions. The Community's main energy source is composed by the solar panels, of which the excess energy is then stored either through the batteries or in form of hydrogen, through the electrolyzer. Not all the energy produced by the PV panels, however, is effectively exploited as an input to the system: when the overproduction also exceeds the storage and hydrogen production capacity, it is exported to the outer grid. On the other hand, when the system's own produced power is not enough to supply the load, the main grid acts as a backup source. Hence in this context, maximizing the self-sufficiency means limiting the share of input power supplied to the system by the grid with respect to the total input energy in the system. The second objective is thus formalized as the minimization of such ratio, referred to as grid dependence, GD:

$$minGD = \sum_{t=1}^{T} \frac{E_{imp,t}}{E_{imp,t} + E_{PV,t} - E_{exp,t}}$$

Where $E_{PV,t}$ is the AC energy produced by the photovoltaic panels during the timestep t, thus after the conversion and losses in the inverter.

44 5. OPTIMIZATION

3. Loss of Power Supply Probability Minimization

Reliability is a capital aspect to be considered in the context of energy communities. The Loss of Power Supply Probability (LPSP) represents an indicator on the energy security of the system throughout a certain period of time. The system's connection to the regional grid is not unlimited, but presents some capacity constraints. Therefore it may occur, in times with high energy demand and scarcity of supply from the system's own sources, that the power imported from the grid is not enough to satisfy the load, resulting in unmet load from the system. LPSP represents the likelihood of this situation to occur over the chosen period (one year in this case). By indicating with UL_t the unmet load during the timestep t and with L_t the total load demand during the time t, the third objective can be formulated:

$$minLPSP = \sum_{t=1}^{T} \frac{UL_t}{L_t}$$

Because of the top priority of ensuring a reliable system, the algorithm is constrained through a penalty function in order to consider solutions that already have a low LPSP. To do so, when a solution results in a Loss of Power Supply Probability higher than 5 percent, a penalty is assigned to the objective functions resulting in extremely high values for the two other objectives. Since the algorithm aims to minimize the objectives, those solutions will be discarded and only the ones with a LPSP lower than 5 percent will be present in the final Pareto Set. Ideally, this value would be as close to zero as possible: as a reference, the grid operator Tennet ensures a reliability of 99.99 % on The Netherlands' power network. In this study, higher failures are accepted within the optimal solutions, mainly because of the facts that TGV can be considered as a testing facility, because of the research character of this project and the absence of critical loads. It is necessary to be aware, however, that even small LPSP values could lead to severe complications especially in the presence of critical loads.

5.1.2. Variables and Constraints

The main scope of the optimization is to find the optimal sizes of the components in order to satisfy the requirements of the Energy Community, expressed in terms of constraints and described by the energy management strategy. To ensure an efficient operation of the system, which is unequivocally related to the system components' sizes, a parameter governing the power flows is also optimized together with the capacities. Each solution vectors is made of 9 components (variables): these are the numbers of PV panels, batteries, fuel cells and electrolyzers to install, together with the total maximum capacity for hydrogen storage (expressed in kg) and ,lastly, the threshold state of charge level of the batteries.

The total number of PV panels is not expressed by a single variable, but by 4 different ones. In order to have a detailed modeling of the PV-produced energy, different orientations for the panels were taken into account, representing the actual three different orientations of The Green Village's rooftops plus the South direction. In fact, together

with the rooftop installations, a certain amount of panels can be disposed on the ground in some of the Village's so called "free zones", open spaces free from buildings or other equipment. In this work, it was supposed that the panels placed in such spaces would be oriented in the optimal direction, which is South for the location of Delft.

Finally, the last optimization variable governs the system's operation. In particular, it gives an indication on the priority between discharging the batteries and starting the fuel cells, in case of deficit power production from the PV to satisfy the load. In fact, in this case, the battery is employed if the state of charge is already at a satisfactory level. Otherwise, the load is served through the fuel cells. This threshold SoC level is the ninth variable of the optimization problem. A high threshold entails a more frequent usage of the fuel cells, with a consequent larger capacity required, also for the H_2 storage. On the other hand, a low threshold has an influence on the battery usage. They will have deeper charge-discharge cycles, which negatively affect their total lifetime, but lower investment costs associated to purchasing more batteries rather than larger H_2 equipment.

The variables are subject to lower and upper bounds, so to limit the search space and only consider solutions that would be feasible for the actual system to be employed at The Green Village. The number of panels are limited by the available areas on the differently oriented rooftops and in the free zones. In particular, according to Zhou et al., 2022, who conducted a study to find the maximum possible PV penetration in The Green Village, the maximum number of Solarge Solo PV panels installable on the flat rooftops is 121. As per the tilted rooftops, a maximum capacity of 17 panels in the DreamHouses' westerly-oriented roofs and 25 on their easterly-oriented roofs were considered. For the so called 'free zones' where to allocate the grounded panels, a limit of 77 panels was considered, which excludes the potential of some areas considered in the cited report, but which were identified as not feasible after consultation with TGV's advisor. The maximum installed capacity is therefore achievable with 240 panels, and equals 87.6 kWp.

The number of batteries, fuel cells and electrolyzers are also subject to upper bounds. An extreme of 32 batteries (4 for each house) was set as the limit for this component. Based on the peak PV power production, another extreme case was used for setting the upper bound for the number of electrolyzers: in case 90 kW of peak power would be used to power some 2.4 kW electrolyzers, 38 of them would be necessary in order to exploit all this peak production. Similarly, if the peak load would need to be satisfied by only using the stored hydrogen, 5 fuel cells of the kind considered for this system would need to be employed. Lastly, the maximum hydrogen Storage capacity was constrained to a 800 kg. Table 5.1 summarizes the maximum sizes of the components imposed.

Additional constraints are imposed on the possible solutions. A non-linear constraint indicates the mutual dependence of electrolyzers and fuel cells: if in a solution one of these two components is not present, the other will also be considered absent (and the capacity of the hydrogen storage tanks will be set at 0). Moreover, because of the previously mentioned capital importance regarding security of supply of the system, not all

46 5. OPTIMIZATION

Variable	Upper Bound
153° Oriented Panels (Flat Roofs)	121
180° Oriented Panels (Ground)	77
255° Oriented Panels (Tilted Roofs - Westerly)	17
75° Oriented Panels (Tilted Roofs- Easterly)	25
Batteries	32
Electrolyzers	38
Fuel Cells	5
Hydrogen Capacity [kg]	800

Table 5.1: Constraints on the Maximum Number of Components

levels of Loss of Power Supply Probability are allowed. In fact, solutions leading to a LPSP higher than 5 percent are discarded and considered as non-feasible. This is done through the introduction of a penalty in the evaluation of the objective functions' values. When a certain solution is associated to a LPSP higher than such value, all the objectives are automatically set as equal to 10^9 . By doing so, since the algorithm's aim is to minimize the objectives, those solutions are automatically considered as unfit and not selected among the feasible ones.

5.2. IMPLEMENTATION

The most relevant aspect of the optimization carried out in this work is the integration between sizing and operation of the system. Because of the interdependence between the power flows and the sizes of the generators and storage components, it was necessary to make the algorithm "aware" of the system's behavior and perform the sizing accordingly. This was done by building a MATLAB external function describing the energy management within the community, and calling it inside the definition of the objective functions of the optimization problem.

The external function *Energymanagement.m* accepts as inputs the hourly electrical load, L, of the whole system and the optimization variables values, namely a matrix X composed of S rows (with S being the population size at each step of the algorithm, hence the number of solutions evaluated at each step) and 9 columns, representing the optimization variables.

For every row vector of the X matrix, the function calculates the hourly difference between the PV production and the Load, Based on the Irradiance data and the number of panels of the given solution. Then, a yearly simulation is performed, following the behavior described in 3.2

The function describing the energy management Strategy is nested inside the definition of the objective functions of the problem. In this way, it is ensured that the iterative process of search for the optimal solution is always dependent on the simulation results for the solution vectors of the previous iteration.

5.2. IMPLEMENTATION 47

The algorithm starts with the generation of a population of random vectors, each representing a feasible configuration of the system satisfying the constraints imposed: the upper and lower bounds for each variable and the non-linear constraints. The *Energy-management* function then evaluates the system's behavior and performances, following the logic earlier described. On the basis of such results, the values of the objective functions for each solution is computed. It is worth noticing that two of the three objectives (i.e. the Loss of Power Supply Probability and the Grid Dependence) can only be computed after the simulation is run, and therefore are strictly dependent on the energy dispatch determined by the *Energymanagement* function.

After simulating the system's behavior and energy flows for a period of one full year and computing the objective functions' values, a fitness value is assigned to each feasible solution and the solutions are ranked on the non-dominance criteria. The operations of mutation and crossover are then applied and the population is updated as described in 2.1.3. Figure 5.1 schematically shows the workflow of such implementation, with the mutual interaction between optimization and operation.

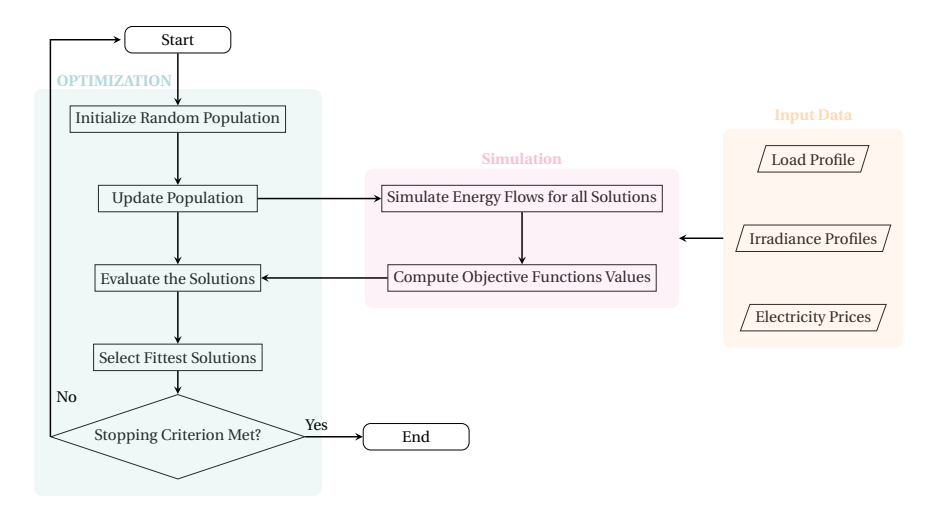


Figure 5.1: Schematic of the Implementation Workflow

In order to ensure proper functioning and accurate results from the *gamultiobj* function in MATLAB, some options have been modified. These options mainly influence the vastness of the search space and the stopping of the algorithm, and are described in Table 5.2.

With these options, the algorithm is ensured enough iterations and accuracy to find a well-defined Pareto Set of equally valid solutions within a vast search space. In particular, the size of the population has an influence on the number of solutions forming the final Pareto Set. It is important to mention that a low value for the tolerance and high

48 5. Optimization

Table 5.2: Options used for the gamultiobj function

Option	Value	Description
Population Size	2000	Size of the population. At each iteration, this is the
		number of vectors of which the population of chro-
		mosomes is composed.
Function Tolerance	10^{-6}	The algorithm stops when the geometric average of
		the relative change in value of the spread over 'Max
		Stall Generations' is less than this value, and the fi-
		nal spread is less than the mean spread over the past
		'Max Stall Generations'
Max Stall Generations	100	The algorithm stops when the geometric average of
		the relative change in value of the spread over this
		number of generations is less 'Function Tolerance',
		and the final spread is less than the mean spread over
		the past 'Max Stall Generations'
Max Generations	5000	Maximum number of iterations for the algorithm, at
		which it ends its search.

values for the other options lead to an increased computational time and effort. The selected values have been tested and gradually increased to favor precise results within a reasonable time.

5.3. OPTIMAL SOLUTION SELECTION

Upon running the model with the specified options, a Pareto Set composed of 700 equally optimal solutions is obtained by the optimization algorithm. As already introduced in 2.1.2, these solutions are said to be equally optimal based on the concept of Pareto dominance, and in particular because not only the three objectives are not comparable, but also because none of them has been identified as a priority with respect to the others.

In order to assist the multi-criteria decision-making process and selecting a suitable solution among the hundreds found by the solver, different methods can be applied. In this work, the TOPSIS (Technique for Order of Preference by Similarity to the Ideal Solution) algorithm is employed, thanks to which the decision can be restricted to very few options. In this section, the optimization objectives (minimization of Annualized Total Costs, Grid Dependence and Loss of Power Supply Probability) will be referred to as *criteria*, in order to avoid confusion with another use of the term *objective*, shortly introduced.

5.3.1. WEIGHTING THE CRITERIA

The method, taken from Alsayed et al., 2013, is firstly based on the definition of a *weight* for each criteria, measuring its relevance with respect to the others. For each criteria, the final weight is given by a subjective and an objective weight. The subjective weight is based on the decision-maker(s) personal preference, and is based on the prioritization

of the criteria. The criteria with the highest subjective priority is associated with a score of 1, the second with a score of 2 and the third with a score of 3. After consultation with an advisor from The Green Village, the priorities have been assigned as follow:

- 1. Minimization of Annualized Total Cost
- 2. Minimization of Grid Dependence
- 3. Minimization of Loss of Power Supply Probability (provided that this value is always below 5 percent)

In order to have a subjective weight in the range [0,1], after assigning the preferences the subjective weight for the j^{th} criteria is determined as per equation 5.7, where n is the number of criteria (3 in this case) and k is the subjective priority assigned to the criteria:

$$w_j^s = \frac{1}{n} \sum_{k=j}^n \frac{1}{k} \tag{5.7}$$

This formula yields three fixed values for the objective weights. The cost objective has a weight of 0.6111, the self sufficiency a weight of 0.2778 and the reliability objective has a weight of 0.1111.

Objective weights are assigned to the criteria on the basis of their *Entropy*. The definition of entropy is based on information theory, and assigns a low weight to an attribute if its values are similar across alternatives, because such attribute does not assist differentiating alternatives Rao, 2013. Objective weights calculated in this way, unlike the subjective, are not always equal but slightly differ for each different simulated scenario, as they are dependent on the actual solutions found by the algorithm and their proximity in the solution space. In order to conduct a fair comparison between scenarios, the objective weights of the Base Case were applied to all cases.

The assignment of such weights is dependent on two matrices obtained as result of the optimization algorithm. The matrix X (of dimensions $S \times K$) contains the S solutions forming the Pareto Set, and the values of the K optimization variables for each solution. The matrix S (dimensions $S \times J$) contains the values of the S objective functions (criteria) for all the S solutions forming the Pareto Set.

To calculate the entropy of a criterion, the Performance index P is first calculated:

$$P_{sj} = \frac{Z_{sj}}{\sum_{s=1}^{S} Z_{sj}}$$
 (5.8)

Entropy is then defined as:

$$E_j = -z \sum_{s=1}^{S} P_{sj} \cdot \ln(P_{sj})$$

$$\tag{5.9}$$

5. OPTIMIZATION

Where:

$$z = 1/\ln S \tag{5.10}$$

The degree of divergence d_j is then introduced. The more divergent is the performance rating P_{sj} for the j^{th} criteria, the higher its d_j value, which will lead to a higher objective weigth.

$$d_i = 1 - E_i \tag{5.11}$$

The objective weights are obtained as:

$$w_j^o = \frac{d_j}{\sum_{i=1}^{J} d_j}$$
 (5.12)

And finally, the subjective and objective weights are combined through the multiplication synthesis combination weighting method (MSCWM), as per equation 5.13:

$$w_{j} = \frac{w_{j}^{s} \cdot w_{j}^{o}}{\sum_{j=1}^{J} w_{j}^{s} \cdot w_{j}^{o}}$$
 (5.13)

The application of this method yields the weights of 0.5511, 0.3418 and 0.1071 for cost, self sufficiency and reliability, respectively. Therefore, the priority introduced by the subjective weights is still preserved, but the relative importance among them is slightly more balanced.

5.3.2. APPLICATION OF THE TOPSIS ALGORITHM

After obtaining a final weight for each of the criteria, solutions can be evaluated and ranked based on their relative performances and their proximity to ideal solutions with the use of the TOPSIS algorithm. The first step of this step consists in making the different criteria comparable with each other. To do so, all elements of the Z matrix need to be normalized:

$$r_{sj} = \frac{Z_{sj}}{\left(\sum_{s=1}^{S} Z_{sj}^2\right)^{1/2}} \tag{5.14}$$

The weighted normalized criteria matrix is obtained:

$$v_{sj} = w_j \cdot r_{ij} \tag{5.15}$$

At this point, the best and worst ideal solutions are found. These are two fictitious solutions: the best ideal is a solution that has the best score among the whole final Pareto set for every criteria, and the worst ideal is the one containing the worst scores. The main idea behind the TOPSIS algorithm is to find the solutions that are closest to the best ideal, and farthest from the worst ideal. For a minimization problem like the one treated in this study, the best ideal is:

$$A^{+} = \{v_{1}^{+}, v_{2}^{+}, v_{3}^{+}\} = Minv_{ij} | j \in J$$
(5.16)

While the worst ideal is:

$$A^{-} = \{v_{1}^{-}, v_{2}^{-}, v_{3}^{-}\} = Maxv_{ij} | j \in J$$
(5.17)

Every solution is analyzed on the basis of its distance from these ideal solutions. In particular, on the positive distance from the best ideal and the negative from the worst. By indicative with l_s^+ the positive distance from the best ideal, and l_s^- the negative distance from the worst ideal, these two lengths are defined as follows:

$$l_s^+ = \sqrt{\sum_{j=1}^{J} (\nu_{ij} - A_j^+)^2}$$
 (5.18)

$$l_s^- = \sqrt{\sum_{j=1}^{J} (\nu_{ij} - A_j^-)^2}$$
 (5.19)

The very last step then consists in calculating the TOPSIS score for each solution forming the Pareto Set. The TOPSIS score is equivalent to the relative closeness of each alternative to the worst ideal, and the solution with the maximum score (that is, the farthest from the worst and closest to the best ideal) is indicated as the best option.

$$TOPSIS_{score} = \frac{l_s^-}{(l_s^- + l_s^+)}$$

$$(5.20)$$

ANALYSIS OF THE RESULTS

After successfully running the optimization model, a Pareto set of 700 equally optimal solution is found. Such solutions are then sorted and ranked with the TOPSIS algorithm detailed in section 5.3. The aim of this chapter is to provide an analysis for the results of the scenarios studied in this research, that shall lead to final conclusions and considerations.

6.1. BASE CASE

The first simulation conducted concerns a Base Case Scenario. The Base Case features the basic load, as introduced in 4.2, and fixed prices for the imports and exports of electricity from the outer grid. In particular, the price for the imports was set as the average electricity retail price in The Netherlands in the last ten years (from 2012 to 2022), equal to 0.33 €/kWh. The revenue gained from selling to the outer grid was set at 0.20 €/kWh, 60 percent of the price charged for imports, in accordance to one of the alternatives proposed by Londo et al., 2020 of abolishing the producer part of the electricity tariffs accounting for approximately one third of the price.

6.1.1. PARETO SET ANALYSIS

The shape of the Pareto Set clearly shows the relationship between the three objectives. As expected, minimizing the system's costs comes at the expenses of decreasing its self-sufficiency and reliability. Figure 6.1 shows the distribution of the non-dominated solutions in the objectives' three dimensional space, while the scatter diagram in Figure 6.2 translates the solutions to a bi-dimensional plane, highlighting such correlation even more. The self sufficiency of the system is clearly clashing with the costs optimization: in fact, the most cost-effective solutions are the ones in which the Energy Community almost solely relies on the grid imports. The reliability objective's behavior also suggests a similar trend with respect to the annualized total costs, with the Loss of Power Supply Probability steeply decreasing with the annualized total cost, especially in the first part.

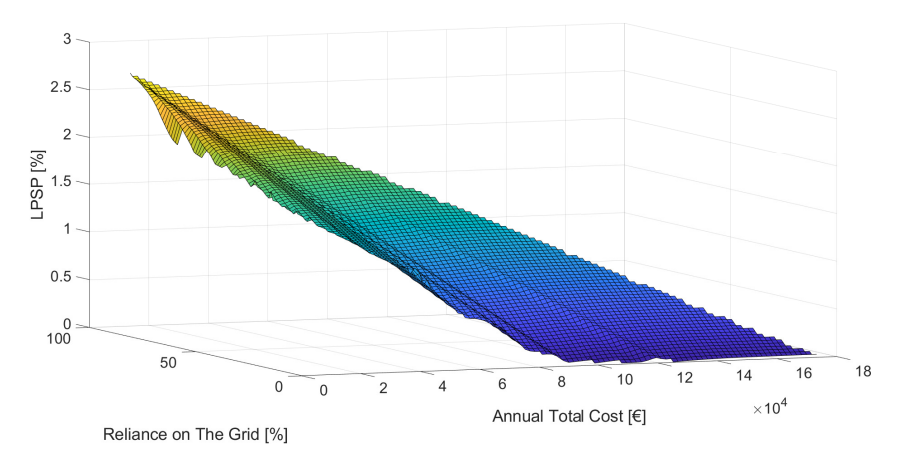


Figure 6.1: 3-Dimensional representation of the Pareto Set, Base Case

Some considerations can also be drawn from the shape of the curve in Figure 6.2. Its hyperbolic trend reaches a plateau when the ATC reach a value of around 100000 €. Even before reaching this region, however, it can be noted that the steepness of the curve is much lees accentuated with respect to the first part. Such behavior translates into the fact that, above a certain cost, the marginal gain obtained by increasing the financial expenses is not effectively balanced by an equal benefit in the other two objectives. It is not surprising, therefore, that all the top-ranked solutions after applying the TOPSIS algorithm can be identified in the steeper part of this curve (more precisely, in the region before the 60,000€).

The curve also clearly shows what previous research about the Energy Community in The Green Village has highlighted: the complete self-sufficiency of the system can only be achieved with extremely high costs. The presence of a grid connection is therefore of utmost importance when aiming at a reduction in the system's cost. In particular, the relatively small penetration potential of PV power and the high costs of storage capacity are the two main factors influencing this result.

6.1.2. USE OF HYDROGEN STORAGE

With the Base Case pricing conditions, there is no particular incentive in storing energy in a period to sell it when it is more profitable, and thus the need for storage is impacting more on the self-sufficiency objective than on the cost-effectiveness. For this reason, the first outstanding result is that, over the 700 ranked solutions, almost half of them (348 solutions) do not employ hydrogen equipment, resulting in the absence of electrolyzers and fuel cells, with no need for hydrogen storage (of which the minimum capacity was set to 50 kg for all the solutions, since some hydrogen storage is already present at TGV). The high costs associated with the production and usage of hydrogen and the low costs for importing energy from the grid when it is necessary make it inconvenient to rely on

6.1. BASE CASE 55

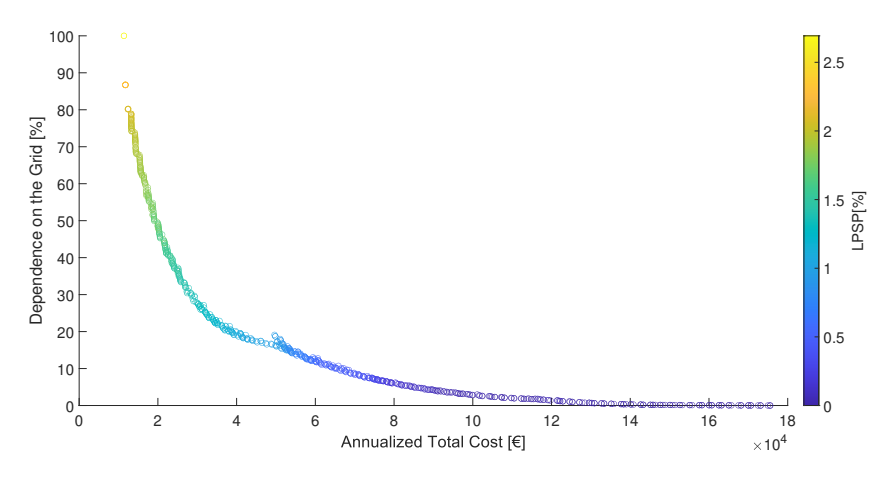


Figure 6.2: 2-Dimensional representation of the Pareto Set, Base Case

long-term storage in favour of using the grid as a backup.

Within the solutions that do employ hydrogen for seasonal storage, the best performing is ranked 92 overall. Table 6.1 shows that the sizing of such solution is very similar to the one achieved for the best-performing solution, with the integration of two electrolyzers and one fuel cell. With exactly the same generation capacity installed, the hydrogen-featuring solution compensates the additional costs with an increase in self sufficiency and reliability, as shown in Table 6.2. The Cost of Electricity here introduced was obtained by dividing the annualized total costs by the annual load.

Table 6.1: First solution overall vs. first H2-featuring solution: Sizing

Ranking	PV Installed Capacity [kWp]	N. Batteries	N. Electrolyzers	N. Fuel Cells
1	85.41 (234 Panels)	5	0	0
92	85.41 (234 Panels)	5	2	1

Table 6.2: First solution overall vs. First H2-featuring solution: Performances

Ranking	Annualized Total Cost [€]	Cost of Electricity [€/kWh]	Grid Dependence [%]	LPSP [%]
1	39,315	1.16	19.10	1.1
92	54,085	1.63	14.15	0.74

A distinctive feature of the Pareto Set noticeable in Figure 6.2 is the presence of a zone in which the steepness of the curve changes, which can be identified by an area where some points are slightly detached from the main curve (in the two-dimensional representation) and from the presence of crests in the surface representing the solution space

(in the three-dimensional representation). Such area represents the transition area from PV-Battery only configurations to solutions including hydrogen storage.

Prior to this area, almost all solutions do not present hydrogen in any forms, while the after that hydrogen storage is present in all solutions. The transition area is where the two configurations alternate, resulting in a very similar overall performance, but differentiated with respect to the single objectives. In particular, hydrogen-featuring solutions perform better in terms of Self-Sufficiency, while Battery-only solutions are preferable in terms of Cost.

6.1.3. ECONOMIC PERFORMANCES

The top rated solutions after the ranking are the most balanced in terms of how they perform with respect to the three objectives. However, as introduced in 5.3, a criterion was selected to assist the decision-making process, which is based on the prioritization of the cost minimization objective over the others. When focusing on such objective, some considerations shall be made.

The less expensive solution found during the optimization is the one relying completely on imports from the outer grid, with no capacity installed whatsoever. In this case, the cost of electricity is of course $0.33 \, \epsilon/kWh$, which is the cost of the imports. Such solution is, on the other hand, the worst possible in terms of reliability and self-sufficiency, with $2.7 \, \%$ of LPSP and $100 \, \%$ of grid dependence. It is crucial to notice that, even if the LPSP percentage seems to be low, it actually corresponds to almost $10 \, days$ of unmet load.

Excluding this and similar extremes, for example solutions featuring an extremely limited amount of panels and grid dependence values over the 80 %, it is worth to notice the economic performances of some of the best solutions, over the 700 found. The topranked solution, introduced earlier, features a cost of electricity of more than $1 \in /kWh$, which is still considerably high if compared to the average electricity price in the recent years. By analyzing other solutions, however, it can be noted that there are some more convenient options under the financial point of view.

Ranking	Cost of Electricity [€/kWh]	Grid Dependence [%]	LPSP [%]
1	1.16	19.10	1.10
93	0.85	28.22	1.35
307	0.70	37.82	1.47
387	0.60	45.87	1.62
493	0.48	60.15	1.86

Table 6.3: Increasingly cost-efficient solutions: Performances

Tables 6.3 and 6.4 show different solutions within the first hundreds of the ranking, in ascending order of cost-efficiency. The Levelized Cost of Electricity (LCOE), calculated by dividing the ATC by the annual total load, is displayed instead of the annualized to-

6.1. BASE CASE 57

Ranking	PV Installed Capacity [kWp]	N. Batteries	N. Electrolyzers	N. Fuel Cells
1	85.41 (234 Panels)	5	0	0
93	71.9 (197 Panels)	2	0	0
307	51.1 (140 Panels)	2	0	0
387	45.26 (124 Panels)	1	0	0
493	35.04 (96 Panels)	0	0	0

Table 6.4: Increasingly cost-efficient solutions: Sizing

tal costs to give a clearer idea about the actual energy costs payed by the Community actors. Once again, the inverse correlation between the cost and the two other objectives is clear: the lower the costs, the lower is the Self-sufficiency and the reliability of the Community. In particular, the most cost effective solutions not only do not ever employ any form of hydrogen storage, but also rely very little on short-term storage in the form of batteries. This is probably relatable to the flat tariffs applied for exchanging electricity with the grid: there is no incentive in storing large amount of energy for a following period, if the prices for importing energy will stay the same over time.

Another important fact to notice is that, even for the most economically convenient solutions, the LCOE is higher than the the average cost of electricity in The Netherlands, at least if average values from recent years are to be considered. On the other hand, it is also true that in this case no Government incentive or economies of scale effects (for example, for the purchase and installment of PV panels) were considered. In a similar way it is important noting that the electricity retail price here considered, despite being an average of recent years, can always be subject to changes that could also be drastic, as happened with the energy crisis of the year 2022.

Such uncertainties, together with the results of this optimization, can lead up to the conclusion that the most cost-effective solutions in this study could actually be applicable for TGV's Energy Community studied, under favourable conditions of pricing (especially for the exports towards the grid) and with policies stimulating investment in renewable energy equipment. Regarding the use of hydrogen storage, it still appears to be a non-efficient choice, especially under the economic point of view.

6.1.4. System's Behavior

A short analysis of the behavior of the system can be conducted by analysing the most promising solutions. As earlier introduced, the top-ranked solution does not feature any long term storage in the form of hydrogen, employing 234 panels in total (85.41 kWp) and 5 batteries to satisfy the load. Figure 6.3 shows the energy flows of a week in the summer period:

This period is characterized by a low load demand, with high solar production. Because of the small storage capacity, considerable amounts of energy are exported during peak energy production hours, while small amounts are stored and used later to fulfill the load during the hours with no sunlight.

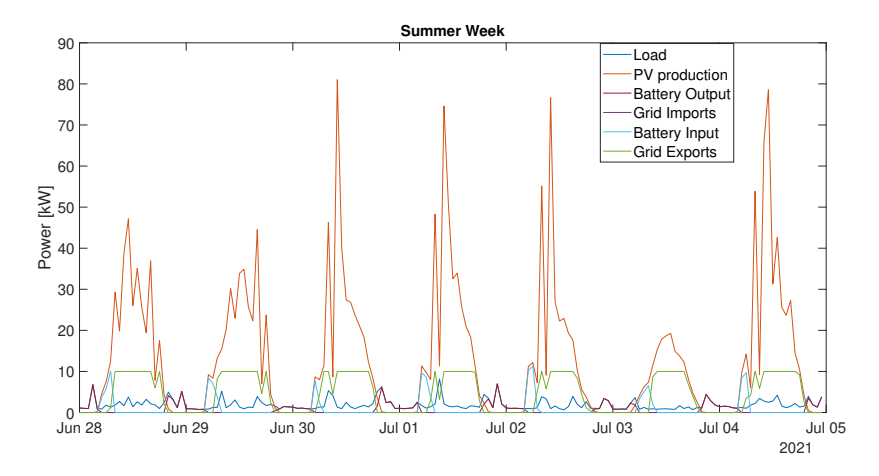


Figure 6.3: Base Case Best solution: Energy Flows during a Summer Week

Figure 6.4 displays the behavior of the system during a typical winter week, characterized by a much higher load and a limited solar energy availability (with the exception of some sharp peaks). The grid imports are much more frequent and consistent than in summer, and sometimes they are not even enough to serve the load, since they are constrained to a capacity of 10 kW. Despite this, the system still needs to export some energy to the outer grid when the batteries are already charging at their maximum rate. Such behavior clearly depicts the trade-off between cost and the other objectives. In this configuration there is some energy that could be stored for later usage, but it was preferred to export it to the grid because of the economic efficiency of this choice over further expanding the storage capacity.

To provide insights on the hydrogen usage, another solution should be analyzed. Figure 6.5 shows the energy flows during the reference summer week for the best performing solution in terms of self sufficiency, which installs the maximum available PV capacity and couples it with 30 batteries, 17 electrolyzers and 2 fuel cells. This solution never imports energy from the outer grid, even though this condition is reached at extremely high costs.

During the summer period, an intense use of the electrolyzers is performed to store energy in the form of hydrogen, while the batteries are employed to serve the load in absence of generation from the PV, and charged until their limit during the day. The hydrogen produced and stored during the summer is then employed to power the fuel cells in winter, as depicted in Figure 6.6.

During winter, the load is mainly supplied by the fuel cells, with a small contribution from the batteries which are occasionally charged during the hours in which the solar production spikes (for no more than 2 hours per day). The presence of seasonal storage

6.1. BASE CASE 59

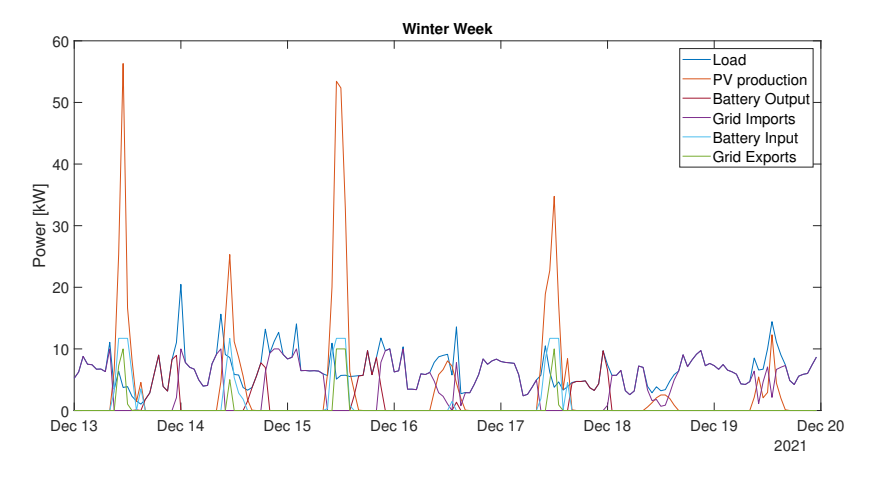


Figure 6.4: Base Case best solution: energy flows during a winter week

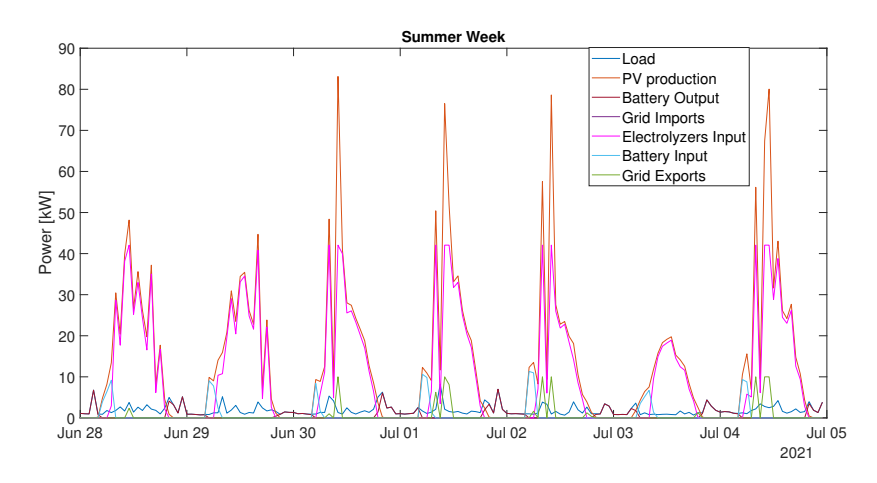


Figure 6.5: Base Case most self-sufficient solution: energy flows during a summer week

in the form of hydrogen not only reduces the energy imports from the outer grid, but also the exports towards it. In fact, the system tends to exploit the long-term storage by prioritizing the load demand, only exporting the eventual excess. Because of the flat pricing mechanism adopted in this scenario, moreover, the system has no economic incentive in exporting during a particular time, and only exports when it is necessary. If comparing Figure 6.3 and 6.5, the differences in exported power in periods of overproduction is evident.

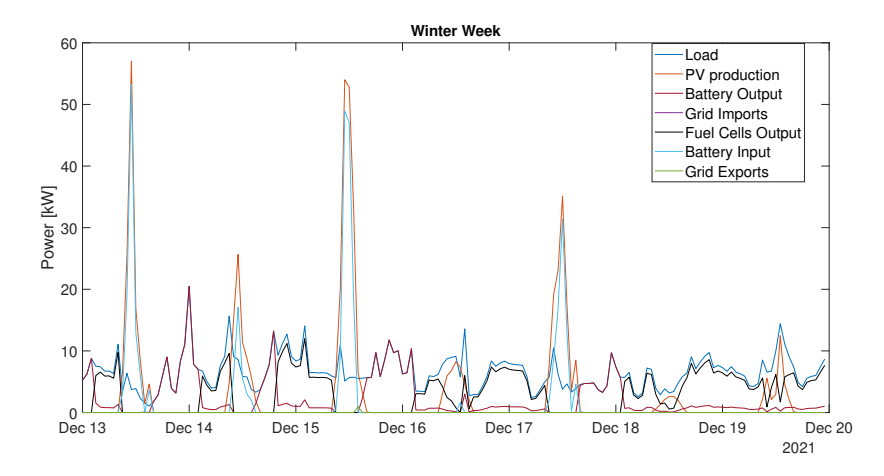


Figure 6.6: Base Case most self-sufficient solution: energy flows during a winter week

6.2. Infinite Grid

The Infinite Grid Scenario investigates the outcome of the optimization and the performances of solutions in a case where the possible interactions of the system with the outer grid are unlimited. Unlimited access to the grid can occur when the network connection is oversized, which is currently the case at The Green Village where a larger transformer is installed with respect to the capacity effectively needed. This could be, however, also a case occurring in the future power network, where distributed energy communities are likely to size their grid connection based on their peak consumption and with a safety margin, in order to have no limitations when they need to import or export energy. The main difference this scenario has with the one described in 6.1 is the removal of the capacity limit for interacting with the outer grid, previously set to 10 kW for both imports and exports.

6.2.1. PARETO SET ANALYSIS

The most relevant consequence of removing the grid capacity constraint occurs with respect to the Loss of Power Supply Probability. As detailed in 3.2, the load cannot be met when all the energy sources present within the system plus the imports from the grid are not enough to satisfy the demand. When the imports are not limited, however, the load can always be met with the help of the outer grid, and thus the LPSP value is always 0. This is the reason why Figure 6.7, displaying the Pareto Set for this Scenario, only features a trade off between two objectives.

Once again, the shape of the Pareto curve anticipates the outcomes of the optimization. Compared to the Base Case (6.2), the Pareto front shown in Figure 6.7 features a less steep transition from the low (below $10,000~\rm e)$) to the high (above $60,000~\rm e)$) cost region, resulting in higher values of grid dependence for solutions falling in the medium-price range. Similarly to the Base Case, the most cost efficient way to supply backup power is

6.2. Infinite Grid 61

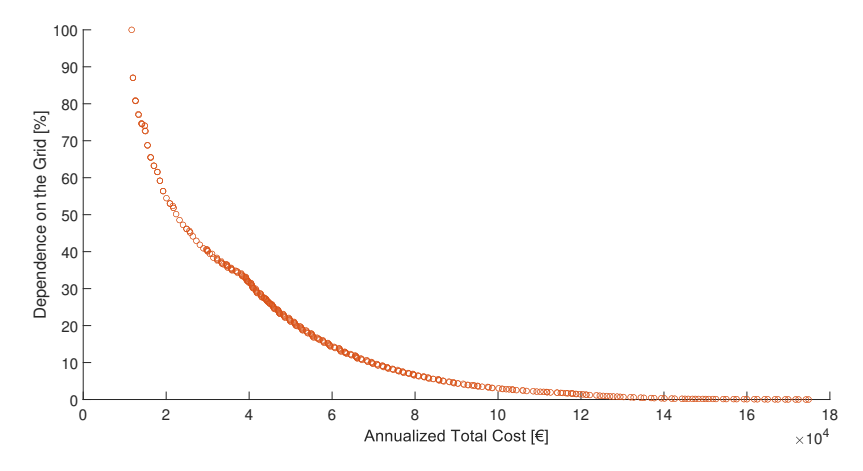


Figure 6.7: Pareto Set, Infinite Grid Scenario

represented by the grid imports, especially when they are not constrained.

The absence of one objective is also reflected on the selection of the best trade off by the TOPSIS algorithm. In fact, the top ranked solution for this scenario (Table 6.5) features a different use of storage capacity with respect to the Base Case, with less batteries but the introduction of hydrogen equipment.

Table 6.5: Infinite Grid Scenario, TOPSIS Best Solution: Sizing

Ranking	PV Installed Capacity [kWp]	N.Batteries	N.Electrolyzers	N. Fuel Cells
1	85.41 (234 Panels)	3	4	1

Table 6.6: Infinite Grid Scenario, TOPSIS Best Solution: Performances

Ranking	Annualized Total Cost [€]	Cost of Electricity [€/kWh]	Grid Dependence [%]	LPSP[%]
1	52,918	1.59	18.70	0

Under the economic perspective, this solution is not preferable over the best selected for the Base Case, but it is comparable to the best hydrogen-featuring solution earlier introduced. In fact, with the help of an infinite grid and a more balanced sizing of the storage solutions, the system can now satisfy the total load demand at a slightly lower cost. The fact that the top-ranked solution for this scenario features a large storage capacity despite being capable of importing virtually infinite energy from the outer grid might seem counter-intuitive. Such result is however a direct consequence of this condition, and is determined by the multi-objective nature of the problem and the goal of the ranking algorithm to find a balanced solution.

As mentioned, because of the absence of grid capacity constraints, only solutions with a maximum reliability are taken into account in the optimization. The load that was previously not met, however, is not fully covered by imports from the outer grid but rather from more balanced sizing solutions. In fact, if this would have been the case, such solutions would have resulted in a higher degree of grid dependence, and would have been excluded from the top-ranked because of the imbalance in the objective function values, mostly favoring the cost abatement goal. An important consequence of this condition is that not only the top-ranked solutions, but most of the solutions within the Pareto Set result to be more expensive with respect to the Base Case. This is detailed better in the next Section.

6.2.2. ECONOMIC PERFORMANCES

Despite the differences in the top-ranked solutions, a broader analysis of the overall results confirms the trends already emerged with the Base Case. Also in this scenario, the top ranked solution is achieved at a considerably high cost of electricity of $1.59~\mbox{\'e}/\mbox{kWh}$. To assess the efficiency of the Pareto set solutions, other solutions were investigated. Tables 6.7 and 6.8 show the sizing and performances of solutions within the Pareto set with increasing degree of grid dependence.

Table 6.7: Infinite Grid Scenario, solutions with increasing Grid Dependence: Performances
--

Ranking	Cost of Electricity [€/kWh]	Grid Dependence [%]
605	0.88	40.07
635	0.65	50.15
656	0.52	61.53
673	0.45	72.59

Table 6.8: Infinite Grid Scenario, solutions with increasing Grid Dependence: Performances

Ranking	PV Installed Capacity [kWp]	N.Batteries	N.Electrolyzers	N. Fuel Cells
605	78.84 (216 Panels)	4	0	0
635	39.42 (108 Panels)	3	0	0
656	39.42 (108 Panels)	1	0	0
673	32.85 (90 Panels)	0	0	0

This analysis confirms that the Energy Community in The Green Village would not be economically competitive with a low degree of grid dependence. At least half of the energy supplying the load demand would need to be satisfied from the outer grid in order to achieve acceptable expenses, while most of the solutions found within the Pareto Set feature much higher costs. This analysis also highlights the non-linearity in the relationship between cost and self sufficiency: this is justified in particular by the high costs of the hydrogen equipment, which is necessary to achieve a year-round high degree of independence. Because of this, the idea of a system relying mainly on its own resources and capable of satisfying the Community's electrical needs seems to be unfavourable at

the moment.

It is worth to emphasize the already mentioned effect of the gird limit removal and the consequent absence of the reliability objective on the solutions. By comparing the Infinite Grid Scenario's Pareto Set with the one relative to the Base Case, the influence of the reliability objective on the optimization's outcome becomes more evident. When accepting a lower security of supply (in this case, still below 1.6 %), monetary savings are conspicuous. Table 6.9 provides an example comparison between two solutions with similar grid dependence values, both around 30 %. The first solution belongs to the Base Case Pareto Set, while the second to the Infinite Grid Scenario's.

Table 6.9: Comparison of solutions with and without Grid Capacity Limit

Grid Capacit	y Limit	PV Capacity	N.Batteries	N.Electrolyzers	N. Fuel Cells	Cost of Electricity
Yes		68.62 kWp	2	0	0	0.84 €/kWh
No		72.27 kWp	3	2	1	1.25 €/kWh

The additional costs necessary to make sure that the system achieves maximum reliability are highlighted in Figure 6.8. The fitted curve represents how much the costs increase in the Infinite Grid Scenario with respect to the Base Case. The cost difference is the highest in the medium GD region, where the full reliability of the system is achieved through the introduction of the hydrogen storage system.

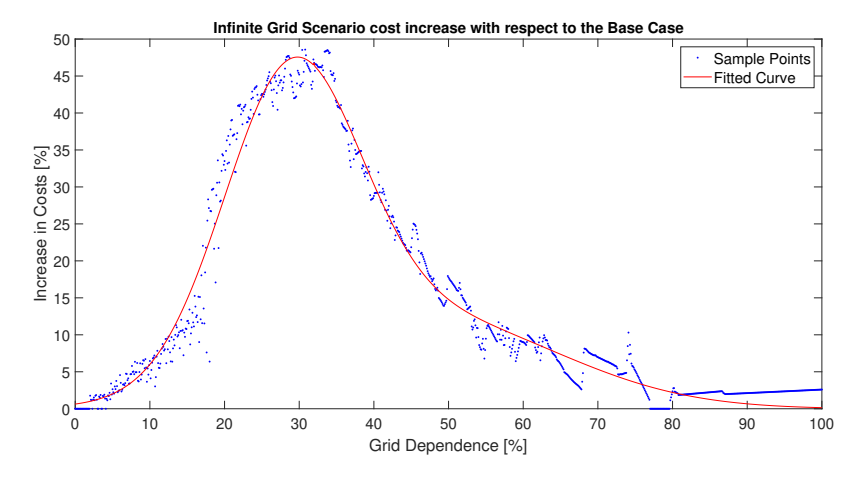


Figure 6.8: Cost increase of Infinite Grid Scenario Solutions with respect to the Base Case

6.3. REAL TIME PRICING

In order to assess the influence of different electricity pricing schemes on the robustness of the sizing model, a Real Time Pricing Scenario was simulated. In this case, the electricity prices reflect the spot market prices, providing immediate and frequent price signals to the Energy Community consumers. The selling price for the exported electricity was

once again set as 60 percent of the buying price, and the grid capacity limit was set as equal to the Base Case.

The first and most relevant result is that, at least for what concerns the top solutions individuated by the TOPSIS algorithm, there is no significant change in the system's sizing when the RTP tariff is applied. In fact, with the exception of one more battery selected in this case, the components' configuration is the same, as shown in Table 6.10.

Table 6.10: Real Time Pricing Scenario, TOPSIS Best Solution: Sizing

Ranking	PV installed Capacity [kWp]	N.Batteries	N.Electrolyzers	N. Fuel Cells
1	85.41 (234 Panels)	4	0	0

The overall performances of such solutions are in line with the ones achieved by the Base Case top solution, with the RTP solution resulting in a lower annualized total cost:

Table 6.11: Real Time Pricing Scenario, TOPSIS Best Solution: Performances

Ranking	Annualized Total Cost [€]	Cost of Electricity [€/kWh]	Grid Dependence [%]	LPSP[%]
1	36,422	1.09	20.34	1.16

The lower costs incurred in this solution can be mainly attributed to two factors. Firstly, despite the high fluctuation in the prices occurring throughout the year and some high peaks reached with this pricing scheme, the average price is slightly lower than the flat tariff used in the Base Case. However, referring to the average of the hourly-varying price is not an effective means to describe this result alone. Figure 6.9 shows that the system manages to avoid imports in correspondence of prolonged periods of high prices, effectively reducing the expenses for the imports through the external grid.

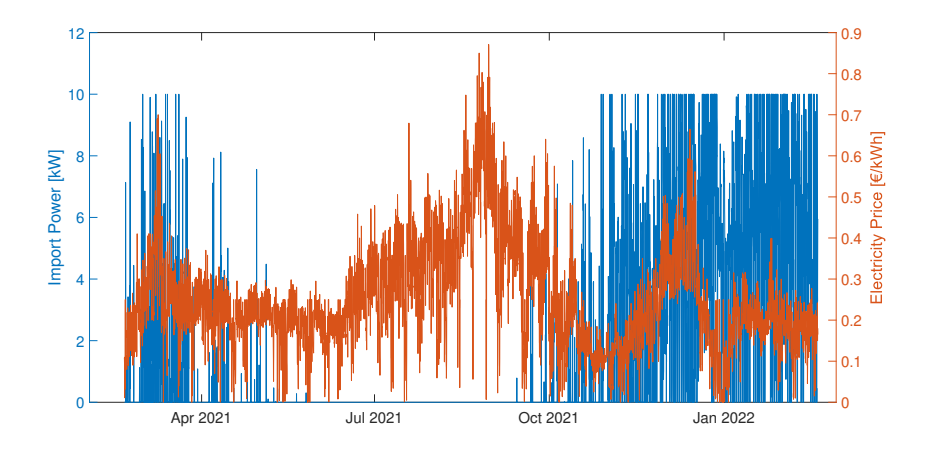


Figure 6.9: Imported power and electricity prices, Real Time Pricing Scenario top solution

Despite this opportunity, the use of a hydrogen storage system which could provide even more flexibility in case of price spikes is still not considered to be favourable. Again, the high investment costs represent an inconvenient barrier to overcome. This result however suggests that, especially in regimes of volatile prices, energy storage equipment in general can represent a significant means to abate costs in the long run. In particular, this could occur in systems with an energy management strategy aware of the real time prices, capable of adjusting the energy flows to minimize the imports' expenses and maximize the exports' revenues.

At the same time, and looked from another perspective, the result can be interpreted as a positive signal regarding the adoption of dynamic tariffs. In the perspective of an energy network with a high penetration of distributed energy sources and communities, these pricing policies not only can better reflect the actual cost of electricity treated as a commodity, but can also benefit both the grid management activities and the prosumers.

6.4. Hydrogen Cost Decrease Scenario

The analysis conducted so far have highlighted how the high capital costs represent a great barrier in the adoption of a hydrogen system for long term energy storage, despite its proved usefulness in the increase of self-sufficiency and reliability. The use of hydrogen in the energy industry, and more generically the demand for hydrogen in key application sectors, has been increasing in recent years (IEA, 2022) and is expected to play a significant role in the pathway to the decarbonization of the energy sector. With the projected investment expansion in hydrogen-related projects, economies of scale effects will likely lead to a drop in the investment costs for the necessary equipment, and in particular of electrolyzers and fuel cells.

This scenario investigates the outcomes of the sizing in the case of, as expected, the investment costs of the hydrogen equipment will decrease as a result of fast development. With respect to the Base Case, no other parameters were changed except for the said costs. The magnitude of such development and the consequent drop in the costs is an uncertain forecast. A report published by TNO (Detz and Weeda, 2022) has analyzed the future development of investment costs trough the construction of learning curves, and according to their most conservative estimation, the cost for PEM electrolyzers could decrease to 1350 €/kW. The AEM technology used by Enapter in the electrolyzers here considered, however, has even greater potential for scalability due to the absence of rare materials. According to the manufacturer (Collins, 2022), a decrease in the costs of 83 percent can be expected in the next years thanks to the opening of a new automated and large-scale production site, leading to a cost of 550 €/kW, which is used for the simulation of this case.

As per the future evolution of fuel cells' costs, a similar research on predictive studies was carried out. An extensive analysis was conducted by Battelle, 2016, where estimates on the costs were given on the basis of the degree of scale production of medium-sized fuel cells by the year 2030. Cigolotti and Genovese, 2021 have considered this and other studies in a more recent report part of IEA's technology platform, hypothesizing a cost

abatement from around 1,000 to 460 %kW, depending on the future degree of penetration of the PEM technology on the market. For this scenario study, the most optimistic of such estimates was considered, in order to assess the hydrogen storage potential in a case of widespread development. Therefore, cost for a single electrolyzer was set to $1,320 \in$, while the cost of each fuel cell was set to $3,100 \in$.

6.4.1. PARETO SET ANALYSIS

Figure 6.10 shows the optimal solutions' set for this case, displayed together with the Base Case for reference. The two curves overlap on the left side of the graph, in the area corresponding to low costs and high self sufficiency, where solutions are characterized by the absence of hydrogen equipment in both cases. The drop in the investment prices is the cause for the subsequent detachment of the lower curve, which is representing the solutions for this scenario. In this case, a plateau is reached significantly before than in the Base Case, as the lower costs make it easier to reach a saturation point with respect to the storage capacity.

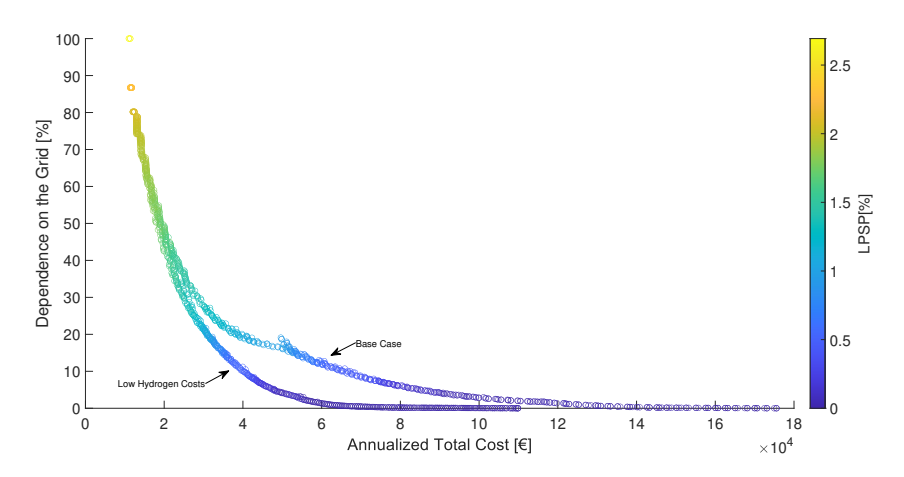


Figure 6.10: Base Case and low Hydrogen Cost Scenario, Pareto Sets comparison

The different configuration of the Pareto Front obviously also affects the results of the ranking algorithm applied. Because of the lower barrier on their application and their undoubted usefulness, the use of electrolyzers and fuel cells is widespread among the best solutions. In fact, only 88 over the 700 Pareto dominant solutions do not employ a hydrogen storage. The PV installed capacity of the best solution is exactly the same of the other cases, despite the optimal storage distribution changes. The recurrence of this value for the generation capacity regardless of changes in the boundary conditions indicates that the optimal trade-off was found between costs and production, in relation to the satisfaction of The Green Village's load. Tables 6.12 and 6.13 summarize the sizing and performances of the best solution in this Scenario.

Table 6.12: TOPSIS best solution: Sizing

Ranking	PV installed Capacity [kWp]	N.Batteries	N.Electrolyzers	N. Fuel Cells
1	85.41 (234 Panels)	3	13	1

The large number of electrolyzers with respect to the amount of fuel cells can be attributed to two factors. First of all, the nominal input power of a single Electrolyzer (2.4 kW) is relatively small compared to the output rated power of 6.8 kW of the fuel cells. Most importantly, however, this is a consequence of the significant energy conversion losses that take place when producing hydrogen with the electrolyzer, making it necessary to oversize the hydrogen production system in order to properly satisfy the subsequent backup generation.

Table 6.13: Low Hydrogen Equipment Cost Scenario, TOPSIS best solution: Performances

Ranking	Annualized Total Cost [€]	Cost of Electricity [€/kWh]	Grid Dependence [%]	LPSP[%]
1	42,294	1.27	6.71	0.21

Despite the price drops, the overall best solution still comes at an uneconomical price for electricity of 1.27 €/kWh, clearly unacceptable at a residential level. It is worth noticing, however, how the performances of this solution with respect to the second and third objective clearly outperform the ones reached in other cases. The greater availability of hydrogen clearly contributes to the abatement of the need for grid backups, and increases the system's reliability.

A more thorough analysis of all the solutions found suggests that, even if the most optimistic cost reduction forecasts for the hydrogen components come true in the next years, most probably they would still not favor their usage in small scale residential applications like this. In fact, as can be also noted in Figure 6.10, the beneficial effect of the components' price drop becomes significant when already high cost levels are reached. As a result, solutions with an acceptable cost of electricity (of maximum $0.4 \, \text{\&le /kWh}$) do not feature any form of hydrogen storage despite the lowered investment costs.

6.5. Unlimited PV Penetration

What the best trade-offs solutions of the previously studied scenarios have in common is the final configuration of PV panels installed. This result can be attributed to several factors: the load demand, the irradiance conditions considered and the physical constraints above all. The latter is of particular importance since the total installed capacity is very close to the maximum installment capacity, which effectively translates into a cap on the Community's own energy production.

As it was noted, these trade-offs also come at a high cost, while solutions characterized by low expenses are heavily relying on the outer grid. The limitation on the number of panels, in fact, affects the outcomes of the sizing in many ways: for example, the high energy conversion losses in the hydrogen equipment usage require the PV system to be oversized. When this is not possible (as in the Base Case), the adoption of this technology is not incentivized. Because of the competitive price of solar generation, moreover, configurations with a higher installed capacity could represent a mean to abate costs by increasing the autonomy of the system from the grid, while using the connection to maximize the reliability.

These considerations led to the formulation of a last scenario, investigating the optimal sizing configurations for The Green Village's community in a case with unlimited space for the instalment of solar panels. The unlimited availability is of course an unrealistic extreme, but it is intended to provide insights on the possible expansion of renewable energy capacity and its effects.

6.5.1. PARETO SET ANALYSIS

The composition of the best solutions found for this scenario does not significantly differentiate from the Base Case Scenario, with the exception of some noteworthy elements. When comparing the Pareto Set for the Unlimited PV penetration case (Figure 6.11) with the one displayed in 6.2, the similarity in shape and trend is evident.

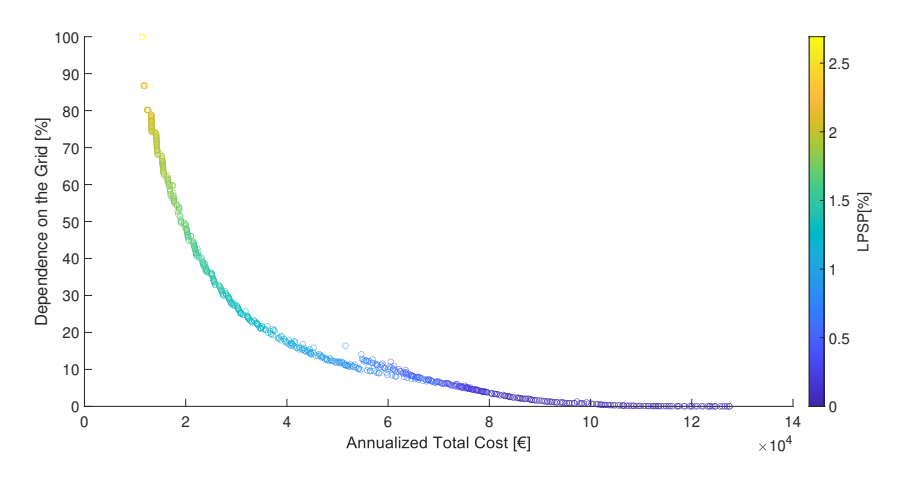


Figure 6.11: Pareto Set, Unlimited PV Penetration Scenario

The most noticeable difference is the forward displacement of the zone in which the steepness of the curve changes, earlier introduced as the transition zone from where hydrogen is introduced in the system. Because of the absence of a limitation in the number of panels, the necessity of investing in hydrogen equipment is "postponed", with low values of grid dependence (up to almost 10 percent) achievable just with a larger PV capacity and with the help of batteries storage.

A second significant result is found when analyzing the extreme solutions in terms of cost. The most expensive solution found in this scenario entails a considerably lower

cost with respect to the most expensive Base Case solution. It consists of 6 electrolyzers and 2 fuel cells, achieving complete and autonomous power supply with the help of 19 batteries and 104 kWp of installed PV capacity. With the possibility of installing a larger capacity of PV panels, the need for large capacities of the hydrogen system ceases because most of the storage can be dealt with the batteries, which are less expensive to employ.

The same reasoning is applied throughout all solutions, also influencing the top-ranked solution. In fact these result to be, on average, more economically convenient with respect to the Base Case, as can be noticed from Table 6.15.

Table 6.14: Unlimited PV Penetration Scenario, TOPSIS Best Solution: Sizing

Ranking	PV installed Capacity [kWp]	N.Batteries	N.Electrolyzers	N. Fuel Cells
1	85.41 (234 Panels)	3	1	1

Table 6.15: Unlimited PV Penetration Scenario, TOPSIS Best Solution: Performances

Ranking	Annualized Total Cost [€]	Cost of Electricity [€/kWh]	Grid Dependence [%]	LPSP[%]
1	34,874	1.05	20.87	1.20

A direct consequence of removing the panels' number limitation lies in their orientation: the easterly and westerly orientations, corresponding to some of the roofs in The Green Village, are completely discarded by the top solutions, which only feature panels mounted on the ground and on flat roofs, since these are the ones receiving the highest irradiation. The same number of panels is, in the two cases, differently distributed. In fact, when the limitations apply, the 75° orientation is the only one not fully exploited, while the others are filled to their limit as per indicated in Table 5.1. Differently, when no limitations are set, the optimal configuration would require most of the panels to be installed towards south, with few installed on the flat roofs.

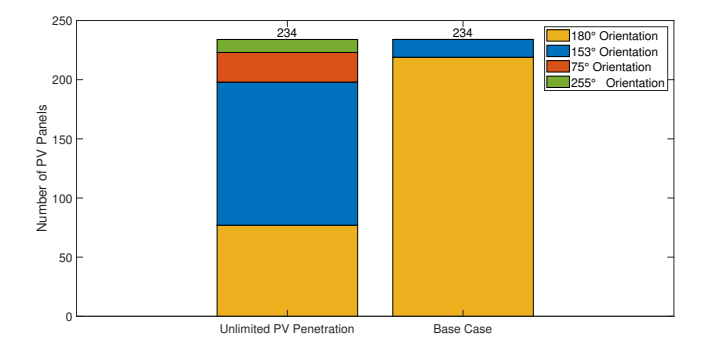


Figure 6.12: Distribution of the PV panels in the best solutions, Base Case vs Unlimited PV Penetration Scenario

As a result, the configurations considered in this scenario would lead to a higher amount of electricity generated, and a need for less storage equipment to achieve similar performances with respect to the Base Case. This is the main reason why not only the TOPSIS best solution results more convenient, but also why under these conditions more costefficient solutions can be found at parity of other parameters.

6.6. BEST SOLUTIONS OVERVIEW

In conclusion, Tables 6.16 and 6.17 show the sizing configurations and the performances of the top-ranked solutions for each scenario.

Table 6.16: Overview of the Best Solutions for all Scenarios : Sizing

Scenario	PV installed Capacity [kWp]	N.Batteries	N.Electrolyzers	N. Fuel Cells
Base Case	85.41 (234 Panels)	5	0	0
Infinite Grid	85.41 (234 Panels)	3	4	1
Real Time Pricing	85.41 (234 Panels)	4	0	0
Hydrogen Cost Decrease	85.41 (234 Panels)	3	13	1
Unlimited PV Penetration	85.41 (234 Panels)	3	1	1

Table 6.17: Overview of the Best Solutions for all Scenarios: Performances

Scenario	Annualized Total Cost [€]	Cost of Electricity [€/kWh]	Grid Dependence [%]	LPSP[%]
Base case	39,315	1.16	19.10	1.1
Infinite Grid	52,918	1.59	18.70	0
Real Time Pricing	36,422	1.09	20.34	1.16
Hydrogen Cost Decrease	42,294	1.27	6.71	0.21
Unlimited PV Penetration	34,874	1.05	20.87	1.20

7

CONCLUSION

The final Chapter of this thesis is focusing on generalizing the main findings of the research, detailing its limitations and suggesting future improvements for similar studies to be carried out. First, Section 7.1 will summarize and discuss the results of the optimization cases. Section 7.2 will provide answers to the research questions introduced at the start of the thesis. Section 7.3 will aim attention at some key features limiting this work, and lastly Section 7.4 will highlight possible areas towards which future studies could focus, using this work as a reference or a benchmark.

7.1. DISCUSSION

The main scope of this work was to find the optimal sizes for the components of the Energy Community in The Green Village, by taking into account different aspects and priorities. The use of a multi objective optimization algorithm, together with a decision making method and the formulation of scenarios has led to the individuation of optimal alternatives, albeit each of those has their points of questions.

The configuration of photovoltaic generation capacity to be installed in the system appears to be one of the factors less dependent on the boundary conditions of the problem. In all the studied cases, the best trade off solutions feature a total capacity of 85.41 kWp, composed of 121 panels placed on flat roofs, 36 on tilted roofs and 77 on the ground, exploiting almost all the available space for solar energy production. This distribution of capacity resulted to be the most convenient in terms of cost-benefit balance, regardless the storage solutions adopted to support the intermittent production. The simulation of a scenario with unlimited potential for solar power penetration highlighted how the overall costs can be further decreased by increasing the solar energy production.

The optimal storage capacity employed not only is the aspect most influenced by the surrounding conditions, but also the one that alters the most the performances of the Energy Community with respect to the three selected objectives: cost, reliability and

72 7. CONCLUSION

self-sufficiency. In the Base Case, where the conditions are the closest to the reality, the optimal configuration presents a storage capacity of slightly more than 75 kWh, only in the form of electrical energy storage with batteries. In cases when an unlimited amount of electricity can be withdrawn from the outer grid, the optimization suggests a more diverse use of storage, in which a part of the electrical storage capacity is replaced by the use of one fuel cell and 4 electrolyzers.

Such result gives reason to believe that, in small grid-connected applications like the one here studied, the use of hydrogen storage is quite inefficient: the high capital costs needed to invest in such equipment make the return of investment particularly small in absence of economies of scale. Furthermore, the need for an oversized PV system to effectively make up for the energy lost in the conversion consists in an implicit additional cost. Site-specific limitations and relatively low PV penetration potential limiting such oversizing, therefore, also contribute in disfavoring hydrogen storage in favor of using batteries for the short term storage, and relying on grid imports in case of necessity.

This is also confirmed by the analysis of a scenario in which the capital costs of the hydrogen components are set to decline, according to optimistic forecasts found in scientific literature. Even with such premises, the benefits in terms of security of supply and self-sufficiency brought by the adoption of such long term storage are not balanced by the additional expenses, and the grid still represents the most favourable mean to supply electricity in times of scarcity. Generally, it can be concluded that this study confirms the skepticism about the adoption of hydrogen storage, although without excluding its potential application on a large scale, for example at the utility level.

Price uncertainties were additionally investigated through the study of two additional scenarios. The simulation of a Real-Time Pricing Scenario, despite confirming the high costs necessary to achieve high degrees of self sufficiency and reliability, has demonstrated that the application of time-varying tariffs can efficiently reduce the prosumers' expenses, as well as being beneficial for grid operators. In particular, smart price-aware energy management strategies can represent a significant further advantage for the Energy Community's users.

The main challenge of this work was to obtain satisfactory solutions despite the clear contradicting nature of the goals considered. While the clash between cost and self-sufficiency was straightforward to predict, the influence of the reliability objective was spotlighted by the analysis of the Infinite Grid Scenario. When the possibility of power failures is completely overlooked, the additional costs to reach full reliability are consistently high (to a varying degree, depending on how much such additional reliability is provided by the system's own production). On the other hand, accepting limited outages (occurring less than 1.5 percent of the time) brings a considerable advantage in terms of cost reduction.

Overall, the clashing nature of the objectives is reflected on the best trade offs found. Despite the best solutions would achieve an optimal compromise considering all the

necessities of the Community, this study has also shown how the overall costs (higher than $1 \notin k$ Wh) would be significantly high if compared to residential energy prices. In order for the costs to be competitive, the system would need to be sized in such a way that at least half of the load would be supplied with imports from the external grid. These solutions feature about half of the PV capacity with respect to the best trade offs, and a maximum of 30 kWh of electrical storage capacity.

7.2. Answering The Research Questions

The thesis work has been conducted in order to give an answer to specific research questions formulated in 1.2, which will be here answered. The first question posed was:

What is the best sizing configuration for a grid-connected energy community in The Green Village under technical and economical aspects?

To answer this question, it is worth to mention that the best solutions individuated could be adopted in The Green Village as part of the pilot 27/7 Energy Lab project, in which the costs are partly covered with research funding and not totally by the Community Users. In this case, both the Base Case and the Infinite Grid Scenario sizing configurations would be suitable, with the latter employing both short term storage in the form of batteries and long term storage in the form of hydrogen. However, when translating such results to real small scale Energy Community cases, the presence of a reliable grid-connection capable of supplying at least half of the load demand is of capital importance to face reasonable costs, and the use of hydrogen storage is still far from being convenient.

Secondly, the uncertainty about the future pricing schemes evolution was addressed through the following question:

What is the influence of different electricity pricing conditions on the design and sizing of a grid-connected energy communities?

This research has shown how the adoption of time-varying electricity tariffs is beneficial for Energy Communities users who can exploit the possibility of selling energy to the outer grid to gain profits. The optimal sizing configuration, however, is not significantly affected with respect to when flat tariffs are applied. A decrease in the Energy Community users' charges can be achieved by employing smart energy management strategies, aware of the current price of electricity. This benefit, however, is not significant enough to justify the adoption of, for example, a larger storage capacity to further exploit the opportunity of windfall profits, at least in small scale applications like the one here studied.

The third research question, regarding the uncertainties about the use of the hydrogen storage, was:

To what extent the adoption of a hydrogen system can benefit a grid-connected energy community under different pricing conditions?

74 7. Conclusion

This research has shown that the adoption of an hydrogen storage system is far from being convenient on a small scale residential level, regardless the pricing conditions. In both the flat and time-varying tariff scenarios, the best trade off solutions do not employ any kind of hydrogen storage, because of the uneconomical capital costs involved and the absence of economies of scale for such small investments. This result is confirmed by the simulation of a case in which such costs significantly decrease, on the basis of forecasts depending on the future growth of the hydrogen market. The analysis, however, has also highlighted the importance of long term storage in achieving full self-sufficiency and extremely high reliability, two conditions that are hardly ever met with the sole use of short term storage in the form of batteries. While this result might less relevant when dealing with grid-connected systems, it acquires more significance for research focused on remote, off-grid configurations.

7.3. LIMITATIONS OF THE WORK

The results of this thesis have been obtained after a thorough application of good engineering practices applied with a critical attitude. Nonetheless, it is important to emphasize some limitations that might have influenced the final findings, to a certain extent.

As per the solar energy output modeling, shading effects were not taken into account. As mentioned, the actual data relative to the incident irradiance in Delft were used to obtain the estimate of the final output, but with the assumption of a clear horizon that is not always respected for some of the areas in which the panels are assumed to be placed. It is true, however, that most of TGV's area does not have significant obstacles to the penetration of sun rays, especially for the rooftops placed at the center of the village. Some trees surrounding the environment could be cause of partial shading, just like the buildings themselves can represent an obstacle for the grounded panels.

Similarly, the simple modeling of the system's components implemented does not account for aspects such as temperature influence (e.g. in the start up phases of the electrolyzers/fuel cells) and other influencing factors. The energy flow modeling doesn't involve electrical parameters like the system's frequency and voltage, but it was meant to have an overview on the electrical energy exchanges throughout all the components. The necessity to look at the system's functioning from a broad perspective made it necessary to simplify some specific aspects in order to be able to focus on the macroscopic aspects of the sizing.

The case study itself, moreover, was of course influenced by the availability of the consumption data. As mentioned in Section 4.2, a post-processing of such data was necessary to deal with some gaps and inconsistencies. Most of it were solved also in consultation with an advisor from The Green Village, but it is necessary to clarify that the load demand used in this study is not completely representative of the real-life load in the year considered. The limited availability also influenced the time span of the simulations, which is now currently of 1 year: clearly, a higher data availability and longer simulations could have brought to more accurate results.

Lastly, the optimization is surely depending on the available computing tools. The simulation parameters were tuned to obtain a satisfactory results in terms of balance between computational time and accuracy of the results, but clearly there is still room for improvement. For example, the adoption of supercomputers and specifically tailored optimization software could bring additional value to the research by expanding the solution space and the vastness of the obtained results. Moreover, more powerful computers would allow to shorten the time required to obtained the results of simulations, allowing to gather more results and increasing the precision.

7.4. RECOMMENDATIONS FOR FUTURE RESEARCH

For future work, some considerations can be drawn on the basis of the findings of this thesis. Based on the available data provided by The Green Village, this work has focused on providing the electricity needs of the Community, assuming all houses to be fully electrified (which is actually the case for the reference houses considered). Following research may include the heating necessities of Energy Community by means of the introduction of an heat grid: because of the residual heat generated by the fuel cells, this technology could play a more relevant role in such cases.

The analysis of the Real Time Price Scenario has brought to light the possibilities for cost abatement with the adoption of a smart energy management strategy. More specific works focusing on the comparison of these strategies could be carried out to find the optimal energy dispatch method with respect to this application.

More diverse configurations can also be part of future research: the simulations of the Unlimited PV Penetration Scenario showed how a larger availability for solar energy capacity can represent a good way to abate costs. Investigating alternative renewable generation sources like biomass generators or the use of small wind turbines can represent a way to overcome the physical constraints of the location studied. Moreover, alternative storage technologies should be considered to balance the need for storage with the high costs involved.

Lastly, as mentioned in the previous section, future work could focus on improving this and similar research by adopting more accurate models for the components used and their interactions. As an example, considerations about the batteries' cycling and its influence on their lifetime can be taken into account, as well as a more detailed modeling of the electrical characteristics of the energy flows.



APPENDIX - LITERATURE REVIEW SUMMARY

The following table summarizes the most relevant studies reviewed about the adoption of Optimization Algorithm to size small and medium-scale Energy Systems.

Authors, Year	System's configuration	Objective(s)	Optimization Method	Alternatives Selection Method
Wang et al., 2020	PV-WT- Biomass- storage, off-grid	Minimize Cost,Land Use and Vi- sual Impact	NSGA-II	TOPSIS (multi-actor criteria)
Attia et al., 2021	PV only, grid- connected	Minimize: Total Costs; Carbon Emissions. Maximize Reliability	Augmented epsilon	TOPSIS constraint 2 (AUGME-CON 2)
Bista et al., 2020	PV-BAT-DG- Biomass, grid connected	-	HOMER PRO	-

Dash et al., 2018	PV-Diesel- WT-Batteries (considered alternatives, configuration oprimized by HOMER), both grid connected and off-grid	Cost	HOMER PRO	-
Akhavan Shams and Ahmadi, 2021	PV-WT-BAT, grid con- nected & PV-WT-H2, grid con- nected	Annual Total Cost (Emissions are taken into account as a cost in the obj. Function) Different degrees of self sufficiency are imposed as a constraint	GA	-
Kusakana, 2019	Storage Only	Cost	Linear Opti- mization	-
Fan et al., 2022	PV-H2-BAT + Heating utilities, Grid connected	Annual Carbon Emissions; Annual Total Costs; Total Grid Interaction	NSGA-II	TOPSIS
Narayan et al., 2019	PV-BAT, off-grid	Minimize Cost (costs are minimized by maximizing the battery lifetime while minimizing their size), LLP, Energy dump	NSGA-II (ga- multiobj in MATLAB)	-

Human et al., 2014	PV-WT-Bat- H2, off-grid	Maximize: Efficiency and Reliabil- ity Minimize: Total costs	SOGA and MOGA	-
Alsayed et al., 2013	PV-WT, grid connected	Minimize Emissions and Costs. Maximize Social Acceptance (based on land use)	Generation of alterna- tives based on step-sized variations ranging from 100% PV to 100% WTs.	Various Multi Criteria Deci- sion Making Approaches.
Dufo-López and Bernal- Agustín, 2008	PV-WT- Bat-H2- Diesel,off- grid	Minimize : Total Cost, Unmet load, Carbon Emissions	Strength Pareto Evolutionary Algorithm (SPEA), for the sizing and a secondary algorithm for the control. The secondary algorithm is a GA that searches for the best control strategy for each combination of components in the main algorithm. This GA is mono- objective (minimization of the costs)	-

Kiptoo et al., 2019	PV-WT- Pumped Heat storage, off grid	Minimize To- tal Cost and Loss of Power supply Prob- ability	MOPSO	-
Baghaee et al., 2017	PV-WT-H2, off-grid	Costs over the 20 years of operation, Loss of Load Expected and Loss of Energy	MOPSO	Fuzzy method
Yu et al., 2021	PV-WT-BAT, off-grid	Minimize Cost, Loss Load, Dumped Energy	NSGA-III	-
Yaghi et al., 2019	PV-WT-BAT- Diesel Gen- erator, grid connected	Minimize Cost and Emissions	NSGA-II	-
Wentao et al., 2018	PV-WT-BAT- Diesel Gen- erator, grid connected	Minimize Cost, Emissions, Loss of Power Supply Probability	MOPSO	-
Jahangir et al., 2016	PV-WT-BAT- Diesel Gen- erator, grid connected	Minimize Investment Cost, Emissions and Power Loss	GA, three objectives inside a single obj. Function	-
C. Zhang et al., 2022	PV-H2-BAT + Heating utilities, Grid connected	Minimize Cost of Energy Maximize ER(Demand/ Total Input Energy); Renewable fraction	Sequential Quadratic Program- ming	" Analytic Hierarchy Process (AHP) and Criteria Importance Through Intercriteria Correlation (CRITIC) mixed weighting method

Shang et al., 2023	PV-WT-H2- GT, grid- connected	Maximize Net Present Benefit. Minimize Carbon emissions and Loss of Energy Conversion	NSGA-II	Entropy model and Cumulative Prospects
Raja and Detroja, 2018	PV-BAT, grid connected	Cost	Single Objective Linear Programming	-
N. Zhang et al., 2021	PV-WT-BAT, off-grid	Minimize Cost, Loss of Power Supply Probability	MOPSO	Selection of the solution based on the normalized values of the objective functions for each solution
Ghorbani et al., 2018	PV-WT-BAT, off-grid	Minimize Cost, Loss of Power Supply Probability	Hybrid GA- PSO	-
B. Li and Roche, 2021	PV-Bat-H2, connected to a Generating station with same charac- teristics	Minimize: Total costs, Exchanged Energy. Maximize: Installed Renewable capacity	NSGA-II	-
Paulitschke et al., 2015	PV-Bat-H2, off-grid	Minimize Cost. Maximize: Security of Supply, Remaining H2 at the end of the year	PSO	-
Gharibi and Askarzadeh, 2019	PV-H2- Diesel, grid connected	Minimize Cost, Loss of Power Supply Probability	Multi Objective Crow Search Algorithm (MOCSA)	-

B

APPENDIX B - RESULTS OF THE OPTIMIZATION

In this Appendix, the results of the optimization algorithm are shown. Because of the large amount of variables and results involved, it was not possible to display every single result of the simulations. Therefore, 20 solutions per Scenario were selected, spanning over the whole Pareto Set. These solutions are shown in ascending order according to the result of the TOPSIS ranking method applied.

Table B.1: Base Case: Sizing Results

Ranking	N. Panels, 153°	N.Panels, 180°	N.Panels, 255°	N.Panels,75°	N. Batteries	N.Electrolyzers	N. Fuel Cells	H2 Storage Capacity [kg]	Threshold SoC
1	121	22	11	25	5	0	0	50	0.01
2	121	77	11	25	4	0	0	51	0.11
3	121	77	6	25	5	0	0	52	0.04
4	121	77	6	25	4	0	0	57	0.08
5	121	77	17	25	4	0	0	51	0.16
176	103	72	0	3	2	0	0	50	0.10
177	121	77	8	25	4	5	1	254	0.16
178	88	77	10	13	2	0	0	50	0.17
179	121	77	11	25	9	4	1	245	0.20
180	103	77	9	10	4	3	1	147	0.18
351	73	09	1	6	1	0	0	50	0.52
352	121	77	17	25	9	10	1	440	0.16
353	64	92	0	0	1	0	0	50	0.41
354	121	77	17	25	6	8	1	395	0.22
355	121	77	11	25	8	6	1	434	0.22
969	121	77	17	25	29	17	2	526	0.76
269	121	77	17	25	29	17	2	529	0.77
869	121	77	17	25	31	16	2	521	0.74
669	121	77	17	25	30	17	2	525	0.76
200	121	27	17	25	30	17	2	525	0.76

Table B.2: Base Case: Objective Functions Values Results

Ranking	Ranking Annualized Total Cost	Grid Dependence [%]	Loss of Power Supply Probability [%]
1	39,315.28 €	19.10	1.10
2	37,006.52 €	20.34	1.17
3	39,244.19€	19.24	1.10
4	36,990.76€	20.49	1.17
2	38,164.05€	19.92	1.15
176	27,327.42 €	30.83	1.38
177	62,581.00€	10.95	0.53
178	28,627.47 €	29.99	1.36
179	64,140.54 €	10.31	0.47
180	51,641.51 €	16.73	0.84
351	22,064.07 €	41.92	1.57
352	86,366.75€	4.79	0.11
353	21,964.21 €	42.01	1.57
354	86,874.23 €	4.65	0.11
355	86,906.64 €	4.76	0.10
969	173,073.91 €	0.01	0.00
269	173,150.91 €	0.01	0.00
869	174,965.33 €	0.00	0.00
669	175,546.55€	0.00	0.00
200	175,546.55€	0.00	0.00

Table B.3: Infinite Grid: Sizing Results

Ranking	N. Panels, 153°	N.Panels, 180°	N.Panels, 255°	N.Panels, 75°	N. Batteries	N.Electrolyzers	N. Fuel Cells	H2 Storage Capacity [kg]	Threshold SoC
1	121	77	11	25	3	4	1	187	0.03
2	121	77	11	25	3	4	1	185	0.24
3	121	92	13	24	4	3	1	166	0.19
4	121	77	10	25	4	3	1	164	0.25
5	121	75	13	25	4	4	1	212	0.12
176	121	77	0	0	3	2	1	78	0.22
177	121	77	8	25	5	5	1	254	0.27
178	121	77	17	25	5	5	1	274	0.22
179	121	77	11	25	4	9	1	288	0.21
180	121	77	5	25	5	5	1	254	0.27
351	85	77	0	0	4	0	0	50	0.23
352	85	77	0	0	4	0	0	50	0.07
353	121	77	12	25	5	7	1	332	0.28
354	121	77	12	25	5	7	1	338	0.24
355	121	77	13	25	5	7	1	343	0.16
969	121	77	17	25	29	17	2	529	0.77
269	121	77	17	25	31	16	2	521	0.74
869	121	77	17	25	31	16	2	523	0.74
669	121	77	17	25	30	17	2	525	92.0
200	121	77	17	25	30	17	2	525	0.76

Table B.4: Infinite Grid: Objective Functions Values Results

Ranking	Ranking Annualized Total Cost	Grid Dependence [%]	Loss of Power Supply Probability [%]
1	52,917.62 €	18.70	0
2	52,879.72 €	18.75	0
3	51,330.53€	19.95	0
4	51,252.57 €	20.03	0
2	55,571.63€	16.75	0
176	41,836.90€	28.98	0
177	61,770.48 €	13.69	0
178	63,245.47 €	12.56	0
179	63,568.72 €	12.34	0
180	61,721.82 €	13.76	0
351	27,272.89 €	42.93	0
352	27,272.89€	42.93	0
353	70,760.17 €	9.62	0
354	70,846.87 €	9.56	0
355	70,946.10€	9.48	0
969	172,499.67 €	0.01	0
269	174,199.92€	0.00	0
869	174,247.73 €	0.00	0
669	174,852.43€	0.00	0
200	174,852.43€	0.00	0

Table B.5: Real Time Pricing Scenario: Sizing Results

Ranking	Ranking N. Panels, 153°	N.Panels, 180°	N.Panels, 255°	N.Panels, 75°	N. Batteries	N.Electrolyzers	N. Fuel Cells	H2 Storage Capacity [kg]	Threshold SoC
	121	77	11	25	4	0	0	50	0.15
2	121	77	8	25	4	0	0	50	0.16
3	120	77	2	17	4	0	0	51	0.24
4	120	77	0	17	4	0	0	50	0.13
5	119	77	11	23	4	0	0	50	0.64
176	121	77	11	25	5	4	1	229	0.14
177	86	75	0	3	1	0	0	50	0.32
178	121	77	12	25	5	3	1	188	0.17
179	119	92	9	24	5	3	ı	174	0.13
180	119	92	12	24	4	4	1	218	0.21
351	121	77	17	25	7	8	1	388	0.19
352	121	77	15	25	7	8	1	390	0.21
353	35	92	0	3	1	0	0	50	0.46
354	121	77	15	25	7	8	1	384	0.31
355	121	77	12	25	7	8	1	378	0.16
969	121	77	17	25	29	17	2	527	0.76
269	121	77	17	25	29	17	2	529	0.77
869	121	77	17	25	31	16	2	521	0.74
669	121	77	17	25	30	17	2	525	0.76
200	121	77	17	25	30	17	2	525	92.0

Table B.6: Real Time Pricing Scenario: Objective Functions Values Results

Ranking Annu	Annualized Total Cost	Grid Dependence [%]	Loss of Power Supply Probability [%]
1	36,422.23 €	20.34	1.17
2	36,258.92 €	20.56	1.17
3	34,615.71 €	21.84	1.20
4	34,493.91 €	22.00	1.20
5	36,205.36€	20.71	1.18
176	61,126.44 €	11.06	0.49
177	24,104.89€	35.04	1.51
178	58,267.08 €	12.44	0.62
179	56,699.30€	13.22	69:0
180	58,413.05 €	12.29	0.62
351	81,812.21 €	5.44	0.11
352	81,730.55 €	5.57	0.13
353	18,599.48 €	48.45	1.66
354	81,641.43€	5.65	0.13
355	81,395.74 €	5.83	0.14
969	173,227.62 €	0.01	0.00
269	173,265.29 €	0.01	0.00
869	175,097.57 €	0.00	0.00
669	175,687.78 €	0.00	0.00
200	175,687.78€	0.00	0.00

Table B.7: Hydrogen Cost Decrease Scenario: Sizing Results

Ranking	Ranking N. Panels, 153°	N.Panels, 180°	N.Panels, 255°	N.Panels, 75°	N. Batteries	N.Electrolyzers	N. Fuel Cells	H2 Storage Capacity [kg]	Threshold SoC
-	121	77	11	25	3	13	1	408	0.15
2	121	77	10	25	3	13	1	406	0.10
3	121	77	11	25	3	15	1	432	0.09
4	121	77	11	25	3	12	1	394	0.20
5	121	77	7	25	3	14	1	411	0.20
176	95	92	2	9	ı	6	1	165	0.03
177	85	75	0	1	2	7	1	185	0.07
178	77	74	0	11	2	7	1	196	0.11
179	96	72	1	6	ı	6	1	189	90.0
180	80	89	0	14	2	7	1	163	0.01
351	09	64	0	2	ı	2	1	56	0.07
352	57	64	0	2	1	2	1	58	0.07
353	49	53	0	4	ı	5	1	09	0.07
354	55	69	0	1	0	4	1	64	0.08
355	121	77	17	25	6	25	2	556	0.53
969	121	77	17	25	26	26	2	556	0.85
269	121	77	17	25	26	26	2	556	0.85
869	121	77	17	25	26	26	2	556	0.85
669	0	0	0	0	0	0	0	50	0.02
200	0	0	0	0	0	0	0	50	0.00

Table B.8: Hydrogen Cost Decrease Scenario: Objective Functions Values Results

Ranking	Annualized Total Cost	Grid Dependence [%]	Loss of Power Supply Probability [%]
1	44,293.82 €	6.79	0.21
2	44,231.60€	6.85	0.23
3	45,360.00€	6.14	0.17
4	43,746.41 €	7.15	0.26
2	44,570.10€	6.78	0.21
176	31,751.40€	18.61	0.98
177	31,245.60€	19.57	0.94
178	31,386.44 €	19.47	0.94
179	31,895.28 €	18.56	0.98
180	31,139.83€	19.78	0.95
351	22,575.29 €	36.34	1.49
352	22,589.38€	36.41	1.49
353	22,807.54 €	35.70	1.55
354	22,030.49€	36.09	1.62
355	67,128.17 €	0.59	0.00
969	109,851.90€	0.00	0.00
269	109,862.18€	0.00	0.00
869	109,862.18€	0.00	0.00
669	11,026.51 €	100.00	2.69
200	11,026.51 €	100.00	2.69

Table B.9: Unlimited PV Penetration Scenario: Sizing Results

Ranking	Ranking N. Panels, 153°	N.Panels, 180°	N.Panels, 255°	N.Panels, 75°	N. Batteries	N.Electrolyzers	N. Fuel Cells	H2 Storage Capacity [kg]	Threshold SoC
-	15	219	0	0	3	0	0	51	0.45
2	29	221	0	0	4	0	0	52	0.40
3	10	221	0	0	4	0	0	52	0.34
4	11	233	0	0	3	0	0	52	0.36
2	34	197	0	0	3	0	0	53	0.38
176	2	184	0	0	1	0	0	51	0.43
177	16	139	0	0	2	0	0	51	0.47
178	8	180	0	0	1	0	0	50	90.0
179	10	144	0	0	2	0	0	50	0.44
180	8	179	0	0	1	0	0	50	0.40
351	8	95	0	0	2	0	0	50	0.51
352	10	110	0	0	1	0	0	54	0.34
353	12	91	0	0	2	0	0	50	0.28
354	42	233	0	0	2	9	1	329	0.21
355	56	237	0	3	9	5	1	323	0.18
969	131	269	3	2	18	9	2	422	0.71
269	141	304	9	6	16	9	2	413	0.72
869	125	259	3	4	19	9	2	411	0.71
669	0	0	0	0	0	0	0	50	0.78
200	0	0	0	0	0	0	0	50	0.00

Table B.10: Unlimited PV Penetration Potential Scenario: Objective Functions Values Results

Ranking	Annualized Total Cost	Grid Dependence [%]	Loss of Power Supply Probability [%]
1	34,874.24 €	20.87	1.20
2	38,780.83 €	17.89	1.12
3	36,962.76€	19.49	1.15
4	36,265.31 €	19.93	1.18
2	34,730.96€	21.23	1.21
176	26,792.92 €	32.22	1.47
177	25,518.28 €	34.20	1.41
178	26,726.15€	32.39	1.47
179	25,466.76€	34.35	1.41
180	26,677.57 €	32.55	1.48
351	21,047.81 €	46.04	1.61
352	20,426.41 €	46.48	1.63
353	21,047.49€	46.07	1.61
354	73,464.21 €	6.04	0.29
355	74,549.21 €	5.39	0.25
969	126,957.11 €	0.00	0.00
269	127,419.45€	0.00	0.00
869	127,465.28 €	0.00	0.00
669	11,381.28 €	100.00	2.69
200	11,381.28 €	100.00	2.69

- Abdmouleh, Z., Gastli, A., Ben-Brahim, L., Haouari, M., & Al-Emadi, N. A. (2017). Review of optimization techniques applied for the integration of distributed generation from renewable energy sources. *Renewable Energy, 113*, 266–280. https://doi.org/10.1016/J.RENENE.2017.05.087
- ACER. (2023). Report on Electricity Transmission and Distribution Tariff Methodologies in Europe (tech. rep.). ACER European Union Agency for the Cooperation of Energy Regulators. Ljubljana. https://www.acer.europa.eu/Publications/ACER_electricity_network_tariff_report.pdf
- Akhavan Shams, S., & Ahmadi, R. (2021). Dynamic optimization of solar-wind hybrid system connected to electrical battery or hydrogen as an energy storage system. *International Journal of Energy Research*, *45*(7), 10630–10654. https://doi.org/10.1002/er.6549
- Alsayed, M., Cacciato, M., Scarcella, G., & Scelba, G. (2013). Multicriteria optimal sizing of photovoltaic-wind turbine grid connected systems. *IEEE Transactions on Energy Conversion*, 28(2), 370–379. https://doi.org/10.1109/TEC.2013.2245669
- Ananth, D., & Vineela, K. (2021). A review of different optimisation techniques for solving single and multi-objective optimisation problem in power system and mostly unit commitment problem. *International Journal of Ambient Energy, 42*(14), 1676–1698. https://doi.org/10.1080/01430750.2019.1611632
- Askarzadeh, A. (2016). A novel metaheuristic method for solving constrained engineering optimization problems: Crow search algorithm. *Computers & Structures*, 169, 1–12. https://doi.org/10.1016/J.COMPSTRUC.2016.03.001
- Attia, A. M., Al Hanbali, A., Saleh, H. H., Alsawafy, O. G., Ghaithan, A. M., & Mohammed, A. (2021). A multi-objective optimization model for sizing decisions of a grid-connected photovoltaic system. *Energy*, 229, 120730. https://doi.org/10.1016/J. ENERGY.2021.120730
- Baghaee, H., Mirsalim, M., & Gharehpetian, G. (2017). Multi-objective optimal power management and sizing of a reliable wind/PV microgrid with hydrogen energy storage using MOPSO. *Journal of Intelligent and Fuzzy Systems*, *32*(3), 1753–1773. https://doi.org/10.3233/JIFS-152372
- Battelle. (2016). *Manufacturing Cost Analysis of PEM Fuel Cell Systems for 5- and 10-kW Backup Power Applications* (tech. rep.). Columbus. https://www.energy.gov/eere/fuelcells/articles/manufacturing-cost-analysis-pem-fuel-cell-systems-5-and-10-kw-backup-power
- Betere Marcos, G. (2022). *Simulation of a Hybrid Short-Term & Long-Term Energy Storage System in Energy Communities* (tech. rep.). Delft University of Technology. Delft. http://resolver.tudelft.nl/uuid:d90b840c-24d5-4056-b790-da848906d092
- Bista, A., Khadka, N., Shrestha, A., & Bista, D. (2020). Comparative analysis of different hybrid energy system for sustainable power supply: A case study. *IOP Confer-*

- ence Series: Earth and Environmental Science, 463(1), 12045. https://doi.org/10.1088/1755-1315/463/1/012045
- Centraal Bureau voor de Statistiek. (2023). Natural gas and electricity, average prices of end users. https://www.cbs.nl/nl-nl/cijfers/detail/81309NED#shortTableDescription
- Cigolotti, V., & Genovese, M. (2021). STATIONARY FUEL CELL APPLICATIONS: CURRENT AND FUTURE TECHNOLOGIES COSTS, PERFORMANCES, AND POTENTIAL (tech. rep.). IEA Technology Collaboration Programme Advanced Fuel Cells. https://www.ieafuelcell.com/fileadmin/publications/2021/2021_AFCTCP_Stationary_Application_Performance.pdf
- Collins, L. (2022). Enapter eyes 83% cost reduction for its unique AEM hydrogen electrolysers by 2025. https://www.rechargenews.com/energy-transition/exclusive-enapter-eyes-83-cost-reduction-for-its-unique-aem-hydrogen-electrolysers-by-2025/2-1-1256489
- Dash, R., Behera, L., Mohanty, B., & Kumar Hota, P. (2018). Cost and sensitivity analysis of a microgrid using HOMER-Pro software in both grid connected and standalone mode. 2018 International Conference on Recent Innovations in Electrical, Electronics and Communication Engineering, ICRIEECE 2018, 3444–3449. https://doi.org/10.1109/ICRIEECE44171.2018.9009218
- Detz, R., & Weeda, M. (2022). *Projections of electrolyzer investment cost reduction through learning curve analysis* (tech. rep.). TNO. Amsterdam.
- de Vries, T. N., Bronkhorst, J., Vermeer, M., Donker, J. C., Briels, S. A., Ziar, H., Zeman, M., & Isabella, O. (2020). A quick-scan method to assess photovoltaic rooftop potential based on aerial imagery and LiDAR. *Solar Energy*, 209, 96–107. https://doi.org/10.1016/J.SOLENER.2020.07.035
- Dufo-López, R., & Bernal-Agustín, J. (2008). Multi-objective design of PV-wind-diesel-hydrogen-battery systems. *Renewable Energy*, 33(12), 2559–2572. https://doi.org/10.1016/j.renene.2008.02.027
- Dutta, G., & Mitra, K. (2017). A literature review on dynamic pricing of electricity. *Journal of the Operational Research Society*, *68*(10), 1131–1145. https://doi.org/10.1057/s41274-016-0149-4
- ENTSO-E Transparency Platform. (2023). Day-ahead Prices. https://transparency.entsoe.
- Fan, G., Liu, Z., Liu, X., Shi, Y., Wu, D., Guo, J., Zhang, S., Yang, X., & Zhang, Y. (2022). Energy management strategies and multi-objective optimization of a near-zero energy community energy supply system combined with hybrid energy storage. Sustainable Cities and Society, 83, 103970. https://doi.org/10.1016/J.SCS.2022. 103970
- Gharibi, M., & Askarzadeh, A. (2019). Technical and economical bi-objective design of a grid-connected photovoltaic/diesel generator/fuel cell energy system. *Sustainable Cities and Society*, *50*. https://doi.org/10.1016/j.scs.2019.101575
- Ghorbani, N., Kasaeian, A., Toopshekan, A., Bahrami, L., & Maghami, A. (2018). Optimizing a hybrid wind-PV-battery system using GA-PSO and MOPSO for reducing cost and increasing reliability. *Energy*, *154*, 581–591. https://doi.org/10.1016/j.energy.2017.12.057

Hammerstrom, D. J. (2022). On Harmonizing Today's Regulated Tariffs and Future Dynamic Electricity Pricing. 2022 IEEE Power & Energy Society General Meeting (PESGM), 1–5. https://doi.org/10.1109/PESGM48719.2022.9916765

- Hledik, R., & Lazar, J. (2016). *Distribution System Pricing With Distributed Energy Resources* (tech. rep.). Ernest Orlando Lawrence Berkeley National Laboratory.
- Human, G., Van Shcoor, G., & Uren, K. (2014). Interdependent multi-objective sizing and control optimisation of a renewable energy hydrogen system. *IFAC Proceedings Volumes (IFAC-PapersOnline)*, 19, 10257–10262. https://doi.org/10.3182/20140824-6-za-1003.02416
- IEA. (2022). *Global Hydrogen Review 2022* (tech. rep.). International Energy Agency. Paris. https://www.iea.org/reports/global-hydrogen-review-2022
- Jahangir, H., Ahmadian, A., & Golkar, M. (2016). Multi-objective sizing of grid-connected micro-grid using Pareto front solutions. *Proceedings of the 2015 IEEE Innovative Smart Grid Technologies - Asia, ISGT ASIA 2015*. https://doi.org/10.1109/ISGT-Asia.2015.7387138
- Kiptoo, M. K., Adewuyi, O. B., Lotfy, M. E., Senjyu, T., Mandal, P., & Abdel-Akher, M. (2019). Multi-Objective Optimal Capacity Planning for 100% Renewable Energy-Based Microgrid Incorporating Cost of Demand-Side Flexibility Management. Applied Sciences, 9(18). https://doi.org/10.3390/app9183855
- Koirala, B. P., Koliou, E., Friege, J., Hakvoort, R. A., & Herder, P. M. (2016). Energetic communities for community energy: A review of key issues and trends shaping integrated community energy systems. *Renewable and Sustainable Energy Reviews*, 56, 722–744. https://doi.org/10.1016/J.RSER.2015.11.080
- Konak, A., Coit, D., & Smith, A. (2006). Multi-objective optimization using genetic algorithms: A tutorial. *Reliability Engineering and System Safety*, 91(9), 992–1007. https://doi.org/10.1016/j.ress.2005.11.018
- Kusakana, K. (2019). Economic performance of a grid-interactive system with storage under a dynamic electricity pricing environment. *Proceedings of the IEEE International Conference on Industrial Technology, 2019-Febru,* 619–624. https://doi.org/10.1109/ICIT.2019.8755243
- Li, B., & Roche, R. (2021). Sizing a 100% renewable energy based power supply system based on multi-objective optimization. *2021 IEEE Madrid PowerTech*, 1–6. https://doi.org/10.1109/PowerTech46648.2021.9495095
- Li, N., Lukszo, Z., & Schmitz, J. (2023). An approach for sizing a PV-battery-electrolyzer-fuel cell energy system: A case study at a field lab. *Renewable and Sustainable Energy Reviews*, *181*, 113308. https://doi.org/10.1016/J.RSER.2023.113308
- Londo, M., Matton, R., Usmani, O., van Klaveren, M., Tigchelaar, C., & Brunsting, S. (2020). Alternatives for current net metering policy for solar PV in the Netherlands: A comparison of impacts on business case and purchasing behaviour of private homeowners, and on governmental costs. *Renewable Energy*, 147, 903–915. https://doi.org/10.1016/J.RENENE.2019.09.062
- Narayan, N., Chamseddine, A., Vega-Garita, V., Qin, Z., Popovic-Gerber, J., Bauer, P., & Zeman, M. (2019). Exploring the boundaries of Solar Home Systems (SHS) for offgrid electrification: Optimal SHS sizing for the multi-tier framework for house-

- hold electricity access. *Applied Energy*, 240, 907–917. https://doi.org/10.1016/J. APENERGY.2019.02.053
- Nikiforow, K., Pennanen, J., Ihonen, J., Uski, S., & Koski, P. (2018). Power ramp rate capabilities of a 5kW proton exchange membrane fuel cell system with discrete ejector control. *Journal of Power Sources*, *381*, 30–37. https://doi.org/10.1016/J. JPOWSOUR.2018.01.090
- Paulitschke, M., Bocklisch, T., & Böttiger, M. (2015). Sizing Algorithm for a PV-battery-H2-hybrid System Employing Particle Swarm Optimization. *Energy Procedia*, 73, 154–162. https://doi.org/10.1016/J.EGYPRO.2015.07.664
- Raja, P., & Detroja, K. (2018). Optimal sizing of PV panels and battery for grid connected load under dynamic pricing. 2018 Indian Control Conference, ICC 2018 Proceedings, 2018-Janua, 166–171. https://doi.org/10.1109/INDIANCC.2018.8307972
- Rao, R. V. (2013). *Decision Making in Manufacturing Environment Using Graph Theory and Fuzzy Multiple Attribute Decision Making Methods*. Springer London. https://doi.org/10.1007/978-1-4471-4375-8
- Reindl, D. T., Beckman, W. A., & Duffie, J. A. (1990). Evaluation of hourly tilted surface radiation models. *Solar Energy*, 45(1), 9–17. https://doi.org/10.1016/0038-092X(90)90061-G
- Ryan, L., Monaca, S., & Mastrandrea, L. (2017). Designing retail tariffs to decarbonise the electricity system. *International Conference on the European Energy Market, EEM.* https://doi.org/10.1109/EEM.2017.7982022
- Sampson, E., & Longe, O. (2021). Review of the role of energy pricing policies in electricity retail market. 2021 IEEE PES/IAS PowerAfrica, PowerAfrica 2021. https://doi.org/10.1109/PowerAfrica52236.2021.9543429
- Shan, K., Wang, S., Yan, C., & Xiao, F. (2016). Building demand response and control methods for smart grids: A review. *Science and Technology for the Built Environment*, 22(6), 692–704. https://doi.org/10.1080/23744731.2016.1192878
- Shang, J., Gao, J., Jiang, X., Liu, M., & Liu, D. (2023). Optimal configuration of hybrid energy systems considering power to hydrogen and electricity-price prediction: A two-stage multi-objective bi-level framework. *Energy*, *263*, 126023. https://doi.org/10.1016/J.ENERGY.2022.126023
- Smets, A., Jäger, K., Isabella, O., Van Swaaij, R., & Zeman, M. (2016). Solar Energy The physics and engineering of photovoltaic conversion, technologies and systems.
- Stein, J. S., Holmgren, W. F., Forbess, J., & Hansen, C. W. (2016). PVLIB: Open source photovoltaic performance modeling functions for Matlab and Python. *2016 IEEE 43rd Photovoltaic Specialists Conference (PVSC)*, 3425–3430. https://doi.org/10.1109/PVSC.2016.7750303
- Tennet. (2023). Costs of a grid connection. https://www.tennet.eu/costs-grid-connection The MathWorks Inc. (2023). gamultiobj Algorithm.
- Wang, N., Heijnen, P. W., & Imhof, P. J. (2020). A multi-actor perspective on multi-objective regional energy system planning. *Energy Policy*, 143, 111578. https://doi.org/10.1016/J.ENPOL.2020.111578
- Weckesser, T., Dominković, D. F., Blomgren, E. M., Schledorn, A., & Madsen, H. (2021). Renewable Energy Communities: Optimal sizing and distribution grid impact

- of photo-voltaics and battery storage. *Applied Energy, 301*, 117408. https://doi.org/10.1016/J.APENERGY.2021.117408
- Wentao, Z., Youfu, Z., Da, L., Yuhong, Z., Xueying, Y., & Huaqiang, L. (2018). Multi-objective optimization of capacity configuration for grid-connected microgrid system. 2017 2nd International Conference on Power and Renewable Energy, ICPRE 2017, 737–741. https://doi.org/10.1109/ICPRE.2017.8390631
- Yaghi, M., Luo, F., Fouany, H., Junfeng, L., Jiajian, H., & Jun, Z. (2019). Multi-objective optimization for microgrid considering demand side management. *Chinese Control Conference, CCC*, 2019-July, 7398–7403. https://doi.org/10.23919/ChiCC. 2019.8865498
- Yu, J., Sun, C., Kong, R., & Zhao, Z. (2021). Multi-objective optimization configuration of wind-solar-storage microgrid based on NSGA-III. *Journal of Physics: Conference Series*, 2005(1). https://doi.org/10.1088/1742-6596/2005/1/012149
- Zhang, C., Xia, J., Guo, X., Huang, C., Lin, P., & Zhang, X. (2022). Multi-optimal design and dispatch for a grid-connected solar photovoltaic-based multigeneration energy system through economic, energy and environmental assessment. *Solar Energy*, 243, 393–409. https://doi.org/10.1016/j.solener.2022.08.016
- Zhang, N., Yang, N.-C., & Liu, J.-H. (2021). Optimal sizing of PV/wind/battery hybrid microgrids considering lifetime of battery banks. *Energies*, 14(20). https://doi.org/10.3390/en14206655
- Zhang, Y., Ma, T., & Yang, H. (2022). Grid-connected photovoltaic battery systems: A comprehensive review and perspectives. *Applied Energy*, 328. https://doi.org/10.1016/j.apenergy.2022.120182
- Zhou, Y., Ziar, H., Zeman, M., & Isabella, O. (2022). *Solar PV Scan at Green Village (TGV)* (tech. rep.). PVMD Group, Delft University of Technology. Delft.